**Doctoral Dissertation (Shinshu University)**

# On the molding method and the mechanical properties of advanced composite materials

March 2014

XU ANCHANG

# Contents

**Chapter 3: Deformation behavior of fiber-reinforced plastic composites under a pure bending moment**



**Chapter 4: Influence of aramid spread tow fabric on the mechanical properties of fiber reinforced plastic composite**

**Chapter5: Determination of Creep Life of Glass Fiber/Phenol Composite Filled with Carbon Nanotubes by Four-Point Flexural Creep Test**

CHAPTER ONE

# Introduction

# Chapter 1: General introduction

## 1.1 Fiber reinforced polymer matrix composite (PMCs) [1-4]

The word composite implies that the material is composed of dissimilar constituents, which means there are two or more individual constituents that retain their identity on the macroscopic level in composite material. Materials composing a composite can be classified as a reinforcement or strengthening phase and a matrix or binder phase. Generally a homogeneous matrix component is reinforced by a stronger and stiffer constituent, which is usually in the forms of continuous fibers, discontinuous or chopped fibers, whiskers, particles, platelets, etc. Matrix materials can be polymers, metals, or ceramics. The composite mentioned in this paper will be concentrated primarily on fiber reinforced polymer matrix composites. Typically the reinforcement fibers are impregnated by a matrix material that acts to transfer load to the fibers. Also the matrix plays a role of protecting the fibers from abrasion and environment attack. The matrix dilutes the properties to some degree, but even so very high specific (weight-adjusted) properties are available from these materials. The excellent lightweight coupled with high stiffness and strength along the direction of the reinforcement is one of the major reasons for their use in aircraft, automobiles, and other moving structures. There are also some desirable properties including superior corrosion and fatigue resistance compared to metals. Currently the PMCs are limited to service temperatures below about 300ºC for the matrix decomposes at high temperature. The PMCs are often divided into two categories: reinforced plastics and so-called

advanced composites based on the distinction of the level of mechanical properties (usually strength and stiffness); however there is unambiguous line separating the two. Reinforced plastics typically consist of polyester resins reinforced with low-stiffness glass fibers, which are relatively inexpensive. And the advanced composites consist of fibers and matrix combinations that yield superior strength and stiffness, which are relatively expensive. They typically contain a large percentage of high performance continuous fibers, such as graphite, aramid or other organic fibers.

The reinforcement, the matrix and the interphase between the matrix and reinforcement determine the properties of PMCs. When designing PMCs, many variables should be put into consideration. The variables like the geometry of the reinforcement, and the nature of the interphase influence the properties of PMCs as well as the types of matrix and reinforcement and their relative proportions. Also the mechanical properties of PMCs are highly interdependent. For instance, cracking associated with shear stresses may result in a loss of stiffness. Impact damage can seriously reduce the compressive strength of PMCs. Compressive and shear properties can be seen to relate strongly to the toughness of the matrix, and to the strength of the interfacial bond between matrix and fiber. All these PMCs characters must be considered comprehensively to produce a structural material optimized for the conditions for which is to be used.

The matrix properties determine the resistance of the PMCs to most of the degradative processes, for instance impact damage, delamination, water absorption, chemical attack and high-temperature creep, which cause failure of the structure. PMCs can be classified in to fiber reinforced thermosetting plastic (FRP) and fiber reinforced thermoplastic (FRTP) by the distinction in the types of matrix resin.

Polyesters, vinylesters, epoxies bismaleimines and polyamines are thermosetting resins. Currently the most commonly used thermosetting resin in advanced composite is the epoxies. Initially, the viscosity of thermosetting resins is low. During their curing process, thermosetting resins undergo chemical reactions that crosslink the polymer chains and thus connect the entire matrix together in a three-dimensional network. Because of the three-dimensional cross-linked structure, the thermosetting resins tend to have high dimensional stability, high-temperature resistance and good resistance to solvents. However, the major short point of fiber reinforced thermosetting resins is hard to be recycled or reused just because of the chemically insert of the cured matrix.

Polymers such as polyetherimide, polyamide imide, polyphenylene sulfide, polyether-etherketone (PEEK) and liquid crystal polymers fall into the same category known as thermoplastic resins, sometimes called engineering plastics. In thermoplastic resins, there are long, discrete molecules that melt to a viscous liquid when heated to process temperature, and after forming, are cooled to an amorphous, semi-crystalline or crystalline solid. Unlike the curing process of thermosetting resins, this process is reversible, and by just heating to the process temperature the thermoplastic resins can be formed into another desired shape. Thermoplastics are more resistant to impact damage and cracking comparing to thermosetting resins, although they are inferior in high-temperature strength and chemical stability to them. Thermoplastics offer a promise way for manufacturing PMCs effectively, because it is easier and faster to heat and cool a material than it is to cure it. Although the thermoplastic resins are reinforced primarily by discontinuous fibers by extrusion, injection molding or compressing molding currently, there are great potential for manufacturing high-performance PMCs reinforced with continuous fibers, because of their high processing cycle.

In order to produce the PMCs with improved properties and manufacture more cost-effectively, the following needs should be addressed: (1) it is urgent to develop a new, low-cost fabrication method for PMCs, because their high cost remains the most important barrier to more widespread use in commercial application; (2) the impact resistance of PMCs should be improved which is crucial to the reliability and durability of PMC structures; (3) delamination is considered to be the most important mode of damage propagation in PMCs with laminar structure so the delamination should be depressed during design; (4) the interphase determines how the load transmitted between the reinforcement and the matrix, has a critical influence on PMCs behavior, should be well understood.

### 1.2 Manufacture of continuous fiber reinforced thermoplastic composite

As a category of matrix resin for fiber reinforced polymer composites, the thermoplastic have several advantages over thermosets. Firstly, their shelf life is unlimited. Because the Thermoplastics are high molecular weight polymers, unlike thermosetting resins, there is no need to cure via a chemical reaction to form a rigid three-dimensional cross-linked chemical structure. They do not have to be stored in freezers. This effectively infinite shelf life is a big advantage and avoids problems with material age and storage. Secondly, many types of manufacturing methods are available for thermoplastics, including compression moulding, pultrusion, filament winding and thermoforming. Prepreg material made from reinforcing fibers pre-impregnated with thermoplastic resin can also be used to build composite parts using autoclave processing. Thirdly, as mentioned before, interconversion between solid and viscous liquid can be

performed by changing temperature of thermoplastics, this character makes them can be formed into the shape required quickly and with the ability to be re-formed; something that cannot be achieved using conventional thermoset resins; by only applying heating and pressure. It is for this reason that thermoplastics have great appeal as composite matrices. During these manufacture or re-forming processes the only factors are how quickly the materials can be heated and cooled, the cycling time is markedly shortened comparing to thermosets. Finally, the thermoplastics are with the properties of low water absorption and high chemical resistance. Moisture uptake results in a decrease in mechanical properties such as stiffness. Moisture uptake is also important in bonded repair procedures since moisture in the parent material is a source of voids in the repair bondline. Thermoplastic matrix composites exhibit excellent mechanical performance in hot/wet environments. The thermoplastics with crystalline morphologies such like PEEK and PPS exhibit excellent resistance to chemical attack which makes them ideal for many aviation operating environments. On the other hand, the thermoplastics are with some disadvantages, for instance, high processing temperatures and high pressures are required. The processing temperatures required to form thermoplastics are far greater than for thermosets and even the thermoplastics are melt at high temperature but still remain fairly viscous which can make it difficult for the resin to flow and the composite part to consolidate consequently high temperature and pressures are required[5-7].

For the purpose of maximization of the reinforcing effect of fiber-reinforcement the continuous fibers were employed to reinforce polymer matrix resin for years. The thermosetting resins traditionally are liquid at room temperature with low viscosity [8], the molding processes such as resin transfer molding (RTM) and vacuum assistant resin

transfer molding (VaRTM) are commonly employed to fabric composite materials[9,10]. On the other hand, the melt viscosity of thermoplastics is two or three orders of magnitude higher [11, 12], make it generally not possible to shift the required viscosity range merely by raising the processing temperature. This makes it difficult for the polymer melt to impregnate into fibrous beds. The poor impregnation leads to poorer product properties. Hence the critical process elements must deal with the effects of this high viscosity. In the impregnation step viscosity affects both fiber/resin uniformity as well as fiber wet-out which is critical for good load transfer in the final part. In processing the final part, viscosity affects consolidation rate, fiber wash or movement of the fibers in the part and cycle time. The most critical phase in processing of thermoplastics is the impregnation step. Here the fiber and resin are brought into intimate contact and the fiber/matrix distribution is essentially set. For most thermoplastic systems this is accomplished first before proceeding to make a part. Accordingly, special equipment and manufacturing techniques are required for continuous fiber reinforced composites in order to facilitate the resin impregnation simultaneously ensure the continuous fibers without being cut during the impregnation process [13, 14]. For this primary limitation, the use of thermoplastic matrices has been limited by the lack of good processing techniques. For the sake of adopting the thermoplastics resin for large volume applications [7, 15], during the last decade, great efforts have been made to overcome the difficulties in impregnation of fiber with thermoplastic resins for manufacturing composites. There are three different types of impregnation process for thermoplastic composites: (1) direct melt impregnation; (2) operations involving intimate mixing of constituents prior to impregnation, and (3) processes involving precursors of low viscosity (solvent methods and techniques

involving reactive chain extension after impregnation). As reviewed by A.G.Gibson [16], there are two stages to prepare a fiber reinforced thermoplastic composite, first is compounding the reinforcing fiber and matrix, the second is impregnation and consolidation using a combination of heat and pressure. In the first stage the flow length known as the distance that the matrix resin must flow in order to complete the impregnation process to the required level, should be minimized in the purpose of achieving better impregnation in the second stage.

Those techniques include film stacking, co-woven yarn, plied matrix, powder impregnation, commingled materials, pseudo-thermoplastic oligomers, and dissolved polymer solution [12, 17, 18]. Illustrated in figure 1.1.

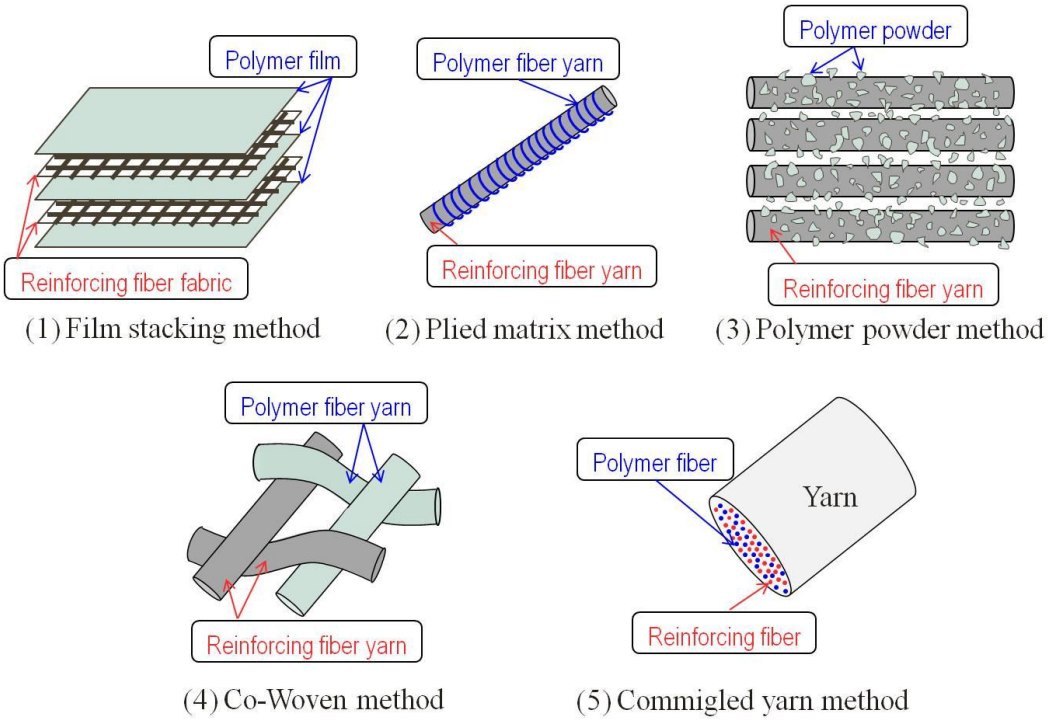


Fig. 1.1. Illustration of impregnation methods

In film stacking method, the fiber and resin beds are stacked in an alternative way,

when temperature increases to melting point the resin film melts and penetrates into the fiber bed attaining the final state of consolidation [15, 19-21]. Due to the low cost and excellent processability for both small and large-scale structures film-stacking method is considered very effective in producing thermoplastic resin composites. Especially the processing time and the resin flow path may be controlled by an appropriate allocation of the resin film and fiber beds. Also vacuum is often employed to reduce the entrapped void [22].

Co-woven fabrics are created by interweaving separate reinforcing and resin yarns. They can be woven in various-harness satin and other styles, depending on user needs [23, 24]. Sometimes an uneven distribution of reinforcement in the matrix may occur.

Plied matrix technique uses a Polymer fiber yarn wound around a reinforcing fiber yarn [25].

Powder impregnation is attractive continuous process that overcomes the difficulty of working with thermoplastics with high melt viscosities and poor solubility. This process generally produces a flexible prepreg by pulling the reinforcement continuously through a bed of powdered resin with diameters arranged 15-150μm. The resin particles are inserted between the fibers at the assistance of opening up technologies [26-31]. The most important advantage of powder impregnation technology is its ability to process matrix systems with very high melt viscosity and high melt temperature. One problem with this method is in handling the constituent materials since the polymer powder can be easily dislodged from the reinforcing filaments.

Commingled yarn consists of a blended combination of reinforcing fiber yarn and a yarn spun from a thermoplastic resin. In the commingled state, the multi-filament yarns are scattered amongst one another at the fiber level [32-37]. This is a relatively

easy process to use. Any thermoplastic resin can be made to work if it can be made into a fiber. Here the trick is to insure that the fiber diameter of the matrix fiber is matched to that of the reinforcing fiber in order to assure good distribution of the two fibers. It also requires a texturing process to open the yam bundle without damaging the brittle fiber.

The oligmers of some thermoplastics are promising materials for good impregnation with fiber bed, because of their low viscosity. After impregnation the oligomers were polymerization in situ, producing fiber reinforced thermoplastic composite [38-41]. However, the unreacted monomers left in the composite system will weaken the properties of the final product.

In solvent impregnation, low viscosity solution with polymer resin dissolved in solvent has been used to impregnate fibrous reinforcement. Subsequently, the solvent will be vaporized to form a fiber reinforced thermoplastic composite [42]. The benefit of this process is derived from the low viscosity of the resulting resin solution which allows both unidirectional tapes and woven fabrics to be used as feed material. However, there are two big drawbacks: the potential for residual solvent in the prepreg, and inability to use higher performance resins that have excellent solvent resistance. Much more endeavors are required in fabrication of continuous fiber reinforced thermoplastic composite with better performance.

The Poly-*p*-phenylenebenzobisoxazole (PBO) is a rigid-rod polymer formed by the polycondensation of terephthalic acid (TA) and diaminoresorcinol (DAR) in polyphosphoric acid (PPA) [43]. Fibers manufactured by this polymer are spun by a dry-jet wet-spinning technique that warrants a high degree of molecular chain orientation through an elongational flow field [44-46]. The aromatic heterocyclic rings

in the polymer provide the fiber with excellent tensile, impact and tribological properties and ensure good chemical resistance under a wide temperature range [47]. Also exceptional fire resistance of PBO was reported by Serge Bourbigot [48]. All those excellent mechanical properties provided great potential applications in advanced composite materials. Although the mechanical properties of composites are primarily determined by the properties of reinforcement and matrix, the reinforcement/matrix interface is also an indispensable factor in influencing the overall properties of the composite, such as off axis strength, fracture toughness and environmental stabilities [49, 50]. Because the interface properties impress the effectivity of stress transferred from matrix to reinforcement. However, the surface of PBO fiber is chemical insert and smooth due to its high crystallinity and the lack of polar functional groups in the polymer repeat unit, which lead to a poor interfacial adhesion with most of the polymer matrix [51]. Several surface treatment methods, such as chemical treatment [52-54], corona, plasma modification [15-58], chemical coupling method [59] and γ-ray irradiation [51] are used to add polar agents improving surface free energy or roughen the fiber surface for better adhesion properties.

Fiber compressive strength is as important as the tensile strength in many composite applications. But extensive studies on compression behavior of PBO fiber found that the compressive strength (200-300MPa) is only a small fraction of its tensile strength. The reason is that unlike carbon and other inorganic fibers, rigid-rod polymeric fibers exhibit failure via kinking instead of a catastrophic failure. The deformation mechanism involving kinking of individual molecules was confirmed by observing sharp, high angle tilt boundaries. Several theoretical models have been developed to explain compressive failure in high performance polymeric fibers. A

model proposed the elastic instability of perfectly oriented rigid-rod chains. From this model, the relationship between compressive strength and shear modulus, depending on buckling mode, is suggested that the compressive failure is dominated by fibrillar instability rather than molecular instability. The other theories concerned the misalignment between fibrils, crystals, or domains of well-oriented molecules and applied load direction [44].

### 1.3 Impact resistance of laminated composite [60-63]

The most significant limitation of composite materials is their susceptible response to out-plate impact loading. In recent years many investigations have been undertaken in an attempt to better understand the impact response of these materials [64-68]. The failure modes of composites are significantly different from those of metals and very complex. In metal structures the impact damage always starts from the surface and of course can be detected by routine visual inspection. However, the ability of composites undergoing plastic deformation is extremely limited, the absorbed impact energies cause significant impact damage in the form of delamination, matrix cracking, or fiber breakage which is totally undetectable by visual inspection. The damage subsequently leads to reductions in both strength and stiffness. For developing composite materials with better impact resistance it is essential to understand the impact phenomenon, damage mechanisms, and develop appropriate mathematical models.

The main damage forms caused by impact energy in composite materials are delamination, matrix cracking and fiber breakage. Among them, delamination and matrix cracking are sensitive to matrix properties, whereas fiber breakage is more

sensitive to the properties of fiber. Generally improvements in the properties of the constituents lead to improved impact damage resistance. Influences on the impact resistance of composites caused by the properties of fiber, matrix and the interfase between them and also the test conditions such like the geometry of the sample and impact velocity will be introduced.

The properties of the fibers in a continuous fiber composite have a significant effect on the impact resistance and subsequent load-bearing capacity of components made from such materials. Higher fiber failure strains, with the same elastic modulus, will result in higher energy absorption, especially since the strain energy absorbed by the matrix represents a large portion of the total strain energy. For the same impact energy, higher capacity to absorb energy results in less fiber breakage and a higher residual tensile strength. Secondary matrix damage which occurs after initial fiber failure will also be reduced so that residual compressive strength is also increased [69]. For low velocity impact loading, the ability of the fibers to store energy elastically appears to be the fundamental parameter in determining impact resistance. Kevlar fibers, which have large areas under their stress/strain curves, offer excellent impact resistance [70].

The polymeric matrix in a fiber-reinforced composite serves to protect, align and stabilize the fibers as well as assure stress transfer from one fiber to another. In general, both the stiffness and strength of the matrix are considerably below those of the reinforcing fiber. Nevertheless the function of the matrix is critical. For example, damage to the matrix such as impact-induced delamination can reduce the load-bearing capability of the composite by up to 50% [71]. As a result of the relatively poor behavior of matrix, in recent years much work has been undertaken in an attempt to

identify the fundamental matrix properties that influence the impact resistance of composite materials. It is clear that matrix properties play a significant role in determining the impact resistance and subsequent load-bearing capability of a fiber-reinforced plastic. Presently, significant efforts have been made to improve the impact resistance and post-impact compressive properties of composites by changing the matrix properties [72-75].

The bonding strength between the matrix resin and the fiber reinforcement is a controlling factor in determining the mechanical performance of most polymer composites. Generally, oxidative treatment on the surface of the fibers is performed in order to improve the level of adhesion between matrix and fiber. Initially, this interracial zone was considered as being a two dimensional surface with effectively zero thickness. However, more recent studies have shown that this region is in fact three-dimensional, having its own distinct properties [76, 77]. The level of treatment applied to the surface of the fibers in a composite material has a significant effect upon both its impact resistance as well as its residual load-carrying capability. In general, impact on composites with low levels of fiber surface treatment generates large areas of splitting and delamination with severe effects on the compressive properties of the material. Localized impact loading on highly treated fiber composites results in a smaller, more localized damage zone, a lower perforation threshold and improved.

Composite materials offer a unique advantage in that properties such as strength and stiffness can be tailored to meet specific design requirements through a careful selection of the fiber stacking sequence. Considerable work has shown that the impact resistance of composite materials also depends upon the specific order in which the plies are stacked. The impact resistance of a multidirectional laminate is strongly

dependent upon the specific orientation of the plies. Unidirectional laminates should be avoided since they split and fail at low energies. The mismatch in bending stiffness between two plies appears to have a significant effect upon the level of damage incurred at that interface. Damage appears to be greatest where ply orientation changes of 90° occur. This suggests that for containment of damage laminates with abrupt changes in fiber direction should be avoided. Other ways to suppress damage include the use of woven fabrics, the use of hybrid composites or stitching at desired locations.

Geometry of the test sample is a fundamental parameter in determining the impact response of a composite component. Researchers found that the energy absorbing capability increases with an increased size of GFRP beam under low velocity impact conditions, however, doubling the size did not leading to a equivalent increasing in the energy absorption[78]. Geometrical effects are significant under conditions of low velocity impact loading. Varying the geometry changes the target's ability to store energy and therefore its impact resistance. Large targets are not necessarily better energy absorbers than small coupons. Consequently attention should be taken when interpreting data from tests on laboratory-size specimens.

Varying the impact velocity and therefore the strain rate affects both the material's properties as well as the target response. Low velocity impact loading by a heavy object induces an overall target response, whereas high velocity impact by a light projectile induces a localized mode of target deformation resulting in energy being dissipated over a small region immediate to the point of impact. In the latest generation of tough composites matrix dominated modes of fracture appear to show a distinct rate dependency and care should be taken when using static tests to characterize dynamic behavior.

## 1.4 Spread tow fabric reinforced composites

Woven fabrics are wildly employed to reinforce polymeric matrix in composites are instead of pre-impregnated warp sheets in many application field. Firstly, fabric can be easily handled, allowing for automation and consequent reduction of labor. Secondly, fibers can conform to complex shapes and have more isotropic in-plate properties than unidirectional materials do [79-81]. However, distortions of the fiber roving at interlacing points in the fabric lead to stress concentration in the composite, result in reduction in strength and stiffness comparing with cross-ply laminates [82-86]. A new technology was developed to change the woven fabric structure for reducing the stress construction and improving their mechanical properties which is known as spread tow fabric (STF) [87-89]. This technology includes the steps of spreading a tow into a thin and flat unidirectional tape, and waving the tapes to a woven spread tow fabric using a special weaving apparatus. The fibers in the woven structure are arranged in the straightest orientation insuring that the fiber properties are used in the most effective way to carry load. There are some advantages of spread tow, for instance, it is possible to achieve better mechanical properties in composite materials, because the diminished fiber distortion at the cross-over points; the flatness of STF makes it impossible for hulk matrix accumulation in the near absence of crimp at the interlacing points, consequently, the dead weight of the final composite materials can be remarkably reduced.

The spread tow fabric technology is commonly employed in producing carbon fiber spread tow fabrics used as reinforcement in composite. It had been confirmed that with using spread tow technology the tensile strength and bending strength of composite

were improved as well as the fatigue property [90, 91]. In addition, the enhancements in damage resistance such like open-hole tensile strength [90] and open-hole compressive strength [92] as well as impact resistance [93] were reported. By the investigation of damage mechanism, it is discovered that transverse crack and delamination are significally restrained along with the reducing in the laminate thickness [94, 95].

### **1.5 Multi-scale fiber reinforced polymer matrix composites** [96]

A new kind of composite combining the micro-scale fibrous reinforcement, nano-scale filler and matrix is defined as three-phase composite because of the different in the length scales of reinforcement and fillers. In the three-phase composite the main reinforcing phase are continuous fibers, which determine the high strength and modulus of the materials, while the matrix can be considered as a nanocomposite, containing particles on the nanometer scale. The high volume fraction will not be influenced, because the nanometer scale fillers only fit in the space occupied by the matrix before.

The relatively poor properties of matrix resin and the weak fiber-matrix interfacial bond limit the though-the-thickness properties in fiber reinforced polymer matrix composites with laminated structure. In fact delamination caused by external loading as in static bending, compression or tension, in cyclic fatigue or by impacts of low-to-high energies, during fabrication or in service is one the most prevalent life-limiting crack mode in laminate composites. Improving the though-the-thickness properties and reducing delamination are urgent for their future structural applications.

Introducing nanotechnology in the field of composite with nano-scale fillers, like carbon nanotubes (CNTs) and carbon nanofibers (CNFs), offers new possibility to

improve the resistance to interlaminar fracture and impact damage and multifunctional properties of FRPs. Because of their excellent modulus and strength, high aspect ratio, large surface area and excellent thermal and electrical properties, these nanofillers can be incorporated into the FRPs to modify the properties of matrix resins.

The most important part of introducing CNTs into a composite is how they are integrated into the three-phase multi-scale composites. The incorporation of nanoscale CNTs with conventional microscale fiber reinforcements in a common polymer matrix can be achieved by modifying either the matrix resin or the fibrous reinforcement using CNTs. Fabrication of multi-scale FRPs with modified matrix resin has some limitations that hinder their development and widespread applications. One of the main problems in this approach is that the viscosity of the matrix increases dramatically with increasing CNT content, even the content is below 1wt%, and the CNTs severely agglomerate together in the composite. The highly viscous and CNT-agglomarated resin systems cannot be processed using the conventional composite manufacturing methods such as RTM or VaRTM. For example, when the frequently used VaRTM is employed to fabricate the multi-scale FRPs, nanofillers can be filled and trapped in the inter-tow regions within the perform mesh, leading to an inhomogeneous microstructure of multi-scale FRPs. Another way is attaching CNTs on the surface of fibrous reinforcement directly. The key advantage of this method is the ability to incorporate CNTs with high concentrations in the composites.

There are many reports [97-100] on the properties of CNTs-polymer composites; according to these researches, the fracture toughness was significantly improved by adding CNTs in the matrix resin. From those promising, there is a possibility to use CNTs in modifying the properties of FRPs that are dominated by the inherent properties

of the matrix materials such as compressive and flexural strength. The compressive strength of composites is considered to depend on the modulus of the matrix [101-104]. The higher the matrix modulus is the better lateral support of the fibers they can provide, which reduces the tendency of micro buckling or kinking of fibers. The compressive strength dominates the flexural strength of the continuous fiber reinforced composites, because, under flexural loading the failure always starts at the compressive side due to the micro buckling and kinking [100]. It is considered that the factors affecting the modulus of polymer composite are complicated. Those factors include the nature of filler and polymer matrix and the compatibility between them, the distribution or dispersion of the fillers in the polymer matrix, as well as the interfacial structure and morphology, and so on [105-107].

The interlaminar shear strength of the multi-scale composite can be improved because of the enhancement in matrix strength and the fiber-matrix interfacial adhesion strength [96]. The nanoscale fillers enhanced the load transfer to the fibrous reinforcements in the adherents so that the failure occurred preferentially in the composite rather than along the adhesive composite interface.

## 1.6 Investigation in this research

The fiber reinforced polymer matrix composite materials (PMCs) attracted many attentions, for their properties of light-weight, high specific strength and specific modulus, good corrosion resistance and etc.. But there are still some properties that may cause problems during the usage in practice. When the composite fiber and matrix materials are combined to form a composite material the properties of the result differs

from most engineering materials in that the mechanical properties of composites are highly dependent on the direction in which the loads are applied. Composite strength and stiffness are generally anisotropic. Strength and stiffness are generally much higher along the fiber direction (isostrain) than perpendicular to the fiber direction (isostress). This property should be pay attention to when design the products made from this kind of materials. Changing the stacked sequence manufactures quasi-isotropic materials for usage in the field like aerospace.

The interface between reinforcing fiber and matrix is with direct influence on the load transforming in PMCs. Poor interface properties will lead to poor mechanical properties of PMCs.

A critical type of damage in the PMCs is delamination which sometimes developed from matrix imperfections. Delaminations form on the interface between the layers in the laminate. Delaminations may form from matrix cracks that grow into the interlaminar layer or from low-energy impact. Debonds can also form from production nonadhesion along the bondline between two elements and initiate delamination in adjacent laminate layers. Under certain conditions, delaminations or debonds can grow when subjected to repeated loading and can cause catastrophic failure when the laminate is loaded in compression. (Behavior of delaminations and debonds depend on loading type. They have little effect on the response of laminates loaded in tension. Under compression or shear loading, however, the sublaminates adjacent to the delaminations or debonded elements may buckle and cause a load redistribution mechanism that leads to structural failure.)

When under compressive load in the fiber long direction, the reinforcing fiber fall into buckling easily which leads to low compression strength.

After the reinforcing fibers and matrix resins are composed together, it is hard to change the shape of the PMCs because of the characteristics (crosslinked structure which cannot be remolded) of the thermosetting resins. Thermoset materials once cured cannot be remelted or reformed. During curing, they form three-dimensional molecular chains, called cross-linking. Due to these cross-linkings, the molecules are not flexible and cannot be remelted and reshaped.

It is inherently difficult to recycle PMCs, because of their complex composition (reinforcing fibers, plastic matrix and fillers), the crosslinked structure of thermosetting resins (which cannot be remolded), and the combination with other materials (metal fixings, honeycombs, foam, etc.).

In order to fasten the material parts together, holes should be drilled on the PMCs parts. Improper hole drilling, poor fastener installation, and missing fasteners may occur in manufacturing and hole elongation can occur due to repeated load cycling in service.

As mentioned before the viscosity of the thermoplastic resin is extremely high which leads to poor impregnation with continuous reinforcing fibers, cause poor mechanical properties in FRTPs.

This research focuses on investigating how to improve the fiber volume fraction in FRTPs, and reshaping and reprocessing ability, impact resistance and creep life time of FRP. The high performance materials including high performance reinforcing fibers (poly(*p*-phenylenebenzobisoxazole), poly para-phenyleneterephthalamide, CNTs) and thermoplastic matrix resin are employed to fabricate the advanced polymer matrix composites. The molding method and the mechanical properties of the advanced fiber reinforced polymer matrix composites were investigated.

The low fiber volume fraction of the continuous fiber reinforced thermoplastic

composite is the main limitation for application as structural materials.To achieve better impregnation and a higher fiber volume fraction, a new vacuum-assisted solution impregnation prepreg thermoplastic composite molding method was proposed. Consequently tensile testing comparison between the final composite and thermosetting composite with the same reinforcement was performed to confirm the feasibility of this method.

Fabric reinforce polymer matrix composites are with complex deformation characteristics, the bending deformation of an organic fabric reinforced thermosetting composite was investigated by performing on a special pure bending apparatus. Also the deformation of carbon fiber reinforce same thermosetting resin was investigated for a comparison.

A new technology of fabricating fabrics with thinner thickness than the ordinary ones is known as spread tow fabric (STF). There are some improvements in the composites with the reduced thickness of reinforcing fabrics. A spread tow fabric produced by aramid fiber is used as the reinforcement of composite. Influences of this spread tow fabric on the properties such like tensile strength compressive strength and the flexural properties of mono- and hybrid composites were investigated.

A three-phase composite of CNTs and glass fiber reinforced phenol matrix was manufactured because there are reports on the enhancements of this kind of composite. It is promising to employ this technology to improve the creep life of fiber reinforce polymer matrix composite. Firstly the interlaminar shear strength was investigated by short beam testing method, and then a flexural creep test was performed. A long term creep data was obtained according to the time-temperature reciprocation law. With these data, the influences of adding CNTs on the durability of composite were investigated.

**References**

[1] Advanced Materials by Design, chapter 3 Polymer matrix composites

[2] D.hull and T.W. Clyne, An introduction to composite materials,

[3] Krishan K. Chawla, Composite Materials: Science and Engineering,

[4] P. K. Mallick, Fiber-reinforced composites: materials, manufacturing and design,

[5] Roger Vodicka, Thermoplastics for airframe applications a review of the properties and repair methods for thermoplastic composites, DSTO-TR-0424.

[6] Thermoplastic composites-rapid processing applications, Composite part A: Applied Science and Manufacturing, 27A (1996) 329-336.

[7] D. M. Bigg, D. F. Hiscock, J. R. Preston AND E. J. Bradbury, High performance thermoplastic matrix composites, Journal of Thermoplastic Composite Materials, 1 (1988) 146-160.

[8] G. Augustin, W. Janke, and G. Hinrichsen, Schmelzepultrusion—ein Verfahren zur Herstellen thermoplastischer Hochleistungsprepregs, Kunsfstoffe, 81 (1991) 403-406.

[9] Lee LJ. Liquid composite molding. In: Gutowski TG, editor. Advanced Composites Manufacturing. New York: Wiley InterScience; 1997. p. 393-456.

[10] Rudd CD, Kendall KN. Towards a manufacturing technology for high-volume production of composite components, Proceedings of the Institution of Mechanical Engineers, Part B: Journal of Engineering Manufacture, 206 (1992) 77-91.

[11] Augustin, G. and Hinrichsen, G. Forschung AktueNl990,7 (5), 7

[12] I.Y. Chang and J.K. Lees, Recent Development in Thermoplastic Composites: A Review of Matrix Systems and Processing Methods, Journal of Thermoplastic Composite Materials, 1 (1988) 277-296.

[13] Kocsis JK. Polypropylene: structure, blends and composites. London: Chapman & Hall; 1995.

[14] Jang BZ. Advanced polymer composites: principles and applications. New York: ASM International; 1994.

[15] Hiscock DF, Bigg DM. Long-fiber-reinforced thermoplastic matrix composites by slurry deposition. Polymer Composites, 10 (1989) 145–149.

[16] A.G.Gibson and J.-A. Månson, Impregnation technology for thermoplastic matrix composites, Composites manufacturing, 3 (1992) 223-233.

[17] K. Fujihara, Zheng-Ming Huang, S. Ramakrishna, H. Hamada, Influence of processing conditions on bending property of continuous carbon fiber reinforced PEEK composites, Composites Science and Technology, 64 (2004) 2525–2534

[18] M. D. Wakeman, T. A. Cain, C. D. Rudd, R. Brooks & A. C. Long, Compression moulding of glass and polypropylene composites for optimised macro- and micro-mechanical properties- 1 commingled glass and polypropylene, Composites Science and Technology, 58 (1998) 1879-1898.

[19] Silverman EM. Effect of glass fiber length on the creep and impact resistance of reinforced thermoplastics, Polymer Composites, 8 (1987) 8-15.

[20] Bigg DM, Bradbury EJ. The impact performance of thermoplastic sheet composites, Polymer Engineering and Science, 32 (1992) 287-297.

[21] Bigg DM, Preston JR. Stamping of thermoplastic matrix composites, Polymer Composites, 10 (1989) 261-268.

[22] Letterman LE. Resin film infusion process and apparatus.US Patent 4622091, 1986.

[23] Stuart M. Lee, Handbook of Composite Reinforcements, 1992.

[24] Sylvie Beland, High Performance Thermoplastic Resins and their Composites, 1990.

[25] Lynch, T., Thermoplastic/graphite fibre hybrid fabrics. SAMPE Journal, 25 (1989) 17-22.

[26] Hartness, T., Thermoplastic powder technology for advanced composite materials systems. Journal of Thermoplastic Composite Materials, 1 (1988) 210-220.

[27] Ye, L., Klinkmtiller, V. and Friedrich, K., Impregnation and consolidation in composites made of GF/PP powder impregnated bundles, Journal of Thermoplastic Composite Materials, 5 (1992) 32-48.

[28] Ye, L., Friedrich, K., Cutolo, D. and Savadori, A., Manufacturing of CF/PEEK composites from powder/sheath-fibre performs, Composites Manufacturing, 5 (1994) 41-50.

[29] Ye, L. and Friedrich, K., Processing of thermoplastic composites from powder/sheath-fibre bundles. Journal of materials processing technology, 48 (1995) 317-324.

[30] Cutolo, D. and Savadori, A., Processing of product forms for the large scale manufacturing of advanced thermo- plastic composites. Polymers for Advanced Technologies, 5 (1994) 545-553.

[31] Miller, A., Wei, C., and Gibson, A. G., Manufacture of polyphenylene sulphide (PPS) matrix composites via the powder impregnation route. 4th International Conference on Automated Composites, Nottingham, The Institute of Materials, (1995)171-181.

[32] Lin Ye, Klaus Friedrich, Joachim Kätel and Yiu-Wing Mai, Consolidation of unidirectional CF/PEEK composites from commingled yarn prepreg, Composites

Science and Technology, 54 (1995) 349-358.

[33] Van West, B.P., Pipes, R.B. & Advani, S.G., The consolidation of commingled thermoplastic fabrics, Polymer Composites, 12 (1991) 417-27.

[34] Svensson N, Shishoo R, Gilchrist M., Manufacturing of thermoplastic composites from commingled yarns – a review, Journal of Thermoplastic Composite Materials, 11 (1998) 22-56.

[35] Fujita A, Maekawa Z, Hamada H, Matsuda M, Matsuo T., Mechanical behavior and fracture mechanism of thermoplastic composites with commingled yarn, Journal of Reinforced Plastics and Composites, 12 (1993) 156-172.

[36] Diao X, Ye L, Mai YW., Fatigue behavior of CF/PEEK composite laminates made from commingled prepreg. Part I: experimental studies. Composite Part A: Applied science and manufacturing, 28 (1997) 739-747.

[37] Long AC, Wilks CE, Rudd CD., Experimental characterization of the consolidation of a commingled glass/polypropylene composite, Composite Science Technology, 61 (2001) 1591-1603.

[38] H. Parton, I. Verpoest, In situ polymerization of thermoplastic composites based on cyclic oligomers, Polymer composites, 26 (2005) 60-65.

[39] Z.A. Mohd Ishak, Y.W. Leong, M. Steeg, J. Karger-Kocsisrd, Mechanical properties of woven glass fabric reinforced in situ polymerized poly(butylenes terephthalate) composites, Composites Science and Technology, 67 (2007) 390-398.

[40] H. Parton, J. Baets, P. Lipnik, B. Goderis, J. Devaux, I. Verpoest, Properties of poly(butylene terephthalate) polymerized from cyclic oligomers and its composites, Polymer, 46 (2005) 9871-9880.

[41] J. Karger-Kocsis, P. P. Shang, Z. A. Mohd Ishak, M. Rösch, Melting and

crystallization of in-situ polymerized cyclic butylene terephthalates with and without organoclay: a modulated DSC study, Express Polymer Letters, 1 (2007) 60-68.

[42] F.v. Lacroix, M. Werwer, K. Schulte, Solution impregnation of polyethylene fibre/polyethylene matrix composites, Composites Part A: Applied Science and Manufacturing, 29 (1998) 371-376.

[43] D.B. Roitman, L.H. Tung, M. Serrano, R.A. Wessling, P.E. Pierini, Polymerization kinetics of poly(p-phenylene-cis-benzobisoxazole), Macromolecules 26 (1993) 4045-4046.

[44] Han Gi Chae, Satish Kumar, Rigid-Rod Polymeric Fibers, Journal of Applied Polymer Science, 100 (2006)791-802.

[45] T. Kitagawa, M. Ishitobi, K. Yabuki, An analysis of deformation process on poly-p-phenylenebenzobisoxazole fiber and a structural study of the new high modulus type PBO HM+ fiber, Journal of Polymer Science Part B: Polymer Physics, 38 (2000) 1605-1611.

[46] T. Kitagawa, K. Yabuki, R.J. Young, An investigation into the relationship between processing, structure and properties for high-modulus PBO fibres. Part 1. Raman band shifts and broadening in tension and compression, Polymer, 42 (2001) 2101-2112.

[47] G.M. Wu, Y.T. Shyng, S.F. Kung and C.F. Wu, Oxygen plasma processing and improved interfacial adhesion in PBO fiber reinforced epoxy composites. Vacuum, 83 (2009) 271-274.

[48] S. Bourbigot, X. Flambard, M. Ferreira and F. Poutch, Blends of Wool with High Performance Fibers as Heat and Fire Resistant Fabrics, *Journal of Fire Sciences, 20* (2002) 3-22.

[49] R.J. Day, K.D. Hewson and P.A. Lovell, Surface modification and its effect on the interfacial properties of model aramid-fiber/epoxy composites, Composites Science and Technology, 62 (2002) 153-166.

[50] Y.D. Huang, L. Liu, J.H. Qiu and L. Shao, Influence of ultrasonic treatment on the characteristics of epoxy resin and the interfacial property of its carbon fiber composites, Composites Science and Technology, 62 (2002) 2153-2159.

[51] C.H. Zhang, Y.D. Huang, Y.D. Zhao, Surface analysis of γ-ray irradiation modified PBO fiber, Materials Chemistry and Physics 92 (2005) 245-250.

[52] G.M. Wu, Y.T. Shyng, Effects of basic chemical surface treatment on PBO and PBO fiber reinforced epoxy composites, Journal of Polymer Research, 12 (2005) 93-102.

[53] G.M. Wu and Y.T. Shyng, Surface modification and interfacial adhesion of rigid rod PBO fiber by methanesulfonic acid treatment, Composite part A: Applied Science and Manufacturing, 35 (2004) 1291-1300.

[54] G.M. Wu, C.H. Hung, J.H. You and S.J. Liu, Surface Modification of Reinforcement Fibers for Composites by Acid Treatments, Journal of Polymer Research, 11 (2004) 31-36.

[55] E. Mäder, S. Melcher, J. W. Liu, S. L. Gao, A. D. Bianchi, S. Zherlitsyn, J. Wosnitza, Adhesion of PBO fiber in epoxy composites, Journal of Materials Science 42 (2007) 8047-8052.

[56] G.M. Wu, Y.T. Shyng, S.F. Kung, C.F. Wu, Oxygen plasma processing and improved interfacial adhesion in PBO fiber reinforced epoxy composites, Vacuum, 83 (2009) S271-S274.

[57] G.M. Wu, Oxygen plasma treatment of high performance fibers for composites,

Materials Chemistry and Physics, 85 (2004) 81-87.

[58] M. Goldman, A. Goldman and R. S. Sigmond, The corona discharge, its properties and specific uses. Pure and Applied Chemistry, 57 (1985) 1353-1362.

[59] S. Yalvac, J.J. Jakubowski, Y.H. So and A. Sen, Improved interfacial adhesion via chemical coupling of cis-polybenzobisoxazole fiber-polymer systems, Polymer, 37 (1996) 4657-4659.

[60] Kevin R. Cromer, Impact and post-impact response of a composite material to multiple non-coincident impacts, 2010

[61] Mmders, P.W. and Harris, W.C., A parametric study of composite performance in compression-after-impact testing, SAMPE Journal, 22 (1986) 47-51.

[62] Curson, A.D., Leach, D.C. and Moore, D.R., Impact failure mechanisms in carbon fiber/PEEK composites, Journal of Thermoplastic Composite Materials, 3 (1990) 24-31.

[63] M.N. Ghasemi Nejhad and A. Parvizi-Majidi, Impact behaviour and damage tolerance of woven carbon fibre-reinforced thermoplastic composites, Composites, 21 (1990) 155-168.

[64] Hong, S. and Liu, D., On the relationship between impact energy and delamination area, Experimental Mechanics, 13 (1989) 115-120.

[65] Takeda, N., Sierakewski, R.L., Ross, C.A. and Malvera, L.E., Delamination-crack propagation in ballistically impacted glass/epoxy composite laminates, Experimental Mechanics, 22 (1982) 19-25.

[66] Takeda, N., Sierakowski, R.L. and Malvern, L.E., Transverse cracks in glass/epoxy cross-ply laminates impacted by projectiles, Journal of Material Science, 16 (1981) 2008-2011.

[67] G.A. Schoeppner and S. Abrate, Delamination threshold loads for low velocity

impact on composite laminates, Composites Part A: Applied Science and Manufacturing, 31(2000) 903-915.

[68] L.H. Strait , M.L. Karasek , M.F. Amateau Effects of Stacking Sequence on the Impact Resistance of Carbon Fiber Reinforced Thermoplastic Toughened Epoxy Laminates, Journal of Composite Materials, 26 (1992) 1725-1740.

[69] W.J. Cantwell, P.T. Curtis and J. Morton, An assessment of the impact performance of CFRP reinforced with high-strain carbon fibres, Composites Science and Technology, 25 (1986) 133-148.

[70] D. F. Adams and A.K. Miller, An analysis of the impact behavior of hybrid composite materials, Materials Science and Engineering, 19 (1975) 245-260.

[71] Cantwell, W.J., P. T. Curtis, and J. Morton, Low velocity impact damage tolerance in CFRP laminates containing woven and non-woven layers, Composites, 14 (1983) 301-305.

[72] Hunston, D. L., Composite interlaminar fracture: Effect of matrix fracture energy, Composites Technology Review, 6 (1984) 176-180.

[73] Valéria D. Ramos, Helson M. da Costa, Vera L.P. Soares, Regina S.V. Nascimento, Hybrid composites of epoxy resin modified with carboxyl terminated butadiene acrilonitrile copolymer and fly ash microspheres, Polymer Testing, 24 (2005), 219-226.

[74] R. S. Raghava, Role of matrix-particle interface adhesion on fracture toughness of dual phase epoxy-polyethersulfone blend, Journal of Polymer Science Part B: Polymer Physics, 25 (1987) 1017-1031.

[75] John E. Masters, Improved impact and delamination resistance through interleafing, Key engineering materials, 37 (1989) 317-348.

[76] Lehmann, S.; Megerdigian, C.; Papalia, R., Carbon fiber resin matrix interphase: effect of carbon fiber surface treatment on composite performance, SAMPE Q, 16 (1985) 7-13.

[77] J. Jang, H. Yang, The effect of surface treatment on the performance improvement of carbon fiber/ polybenzoxazine composites, Journal of Materials Science, 35 (2000) 2297-2303.

[78] L.J. Broutman and A. Rotem, Impact strength and toughness of fiber composite materials, 1972**.**

[79] P.T. Curtis, S.M. Bishop, An assessment of the potential of woven carbon fibre-reinforced plastics for high performance applications, Composites, 15 (1984) 259-265.

[80] A.P. Mouritz, M.K. Bannister, P.J. Falzon, K.H. Leong, Review of applications for advanced three-dimensional fibre textile composites, Composites Part A: Applied Science and Manufacturing, 30 (1999) 1445-1461.

[81] C.D Rudd, M.R Turner, A.C Long, V Middleton, Tow placement studies for liquid composite moulding, Composites Part A: Applied Science and Manufacturing, 30 (1999) 1105-1121.

[82] T. Ishikawa and T. W. Chou, Stiffness and strength behaviour of woven fabric composites, Journal of Materials Science, 17 (1982) 3211-3220.

[83]T. Fujii, S. Amijima, K. Okubo, Microscopic fatigue processes in a plain-weave glass-fibre composite, Composites Science and Technology, 49 (1993) 327-333.

[84] J. Whitcomb, G. Kondagunta, K. Woo, Boundary effects in woven composites, Journal of Composite Materials, 29 (1995) 507-524.

[85] J.L. Kuhn and P.G. Charambides, Elastic Response of Porous Matrix Plain Weave Fabric Composites: Part I Modeling, Journal of Composite Materials, 32 (1998) 1426-1471.

[86] M. Todo, K. Takahashi, P. Béguelin, H.H. Kausch, Strain-rate dependece of the tensile fracture behavior of woven-cloth reinforced polymide composites, Composites Science and Technology, 60 (2000) 763-771.

[87] N. Khokar, A Method for Weaving Tape-like Warp and Weft, Journal of the Textile Institute, 90 (1999).

[88] N. Khokar, Method and apparatus for weaving tape-like warp and weft and material thereof, Canadian Patents CA 2594350.

[89] K. Kawabe, T. Matsuo and Z. Maekawa, New technology for opening various reinforcing fiber tows, Journal of society of materials science Japan, 47 (1998) 727-734.

[90] S. Sihn, R. Y. Kim, K. Kawabe, S. W. Tsai, Experimental studies of thin-ply laminated composites, Composites Science and Technology, 67 (2007) 996-1008.

[91] Y. Nishikawa, K. Okubo, T. Fujii and K. Kawabe, Fatigue crack constraint in plain-woven CFRP using newly-developed spread tows, International Journal of Fatigue, 28 (2006) 1248-1253.

[92] T. Yokozeki, Y. Aoki, T. Ogasawara, Experimental characterization of strength and damage resistance properties of thin-ply carbon fiber/toughened epoxy laminates**,** Composite Structures, 82 (2008) 382-389.

[93] M. Kanesaki, H. Saito, M. Tanaka, M. Hojo and I. Kimpara, Improvement of CAI strength and its mechanisms on FFRTP laminate with thinning in ply-thickness, Journal of the Japan Society for Composite Materials, 39 (2013) 89-98.

[94] H. Takiuchi, H. Saito and I. Kimpara, Investigation of crack suppression mechanism of thin ply CFRP cross-ply laminate by cohesive element method, Journal of the Japan Society for Composite Materials, 38 (2012) 30-37.

[95] H. Saito, H. Takiuchi and I. Kimpara, Experimental evaluation of the damage growth restraining in 90° layer of thin-ply CFRP cross-ply laminates, Advanced composite materials, 21 (2012) 57-66.

[96] S. U. Khan and J. Kim, Impact and delamination failure of multiscale carbon nanotube-fiber reinforced polymer composites: a review, International Journal of Aeronautical and Space Science, 12 (2011) 115-133.

[97] F. Hussain, M. Hojjati, M. Okamoto and R. E. Gorga Review article: Polymer-matrix Nanocomposites, Processing, Manufacturing, and Application: An Overview, Journal of Composite Materials, 40 (2006) 1511-1575.

[98] D.R. Paul and L.M. Robeson, Polymer nanotechnology: Nanocomposites, Polymer 49 (2008) 3187-3204.

[99] C. Velasco-santos, A. L. Martinez-hernandez and V. M. Castano, Carbon nanotube-polymer nanocomposites: The role of interfaces, Composite Interfaces, 11(2005) 567-586.

[100] D.P.N. Vlasveld, W. Daud, H.E.N. Bersee, S.J. Picken, Continuous fibre composites with a nanocomposite matrix: Improvement of flexural and compressive strength at elevated temperatures, Composites Part A: Applied Science and Manufacturing, 38 (2007) 730-738.

[101] J.R. Lager and R.R. June, Compressive strength of boron–epoxy composites, Journal of Composite Materials, 3 (1969) 48-56.

[102] K.H. Lo, E.S.M. Chim, Compressive Strength of Unidirectional Composites, Journal of Reinforced Plastics and Composites, 11(1992) 838-896.

[103] C. R. Schultheisz, A. M. Waas, Compressive failure of composites, part I: Testing and micromechanical theories, Progress in Aerospace Sciences, 32 (1996), 1-42.

[104] A. M. Waas, C. R. Schultheisz Compressive failure of composites, part II: Experimental studies, Progress in Aerospace Sciences, 32(1996) 43-78.

[105] J-Z. Liang, Li Rky, Mechanical properties and morphology of glass bead filled polypropylene composites, Polymer composites, 19 (1998) 698-703.

[106] J-Z. Liang, Li Rky, SC. Tjong, Tensile properties and morphology of PP/EPDM/glass bead ternary composites, Polymer composites, 20 (1999) 413-422.

[107] J-Z. Liang, Predictions of Young's modulus of short inorganic fiber reinforced polymer composites, Composites part B: Engineering, 43 (2012) 1763-1766.

CHAPTER TWO

# Molding of PBO Fabric Reinforced Thermoplastic Composite to Achieve High Fiber Volume Fraction

# Chapter 2: Molding of PBO Fabric Reinforced Thermoplastic Composite to Achieve High Fiber Volume Fraction

## 2.1 Introduction

Fiber-reinforced composites are used as high-performance structural materials in fields such as the aerospace and automotive industries because they have higher specific strengths and stiffnesses than metallic materials. These materials are fiber-reinforced thermosetting plastics (FRPs) or fiber-reinforced thermoplastics (FRTPs), depending on the polymer used as the matrix. The advantages of FRTP composites over FRP composites include superior toughness and greater recyclability, and the possibility of a rapid processing cycle that does not involve a chemical reaction [1]. A unique property of thermoplastic composites is their thermoformability. A fibre reinforced thermoplastic sheet is formable into a two- or three-dimensional product by heating it to a temperature well above its glass transition temperature and by applying pressure. This property makes it possible to achieve a relatively low cycle time for the production of thermoplastic composite parts. The cycle time is determined by the time necessary for the heating, (de)forming and cooling of the composite material. The thermoforming techniques are distinguished by their different forming devices [2]. Commonly used molding methods for FRTP composites are injection and compression molding, in which discontinuous fibers are dispersed in thermoplastic matrices as reinforcement; the enhancement therefore cannot be compared with that using continuous fibers. Thermoplastic composites reinforced with continuous fibers are expected to have

superior mechanical properties.

The main problem in using thermoplastic matrices for composites is the difficulty in impregnating the fibrous reinforcing materials with the resins, which have higher viscosities (500 to 5000 Pa s) than thermosetting resins (typically less than 100 Pa s) [3, 4]. A high melt viscosity requires a significantly high processing temperature and pressure during fabrication. Thermoplastic matrices usually have very high melting or softening temperatures that are close to their decomposition temperatures; it is therefore not possible to reduce the viscosity by raising the processing temperature. This major drawback of thermoplastic composites limits their extensive use. Over the years, various methods have been developed in efforts to improve the impregnation of reinforcing fibers with thermoplastic matrices [5, 6]; these include the following methods. (1) Film-stacking method: the matrix film and reinforcing fabrics are alternately arranged and hot pressed to achieve impregnation. This method is suitable for matrices with low viscosities at the melting temperatures. (2) Plied-matrix method: the matrix fiber yarn is wound around a reinforcing fiber yarn. (3) Powder method: a matrix powder is combined with reinforcing fibers; also, a matrix film can be used to encapsulate exterior fiber yarns. One problem with this method is in handling the constituent materials, since the matrix powder can be easily dislodged from the reinforcing filaments. (4) Co-woven method: the matrix fiber yarn and the reinforcing fiber yarn are combined in a woven preform which possesses good drape ability. The warp direction of the fabric contains all of the reinforcing fiber yarns, whereas the weft direction contains all of the matrix yarns. (5) Commingled yarn method: the reinforcing and matrix fibers are evenly mixed in one yarn. Good impregnation of the matrix in the fibers and a homogenous distribution of the reinforcing fiber can be expected, since the matrix fibers and

reinforcing fibers are intimately mixed altogether. These methods attempt to mix the matrix and reinforcing material to reduce the impregnation length, which is the distance that the matrix resin must flow in order to complete the impregnation process to the required level under appropriate heat and pressure [7]. In addition, efforts have been made to reduce the viscosity of the matrix during impregnation. For example, in Nakamura's paper [8] the reinforcing fabric was first impregnated with a low-viscosity matrix monomer, and then the matrix monomer was polymerized in situ to form polymer macromolecules. In this process, it is easy to get good impregnation, but hard to achieve 100% polymerization, and the method is limited to matrices that can be polymerized in situ. Another fruitful variant of the in-situ polymerization approach is to use a low-molecular-weight thermoplastic polymer for impregnation and increase the molecular weight by chain extension after impregnation [9]. Other examples of impregnation using low-viscosity polymer matrices involve the use of a solvent or plasticizer [10, 11]. In these methods, the most important aspect is that the solvent must be removed from the manufactured composite after impregnation.

Most of the methods mentioned above work at the fiber bundle level, and both the mixing and low-viscosity methods have beneficial effects on the impregnation process. However, warp and weft yarns have interweaving points in the produced reinforcement fabric, which doubles the impregnation length compared to that of a fiber bundle. According to the law of mixture, the mechanical properties of the final composite are greatly influenced by the fiber volume fraction [12]. A high fiber volume fraction is important in transferring the properties of the reinforcing material to the composite. It is therefore necessary to improve the fiber volume fraction as much as possible; under ideal conditions, most of the composite is occupied by fibers, and the rest is matrix

which expected to form good adhesion among the fibers. It is therefore considered that impregnation at low viscosity is preferable in manufacturing fiber-reinforced thermoplastic composites.

To achieve better impregnation and a higher fiber volume fraction, this study proposed a new vacuum-assisted solution impregnation prepreg thermoplastic composite molding method. Tensile testing of the final composite confirmed the feasibility of this method. In this method, poly(*p*-phenylenebenzobisoxazole) (PBO) fabric with a plain weave was used as the reinforcing material. To improve the bonding strength between the reinforcing fibers and the thermoplastic matrix, corona discharge surface treatment was first applied; then the treated fabric was impregnated with a thermoplastic solution under vacuum. After volatilization of the solvent, a thermoplastic prepreg was obtained. The laminated prepreg sheets were hot pressed for manufacture into a fiber-reinforced thermoplastic composite. The fiber volume fraction was calculated, and the tensile properties were investigated and compared with those of thermosetting composites reinforced with the same fiber.

## 2.2 Experimental

### 2.2.1 Materials

Fibers of PBO, a rigid-rod isotropic crystalline polymer material, are high-performance polymeric fibers that have many excellent properties (e.g., a high Young modulus, superior tensile strength, and excellent thermal resistance) [13–15] compared with those of traditional polymeric materials. PBO fibers can be used to

reinforce advanced composites and have many potential applications in the aeronautical and space industries, the military industry, general industry, and other advanced fields [16]. The PBO fabric used for reinforcement in this study was Zylon® High Modulus (HM), supplied by the Toyobo Co., Ltd. It has a tensile strength of 5.8 GPa and a modulus of 270 GPa. Also the carbon fiber (Torayca® CO6343 woven fabrics) purchased from Toray Industries, Inc. was used as reinforcement.

The thermoplastic matrix used in this study was crystalline co-polyester obtained from Toyobo Co., Ltd. It has a glass-transition temperature of 78 °C, no established melting point, but a softening point at 185 °C, and a melt viscosity of 7000 dPa s at 250 °C.

*N*-methyl-2-pyrrolidone (NMP), obtained from the Kanto Chemical Co., Inc., served as the solvent for preparing the solution of the thermoplastic matrix.

### 2.2.2 Composite Manufacturing

In order to achieve better impregnation, the crystalline co-polyester resin was dissolved in NMP using a hot-plate magnetic stirrer (Coring PC-420D) at different weight percentages (15, 20, 25, and 30 wt%) at 100 °C. The viscosity of the solution was measured using viscosity-measuring equipment (Brookfield Viscometer DV-I Prime), based on JIS K 7117-1 (plastic resins in the liquid state or as emulsions or dispersions; determination of apparent viscosity by the Brookfield Test Method) and compared with that of an epoxy resin.

PBO fabric is produced for clothing applications and has a chemically inert smooth surface and few oxygen-containing functional groups. The performance of a composite

depends largely on the interfacial adhesion between the matrix and the reinforcement, which determines how stress is transferred from the polymer to the reinforcing fiber. It is therefore necessary to improve the adhesion properties using a fiber surface treatment [17–19]. In this work, a corona discharge (Corona Master PS-1M, Shinko Electric & Instrumentation Co., Ltd.) surface treatment was used as a chemical reactor to add polar bonds and hydrogen bonds to the fiber surface; the bonds most frequently encountered are C–O, C=O, C–O–O·, and C–OOH [20]. These bonds are promising for increasing the bonding strength between the PBO fibers and the thermoplastic matrix.

Next, the hand layup method was used for pre-impregnation of the reinforcing fabric with the matrix solution, which has a much lower viscosity than the melted resin. After hand layup pre-impregnation, the fabric was placed in a vacuum oven, and the temperature was increased from ambient temperature to 200 °C under vacuum over 2 h. During this process, the vacuum helped to achieve better impregnation and complete volatilization of the solvent NMP. The prepreg was obtained after returning to room temperature and atmospheric pressure, during which the thermoplastic resin froze to a rigid state.

During prepreg manufacture, to verify that the solvent was completely removed, the weight of the reinforcing fabric ($w_F$) and the weights before and after solvent evaporation ($w_b$ and $w_a$, respectively) were measured. Then equation (2.1) was used to calculate the weight percentage (wt%) of the solution used in the experiment. By comparing the result with the weight percentage of a prepared solution, it could be determined whether or not the solvent was completely removed.

$$\text{wt\%} = \frac{w_a - w_F}{w_b - w_F} \times 100\% \qquad \text{Eq. (2.1)}$$

The prepreg sheet was then hot pressed (table-type test press, SA-302, Tester Sangyo

Co., Ltd.) at 200 °C and 0.26 MPa to tidy the surface and squeeze out excess resin before the next manufacturing step. This step is helpful for improving the fiber volume fraction in the final composite product. Figure 2.1 shows the manufacturing procedure described above.

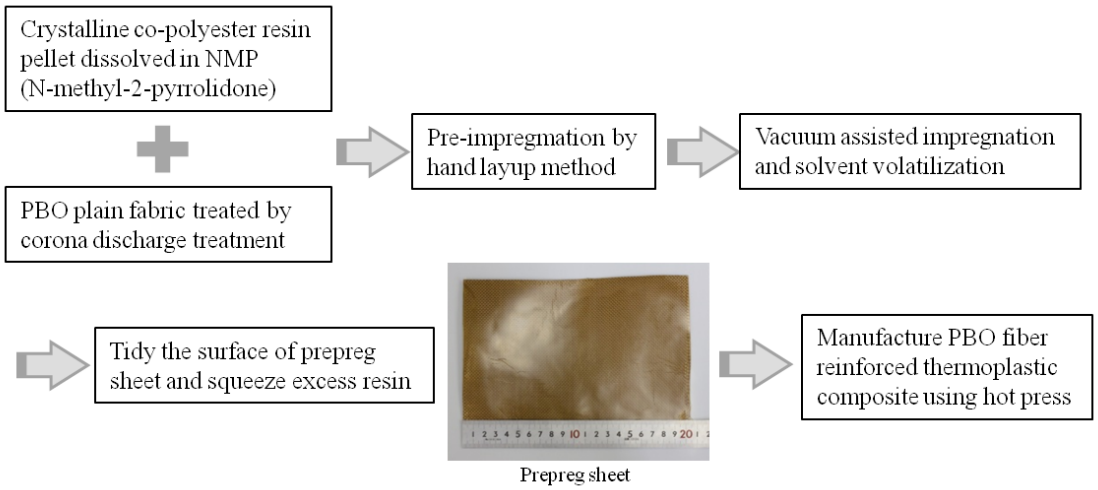


Fig. 2.1. Manufacturing procedure.

In the composite manufacture, the prepreg sheets were laminated in metallic molds (Figure 2.2) with different thicknesses, and hot pressed at 8.70 MPa and 200 °C with a pressure residence time of 30 min. After process cycling, test samples with different fiber volume fractions were prepared. An epoxy resin (epoxy resin XNR 6815, harder XNH 6815, Nagase ChemteX Corporation) reinforced with the PBO fabric subjected to corona discharge treatment was produced using the hand layup method for comparison of the tensile properties.

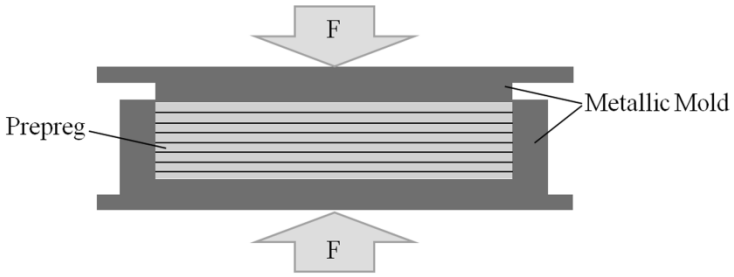


Fig. 2.2. Diagram of metallic mold used in the hot-pressing process.

### 2.2.3 Bonding Tests and Tensile Tests

In the bonding tests, the prepreg was arranged according to the diagram in Figure 2.3. After hot pressing for 30 min at a pressure of 6.97 MPa, a bonding test was performed using a Shimadzu Autograph at a drawing velocity of 10 mm/min. The average bonding strength was calculated from at least five specimens. The bonding strength of a PBO-fiber-reinforced epoxy resin was also investigated for comparison.

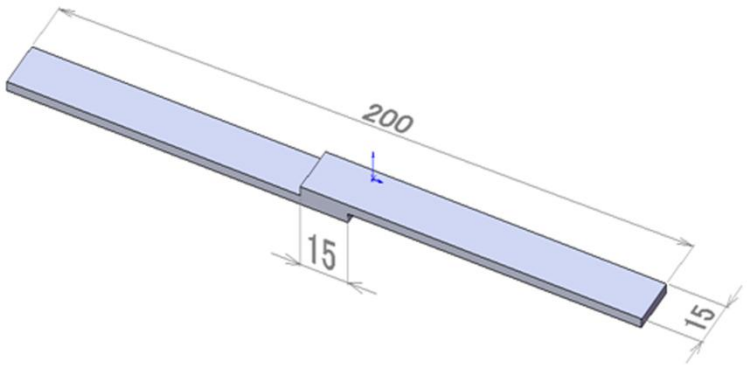


Fig. 2.3. Diagram of bonding test sample.

Samples were cut from the fiber-reinforced composites and tensile experiments were performed using a Shimadzu Autograph, based on JIS K 7054 (testing method for

tensile properties of glass-fiber-reinforced plastic). The size of the test sample is shown in Figure 2.4, and the drawing velocity was 1 mm/min. In order to obtain the actual tensile modulus, two strain gages (KFG-5-120-C1-11L1M2R, Kyowa Electronic Instruments Co., Ltd.) were longitudinally bonded at the center of both sides of each test specimen. An average was taken from at least five specimens of each sample.

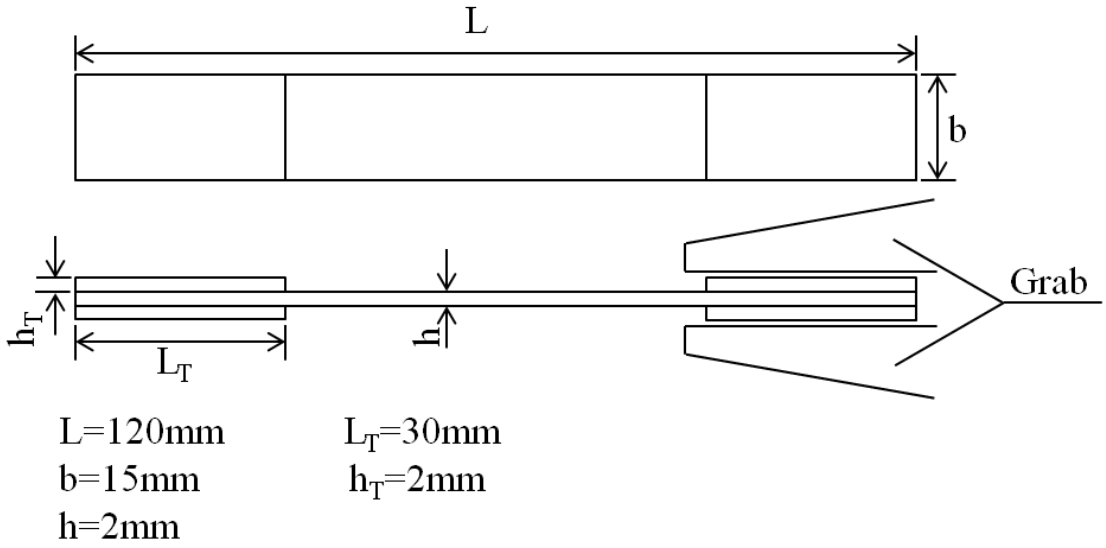


Fig. 2.4. Diagram of tensile test sample.

## 2.3 Results and discussion

### 2.3.1 Bonding Properties

To determine the influence of the corona discharge treatment on bonding, fabrics with different treatment times (fabric length of 20 cm be treated for 0, 5, 10, 15, and 20 s, respectively) under the same discharge voltage were impregnated using the same matrix solution (matrix mass fraction in the solution was 25%) and used as bonding test

samples. The bonding experiment results are presented in Figure 2.5. The graph shows that the bonding strength changed with treatment time; the maximum bonding strength was for a treatment time of 10 s, so the treatment time was set at 10 s as this gave the best treatment effect, according to the experimental results.

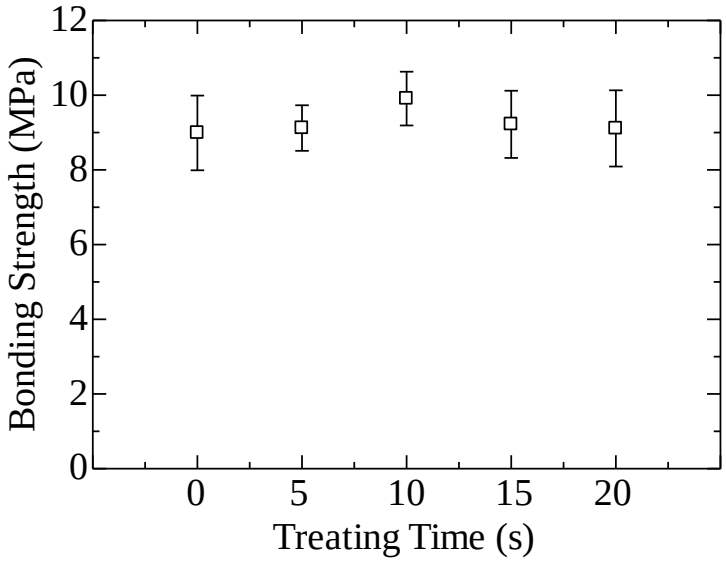


Fig. 2.5. Influence of corona discharge treatment time on bonding strength.

The bonding strengths of fabrics with the same treatment time (10 s) impregnated with different matrices, thermoplastic solutions (matrix mass fraction 15%, 20%, 25%, and 30%) and epoxy resin were studied to determine the influence of the matrix mass fraction on bonding. The results are presented in Figure 2.6. Vacuum assistance in the prepreg manufacture when the resin mass fraction was 30 wt% increased the bonding strength by 35%. This result indicated that vacuum-assisted manufacture is an effective method of producing FRTP composites. Vacuum assistance facilitated both impregnation and solvent volatilization. The void remaining in the fabric after hand

layup pre-impregnation was eliminated by the pressure difference, and was filled by the matrix. In addition, the solvent was gasified during the temperature increase from ambient temperature to 200 °C, and the gaseous solvent was immediately removed from the fabric laminations without leaving voids.

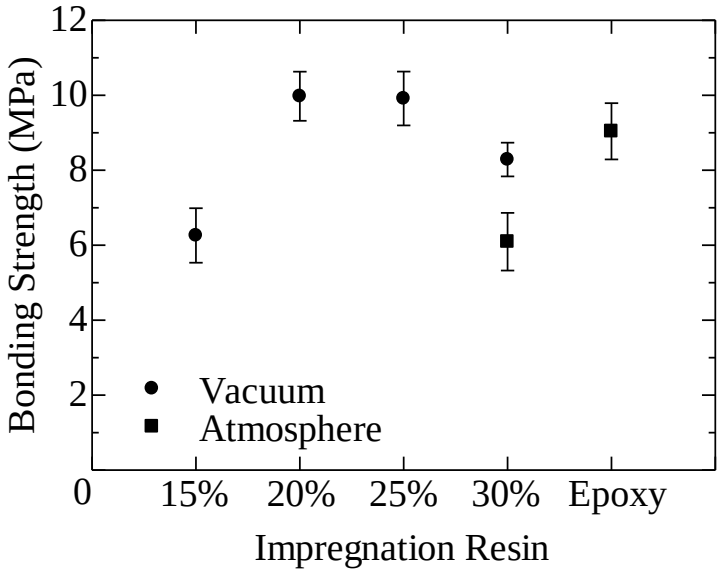


Fig. 2.6. Influence of resin on bonding strength.

Table 2.1 shows the weights measured during prepreg manufacture and the calculated solution weight percentage; these confirmed that there was no residual solvent left in the prepreg. It is therefore unnecessary to worry about the negative impact of residual solvent on the final composite properties.

Table 2.1. Calculated solution weight percent when the prepared solution weight percent is 25%.

| | $w_F$ (g) | $w_a$ (g) | $w_b$ (g) | wt% |
|---|---|---|---|---|
| 1 | 137 | 151 | 192 | 25.45% |
| 2 | 139 | 151 | 187 | 25.00% |
| 3 | 138 | 151 | 189 | 25.49% |

In terms of the influence of the resin mass fraction, the best bondings were observed at 20 wt% and 25 wt%, similar to that of the epoxy resin. As indicated by the viscosity curve of the matrix in Figure 2.7, these solutions (20 wt% and 25 wt%) had viscosities similar to that of the epoxy resin, and an appropriate amount of matrix, which is helpful in achieving perfect impregnation. When the mass fraction was 15 wt%, impregnation was easy. However, there was not enough matrix, leaving voids between fiber laminations and causing weak bonding among them, so this sample had the worst bonding. When the mass fraction was 30 wt%, the viscosity was higher than that when the mass fraction was 15, 20, or 25 wt%. However, impregnation was not as good as at it was at 20 and 25 wt%; thus, the bonding strength was low even when the amount of resin was the highest. In the matrix solution, the solution viscosity and amount of resin are opposing parameters, both of which strongly affect the final product. In this study, the bonding test results indicate that the mass fraction equilibrium points are at 20 and 25 wt%. For the tensile tests, a prepreg produced using a 25 wt% matrix solution for impregnating the PBO fabric was prepared to make a composite plate.

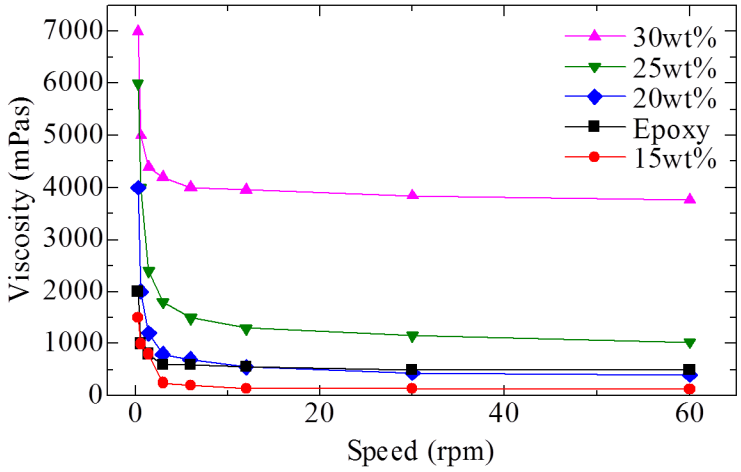


Fig. 2.7. Matrix viscosity curves.

### 2.3.2 Tensile Properties

The fiber volume fraction is calculated on the assumption that the fibrous reinforcements are arranged cheek by jowl in the composite, as shown in figure 2.8. The area of foursquare A is $(2+\sqrt{3})d^2$, the area occupied by circular fibrous reinforcement is $\pi d^2$, when the fiber is covered with $\Delta d$ matrix the composite area A' is $(2+\sqrt{3})(d+\Delta d)^2$. The fiber volume fraction can be calculated according to the equation (2.2):

$$V_f = \frac{A \cdot L}{A' \cdot L} = \frac{\pi d^2}{(2+\sqrt{3})(d+\Delta d)^2} \qquad \text{Eq.(2.2)}$$

where $V_f$ is fiber volume fraction, L is the length of the composite. If the matrix covered on the fiber is 0.1d the fiber volume fraction reduces to 69.53%. The matrix in composite serves to protect, align and stabilize the fibers as well as assure stress transfer from one fiber to another, the function of the matrix is critical. Improving fiber volume fraction by reducing the amount of matrix must fulfill the prerequisite of ensuring the matrix function.

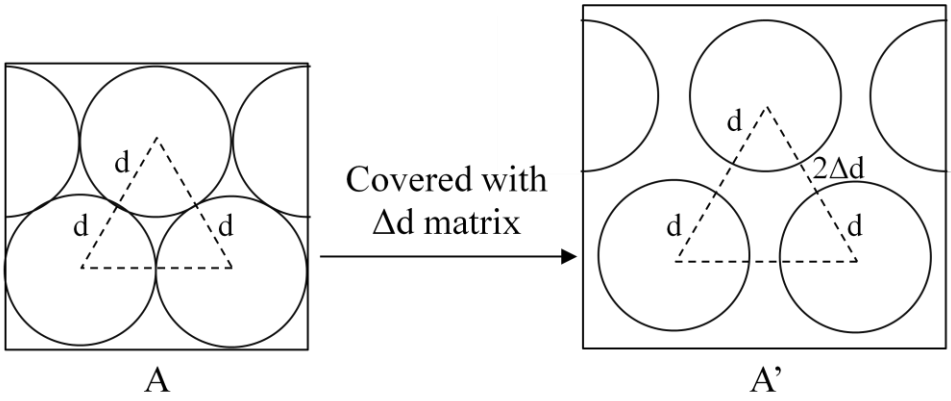


Fig. 2.8. Illustration of calculating fiber volume fraction.

An ion milling system is used to cut the PBO fiber reinforced composite, and the cross section was observed using Hitachi SEM equipment, the SEM images are presented in figure 2.9. The fibers are well dispersed in the matrix without obvious void in the composite. With the increasing in fiber volume fraction, the fiber is pressed close to each other; in 65.24%, fibers don’t remain in circular. It is apprehensive for the changing in the composite mechanical property, so the tensile test was performed to confirm the relationship between fiber volume fraction and mechanical property.

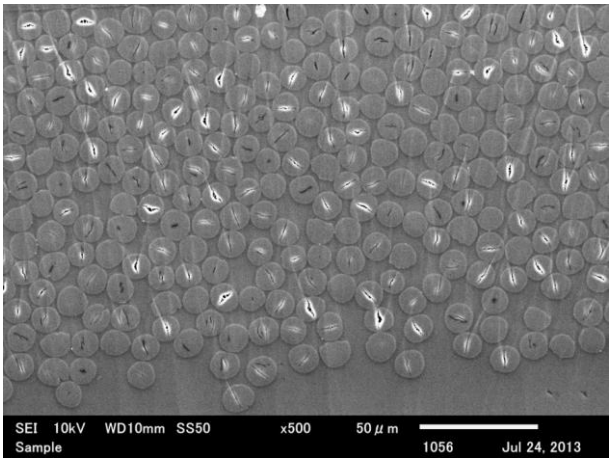

(a)

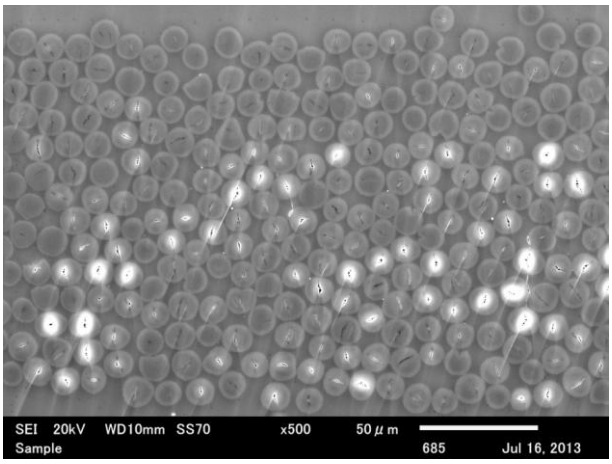


(b)

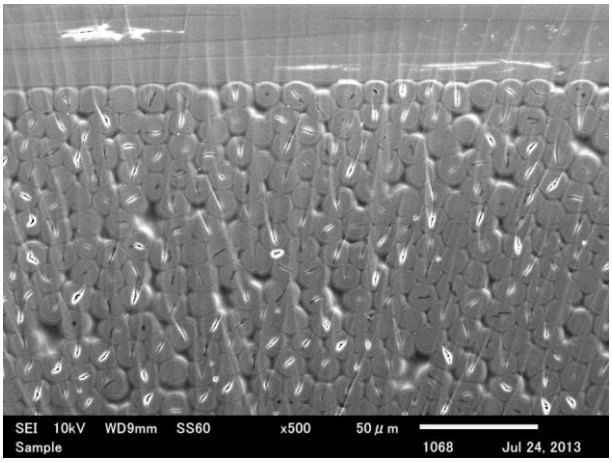


(c)

Fig. 2.9. SEM images with different fiber volume fractions (a) 53.61%, (b) 56.12%, (c) 65.24%.

Figure 2.10 shows a representative tensile stress–strain curve for a PBO-reinforced thermoplastic composite with a fiber volume fraction of 61%. The sample broke at the point marked "×", and the tensile strength was taken from this point. The gradient of the dashed line in the graph is considered to be the tensile modulus of the test sample. Figure 2.11 indicates the average tensile strength, and Figure 2.12 indicates the tensile

modulus.

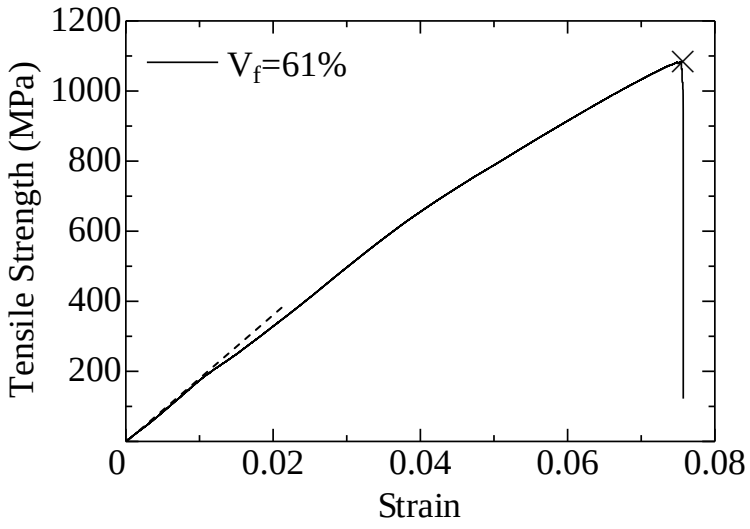


Fig. 2.10. Representative tensile stress–strain curve of PBO-reinforced thermoplastic composite.

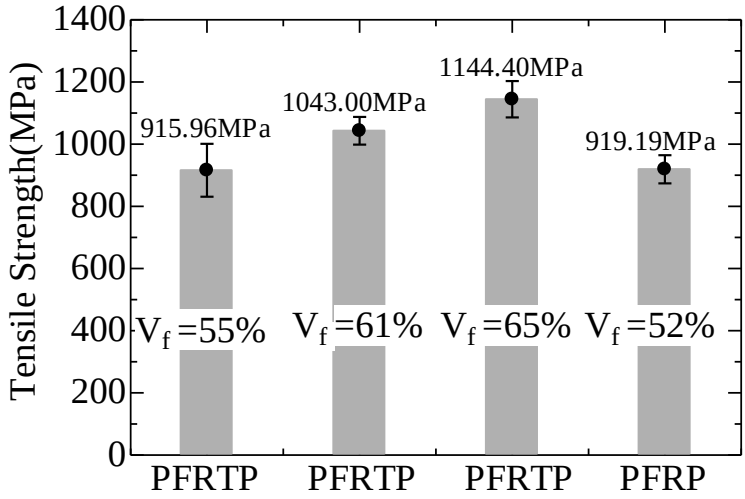


Fig. 2.11. Tensile strength comparison.

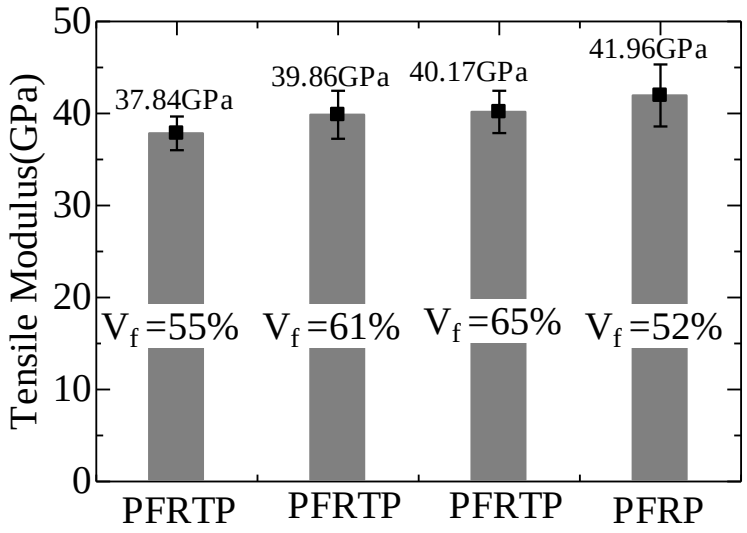


Fig. 2.12. Tensile modulus comparison.

In PBO-FRTP (PFRTP), both the tensile strength and the tensile modulus improved with increasing fiber volume fraction. In PBO-FRP (PFRP), the fiber volume fraction was slightly lower than that of PFRTP; this depends on the manufacturing conditions. The calculated tensile strengths of PFRTP and PFRP are similar, and PFRP has a higher tensile modulus than PFRTP if the fiber volume fractions are the same.

The investigation of the tensile properties of PFRTP and PFRP indicated that they had similar tensile properties. Molding using thermoplastic resin solutions and vacuum-assisted impregnation is therefore suitable for the manufacture of thermoplastic composites.

In the primary experiment, film-stacking was also used to produce the prepreg, and after hot pressing into a composite under the same conditions as those used for the solution impregnation prepreg, the fiber volume fraction was less than 49%, lower than that achieved using the solution impregnation method, which indicated that solution impregnation was better than film-stacking.

By employing the same vacuum assistant solution impregnation method carbon fabric reinforced thermoplastic composite was manufactured, and the tensile properties are evaluated on the Autograph testing machine. The highest fiber volume fraction achieved is 65%. The tensile properties improved with the increasing fiber volume fraction. Similar tensile properties as CFRP were achieved in CFRTP when the fiber volume fraction is similar (shown in figure 2.13).

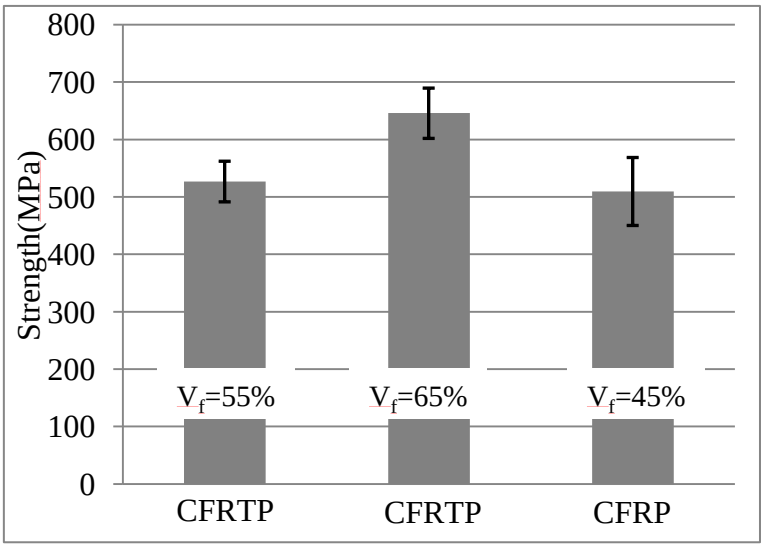


(a)

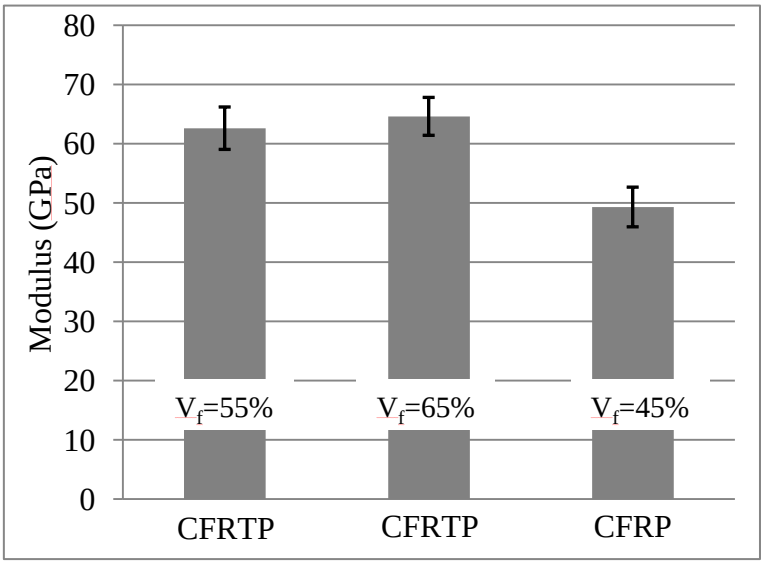

(b)

Fig. 2.13. Tensile properties comparison between CFRTP and CFRP (a) tensile strength and (b) tensile modulus.

After the tensile test, fracture surface observation was also performed. The photo graphs and SEM image are presented in figure 2.14. Fiber rupture is the main fracture model observed at the fracture surface both in CFRTP and CFRP, rather than delamination. In the SEM image of CFRTP at the fracture surface it is found that the matrix resin gets into the interspaces between the fibers which indicated that the impregnation method proposed in this paper is conducive for good impregnation of thermoplastic in continuous fiber.

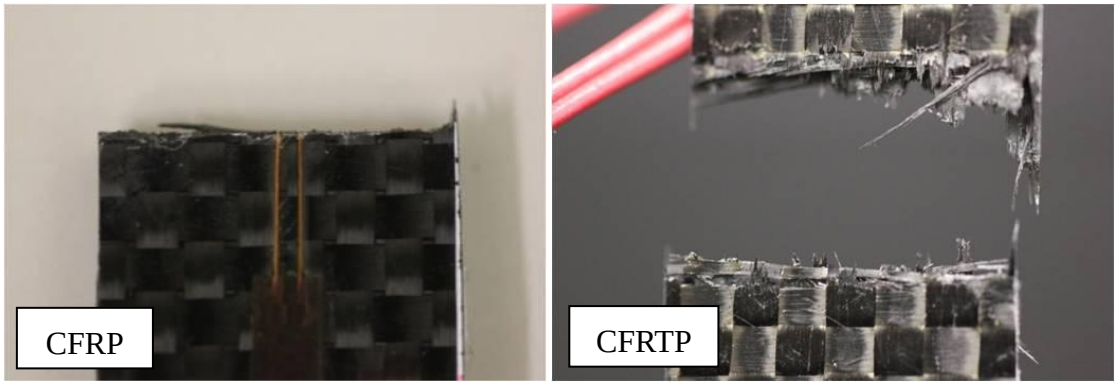


(a)

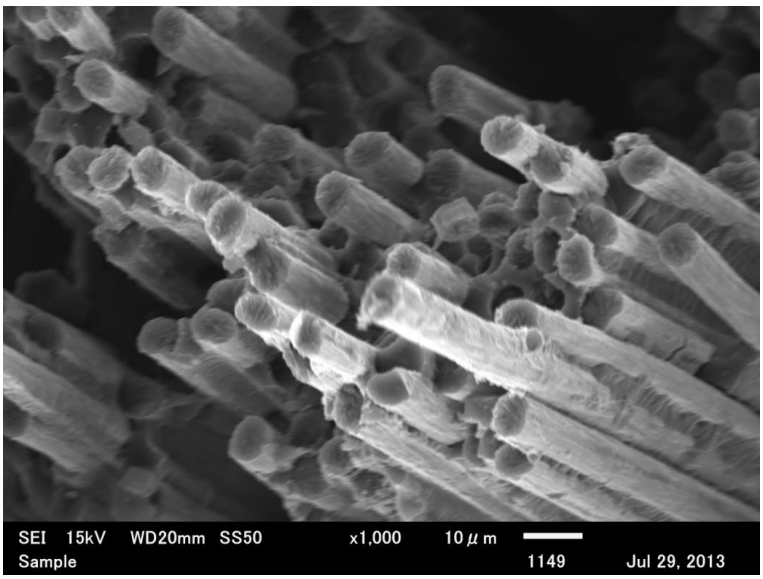


(b)

Fig. 2.14. Observation of the fracture surface (a) photo graph of the fracture surface and (b) SEM observation of CFRTP at fracture surface.

## 2.4 Summary

Vacuum-assisted solution impregnation prepreg thermoplastic composite molding, to improve the fiber volume fractions in FRTP composites, was investigated. After pre-impregnation of the reinforcing fibers with thermoplastic resin solution, a vacuum was employed for further impregnation and solvent volatilization in the prepreg manufacturing process. The treatment time for the fabric and the solution conditions were determined (10 s/20 cm and 25 wt%, respectively) based on bonding tests. Under the determined manufacturing conditions, the fiber volume fraction in the thermoplastic composite material reached 60%, which is similar to those of laboratory-produced fiber-reinforced thermosetting composites. The tensile strength and tensile modulus were improved to levels similar to those of PFRP after the fiber volume fraction of

PFRTP was improved. Tensile tests and comparisons confirmed the effectiveness of vacuum-assisted solution impregnation. The feasibility of the proposed method was confirmed.

Application of the method in manufacturing continuous carbon fiber reinforced thermoplastic indicated that it is promising in the manufacture of other continuous fiber reinforced thermoplastic composites with high fiber volume fraction when the reinforcing materials are in the form of fabric.

**References**

[1] A.H. Miller, N. Dodds, J.M. Hale and A.G. Gibson, High speed pultrusion of thermoplastic matrix composites. Composites Part A: Applied Science and Manufacturing, 29 (1998) 773-782.

[2] H.E.N.Bersee and L.M.J. Robroek, The role of the thermoplastic matrix in forming processes of composite materials, Composite manufacturing, 3 (1991) 217-222.

[3] N. Svensson, R. Shishoo and M. Gilchrist, Manufacture of thermoplastic composites from commingled yarns - a review, Journal of Thermoplastic Composite Materials, 11 (1998) 22-56.

[4] I. Y. CHANG and J. K. LEES, Recent development in thermoplastic composites: a review of matrix systems and processing methods, Journal of Thermoplastic Composite Materials, 1 (1988) 277-296.

[5] Haibin Ning, Uday Vaidya, Gregg M. Janowski, George Husman, Design, manufacture and analysis of a thermoplastic composite frame structure for mass transit. Composite Structures, 80 (2007) 105-116.

[6] K. Fujihara, Zheng-Ming Huang, S. Ramakrishna and H. Hamada, Influence of processing conditions on bending property of continuous carbon fiber reinforced PEEK composites. Composite Science and Technology, 64(2004) 2525-2534.

[7] A.G. Gibson and J.-A. Månson, Impregnation technology for thermoplastic matrix composite. Composites manufacturing, 3 (1992) 223-233.

[8] Koichi Nakamura, Goichi Ben, Norio Hirayama and Hirofumi Nishida, Effect of molding condition on mechanical properties of glass fiber reinforced thermoplastic using in situ polymerizable polyamid6 as the matrix, Journal of the Japan Society for Composite Materials, 37 (2011) 182-189.

[9] M. V. Ward and E. Neield, Method of increasing molecular weight of poly (aryl ethers), US pat 4722980(1988).

[10] K. E. Goodman and A. C. Loos, Thermoplastic prepreg manufacture, Journal of Thermoplastic Composite Materials, 3 (1990) 34-40.

[11] F.N. Cogswell and P. A. Staniland, Method of producing fiber reinforced composition. US pat 4541884 (1985).

[12] A.A. Abdulmajeed, T.O. Närhi, P.K. Vallittu and L. V. Lassila, The effect of high fiber fraction on some mechanical properties of unidirectional glass fiber-reinforced composite. Dental Materials, 27 (2001) 313-321.

[13] S. Bourbigot, X. Flambard and B. Revel, Characterisation of poly( p-phenylenebenzobisoxazole) fibres by solid state NMR, European Polymer Journal, 38 (2002) 1645-1651.

[14] X.D. Hu, S.E. Jenkins, B.G. Min, M.B. Polk and S. Kumar, Rigid-rod polymers: synthesis, processing, simulation, structure, and properties, Macromolecular Material and Engineering, 288 (2003) 823-843.

[15] S. A. Fawaz, A. N. Palazotto and C. S. Wang, Axial tensile and compressive properties of high performance polymeric fibers, Polymer, 33 (1992) 100-105.

[16] L. Yu and X. Cheng, Tensile property of surface- treated poly-*p*-phenylenebenzobisoxazole (PBO) fiber-reinforced thermoplastic polyimide composite, Journal of Thermoplastic Composite Materials, (2011) 1-15, doi:10.1177/089270571 1423290.

[17] J.M. Park, D.S. Kim and S.R. Kim, Improvement of interfacial adhesion and nondestructive damage evaluation for plasma-treated PBO and Kevlar fibers/epoxy composites using micromechanical techniques and surface wettability. Journal of Colloid and Interface Science, 264 (2003) 431-445.

[18] T. Zhang, D. Hu, J. Jin, S. Yang, G. Li and J. Jiang, XPS study of PBO fiber surface modified by incorporation of hydroxyl polar groups in main chains, Applied Surface Science, 256 (2010) 2073-2075.

[19] G.M. Wu, Y.T. Shyng, S.F. Kung and C.F. Wu, Oxygen plasma processing and improved interfacial adhesion in PBO fiber reinforced epoxy composites. Vacuum, 83 (2009) 271-274.

[20] M. Goldman, A. Goldman and R. S. Sigmond, The corona discharge, its properties and specific uses. Pure Appl Chem, 57 (1985) 1353-1362.

CHAPTER THREE

# Deformation behavior of fiber-reinforced plastic composites under a pure bending moment

# Chapter 3: Deformation behavior of fiber-reinforced plastic composites under a pure bending moment

## 3.1 Introduction

Fiber-reinforced plastics (FRPs) encompass composite materials that use fibers to mechanically enhance their strength and elasticity of plastics. FRPs are commonly used in the aerospace, automotive, marine, and construction industries for their high strength, lightweight and good corrosion resistance. FRPs can be shaped into forms that are difficult or impossible using conventional steel materials. This flexibility stems from the virtually limitless combination of ply materials, ply orientations, and ply stacking sequences possible when constructing a laminate material. FRPs can be used to easily construct for light-weight and preassembled shapes of high complexity [1-3]. However, this flexibility of design complicates analyses of composite structures. In particular the anisotropic and inhomogeneous properties of fiber-reinforced composite materials lead to more possible modes of damage and failure that are much more complex than those of conventional materials [4-7]. Hansen et al. [8] used a unique effective stress-strain (S-S) relationship for fiber-reinforced composites to fit experimental results obtained under various loading conditions in fiber-reinforced composites; however, they found this fitting to be difficult. Many efforts have been made to understand the response of polymeric composites undergoing different loadings; researchers have found that these composites generally exhibit highly nonlinear and rate-dependent behaviors in off-axis

directions [9-11]. Researchers consider these nonlinear behaviors of polymeric composites to include plastic deformation, microscopic failure (such as matrix cracking and fiber-matrix debonding), geometric nonlinearity (such as fiber rotation), and other mechanisms [11]. Many theories have been developed to model these nonlinear S-S relationships [9,10,12,13]. Thus, it is important to test and use these formulations to predict the properties of fiber-reinforced polymeric composites and the design implications of those properties.

Polymeric composites are often reinforced using woven fabric instead of pre-impregnated warp sheets for many reasons. First, fabric can be easily handled, allowing for automation and consequent reduction of labor. Second, fibers can conform to complex shapes and have more isotropic in-plate properties than unidirectional materials do. However, distortions of the fiber roving in the fabric can reduce strength and stiffness [14]. One disadvantage of using FRPs is that, unlike metals, reshaping them after their matrix has hardened is very difficult, especially for thermosetting polymers and regardless of the type of reinforcement used. In this paper three kinds of fibers formed into plain woven fabrics were used as reinforcing materials to manufacture polymeric composites then the pure bending and load-unload cycled tests were performed on these composites to investigate their responses.

## 3.2 Material and methods

### 3.2.1 Materials

In this paper, in order to find out the influence of different fibers on the bending property of fiber reinforced plastic composites, three kinds of fibers are used to

reinforce an epoxy resin matrix (epoxy resin XNR 6815, hardener XNH 6815, Nagase ChemteX Corporation) and then explored how those fibers affected the bending properties of the resultant plastic composites. The fibers employed to reinforce the epoxy resin are a glass fabric got from Nitto Boseki Co., Ltd., a carbon fabric (Torayca® woven fabrics) purchased from Toray Industries Inc., and a poly(*p*-phenylenebenzobisoxazole) (PBO) fabric (Zylon® High Modulus (HM)) supplied by the Toyobo Co., Ltd. Each of the fiber sheets had a plain weave [0°/90°]. Unlike glass, glass fiber is a lightweight, extremely strong and robust material after being heated and drawn into fine fibers. Carbon fiber is somewhat stronger and stiffer than glass fiber, but glass fiber is typically far less brittle and the raw materials are much less expensive. Carbon fiber is composed mostly of carbon atoms and has a high strength-to-volume ratio because its crystals are aligned almost parallel to the long axis of the fiber, along which the carbon atoms are bonded together. Many properties of carbon fiber make it very popular in aerospace, civil engineering, military, and motorsports, including its high stiffness, high tensile strength, low weight, high chemical resistance, high temperature tolerance, and low thermal expansion. Fibers of PBO, a rigid-rod isotropic crystalline polymer with molecular chains oriented in the fiber-longitudinal direction, have excellent tensile strength, Young's modulus, and thermal resistance compared with traditional polymeric fibers. PBO fiber is currently the strongest commercially available organic polymeric fiber [15-18]. These fibers can be used to reinforce advanced composites and have many potential applications in the aeronautical, space, and military industries, among others [19].

For the glass fiber fabric with a lower grammage than our chosen carbon fabric and PBO fabric, to ensure the final composites with equal thicknessthe same thickness, the

FRPs with 6-ply glass fabrics, 4-ply carbon fabrics and 4-ply PBO fabrics are manufactured using vacuum-assisted resin transfer molding (VaRTM) respectively. Carbon (2-ply) and PBO (2-ply) interply hybrid FRPs were also manufactured to study how the position of the fabric reinforcement influenced bending properties. In this paper, GFRP refers to glass-fiber–reinforced epoxy, CFRP refers to carbon-fiber–reinforced epoxy, PFRP refers to PBO-fiber–reinforced epoxy, CPFRP refers to hybrid FRP with carbon fabric on the compression side, and PCFRP refers to hybrid FRP with PBO on the compression side. Then the composite plates were cut into rectangular specimens according to the schematic diagram show in Figure 3.1. By adding tabs to the two ends of the specimen, it is protected from clamping damage.

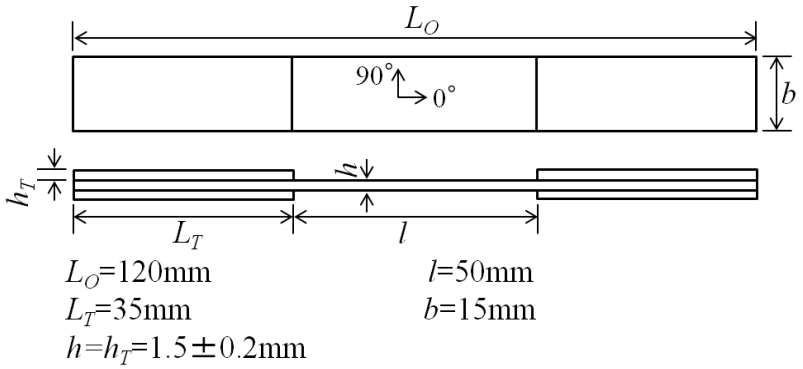


Fig. 3.1. Schematic showing the dimensions of the bending test specimens.

3.2.2 Experimental equipment and method

As shown in Figure 3.2(a) is the schematic of pure bending apparatus, it is assembled on a Shimadzu Autograph test machine when a test is about to perform. Each specimen was clamped at its ends by two clamps. The clamp at point A is attached to an

arm AO, which can swing around the axis through point O, while the position of the center of the clamp at point B is fixed. In addition, the clamps at points A and B can rotate around the center point in response to forces applied by the Autograph test machine in a tensile test mode via a steel wire rope attached to the two wheels at point A and B. The steel wire rope passes through point O to prevent forces other than the bending moment to affect the test specimen. Figure 3.2(b) shows a schematic diagram of a bent specimen. After bending each specimen, the curvature *k* of the specimen can be calculated from the rotation $\delta$ of the clamps and the displacement *x* (*x* is the distance of OA rotated during the bending test which is measured at the midpoint of arm OA). The bending moment (*M*) per unit width applied to the specimen is calculated from the force *F* and lever arm *a*.

$$k = 1/R = \frac{2\delta - \arctan(2x/L)}{l} \quad \text{Eq. (3.1)}$$

where *k* is the curvature of the specimen, *R* is the radius of curvature, $\delta$ is the rotation of the clamp, *L* is the length of both arms OA and OB, and *l* is the distance between the two clamps.

$$M = (F/2)a \quad \text{Eq. (3.2)}$$

where *M* is the bending moment per unit width applied to the specimen, *F*/2 is the force in each steel wire rope, and *a* is the radius of both wheels A and B.

Thus, the bending stress $\sigma$ and strain $\varepsilon$ can be calculate according to the following equations:

$$\sigma = \frac{3Fa}{bh^2} \quad \text{Eq. (3.3)}$$

$$\varepsilon = \frac{hk}{2} = \frac{h[2\delta - \arctan(2x/L)]}{2l} \quad \text{Eq. (3.4)}$$

where *b* and *h* are the width and the thickness of the specimen, respectively.

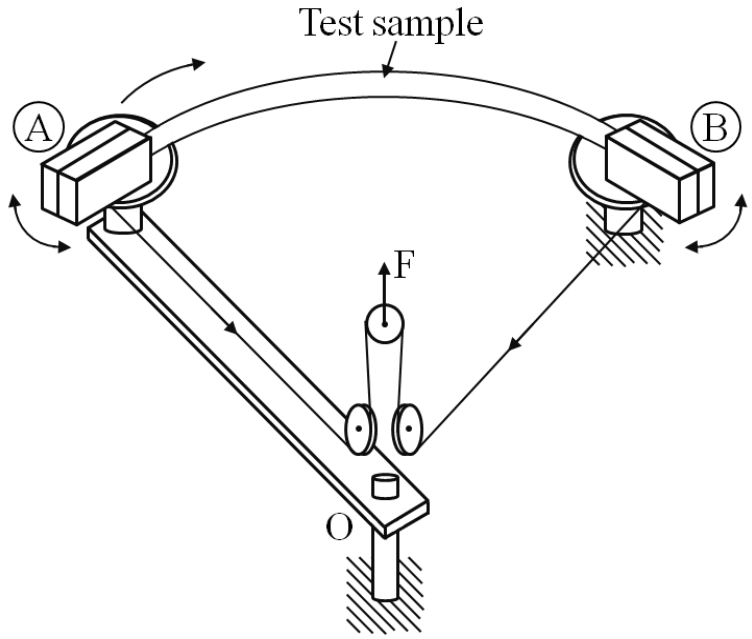


(a)

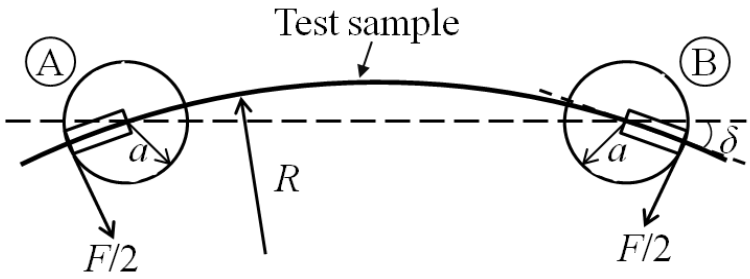


(b)

Fig. 3.2. (a) Schematic of pure bending apparatus; (b) schematic of a bent specimen.

First, a bending moment was applied to each specimen until breakage, from which its load at rupture point can be acquired. Then an equivalent specimen was subjected to a load-unload cycled test according to the conditions in table 3.1. Afterwards, the relationship between stress and strain was investigated for each specimen. All data are averages from at least five equivalent specimens.

Table 3.1 Load-unload cycling test conditions

| | First cycle | | Second cycle | | Third cycle | | Fourth cycle | | Fifth cycle |
|---|---|---|---|---|---|---|---|---|---|
| | Load | Unload | Load | Unload | Load | Unload | Load | Unload | Load |
| Velocity (mm/min) | 20 | 20 | 20 | 20 | 20 | 20 | 20 | 20 | 20 |
| Boundary condition Load (N) | 1/5*F** | 5N | 2/5*F* | 5N | 3/5*F* | 5N | 4/5*F* | 5N | Rupture |

**F* indicates the load at rupture point or maximum load.

### 3.3 Results and discussion

Figure 3 shows the representative S-S curves of CFRP, GFRP, and PFRP. Both CFRP and GFRP broke and have nearly linear S-S relationships. CFRP has a higher Young's modulus than GFRP does, and the strain induced in GFRP is larger than for CFRP, corresponding to the properties of these two fibers. PFRP had a similar modulus to CFRP at a very low stress, but its S-S curve quickly flattens and eventually becomes almost parallel to the coordinate axis. The bending stress for PFRP does not change linearly with strain because the PBO fiber has different properties than the carbon fiber and glass fiber. Although the tensile strength and modulus of the PBO fiber are higher than those of the carbon fiber, it is easy for PFRP to fail on the compression side, leading to a lower strength than CFRP or GFRP [20]. During the bending test, CFRP and GFRP broke into two parts. In contrast, PFRP bent into a circularly deflected shape; after unloading, the PFRP mostly kept its loaded shape. The inset of Figure 3 shows a photo of PFRP after bending.

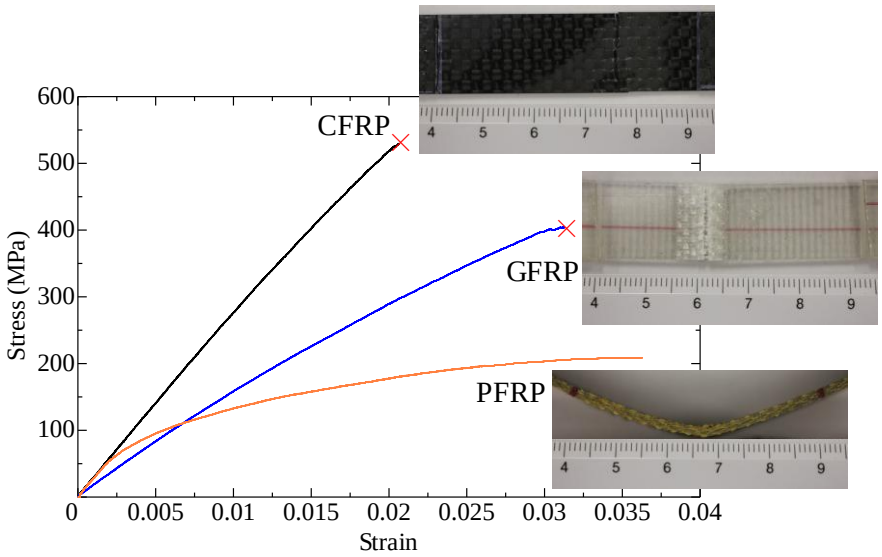


Fig.3.3. Representative S-S curves of CFRP, GFRP, and PFRP after a pure bending test. The × symbol denotes breakage. The inset shows a PFRP specimen after bending.

Figure 3.4(a) shows typical S-S curves for CFRP, GFRP, and PFRP after four cycles of load-unload bending tests. The shapes of these curves are similar to those shown in Figure 3.3. For the CFRP curve, the loading and unloading portions are too close to the continuous main curve to tell apart; in GFRP the loading and unloading parts slightly depart from the main curve, and in PFRP the loading and unloading parts differ obviously. As shown in Figure 3.4(b), for example, when a specimen is bent during the fourth load-unload cycle, a certain stress leads to a corresponding strain; during unloading, the stress decreases and the strain partially reverts. The total strain after the loading process is considered to be composed of recoverable strain which is considered to be reversible elastic strain, and residual strain, which is defined as an irreversible plastic strain. Upon resuming the test after each unloading, the stress gradually rejoins the continuous main curve without any stress overshoot peaks [21]. Figure 3.5 summarizes the total and elastic strains during each cycle, which

demonstrates how the plastic strain depends on the total strain.

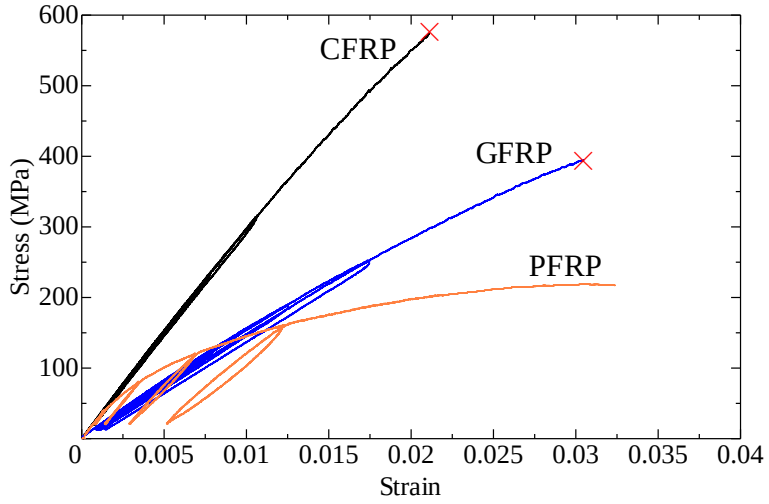


(a)

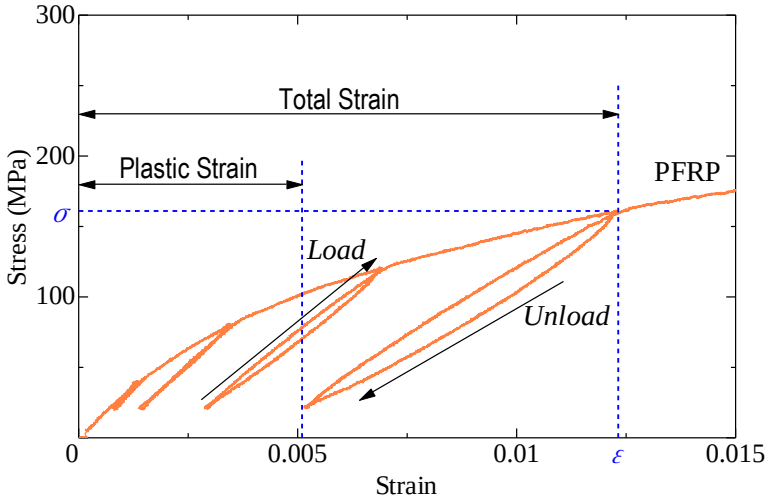


(b)

Fig. 3.4. (a) Representative S-S curves of CFRP, GFRP, and PFRP after cycled pure bending tests; (b) magnification of (a), showing the total strain and elastic strain in one load-unload cycle.

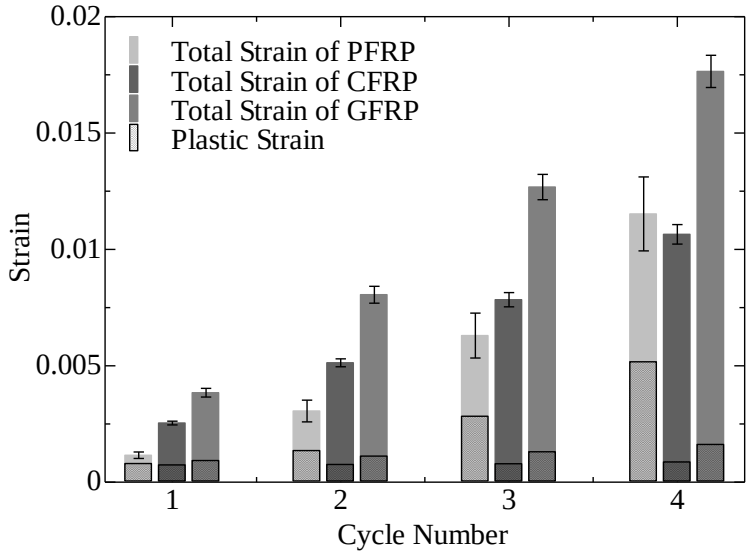


Fig. 3.5. Dependence of plastic strain on total strain during cycled pure bending tests.

As it can be ascertained in Figure 3.5 that the total strain at the boundary condition of each sample increases for each additional cycle, as does the elastic strain. In PFRP about half of the total strain is plastic strain, but in CFRP and GFRP the plastic strain occupies a small portion of the total strain. Without being bent to breakage, CFRP and GFRP recover more readily than PFRP, but PFRP has good plasticity.

As shown in Figure 3.4(b) a cycle performance includes load and unload portions. At the end of the unload portion the specimen was bent once again, going to the next loading portion, the slope of the loading portion, defined as the instantaneous modulus of the loaded material. This parameter is considered to be as important as the material's modulus of elasticity, which can be derived from the initial loading slope. The degradation of the mechanical properties of the loaded material can be characterized by its stiffness loss, which can be calculated by assessing how the elastic modulus changes between load cycles in the S-S curve [2]. Figure 3.6 shows how the modulus varies over many cycles with fit curves. Although the instantaneous modulus of PFRP decreases

remarkably after cycled tests, it is still larger than that of GFRP As mentioned previously, the PFRP has good plasticity after bending and can be highly strained without failing; thus, PFRP meets the requirements for re-processing. The curves fit to the moduli of CFRP and GFRP are almost horizontal because these composites can easily recover their mechanical properties after loading.

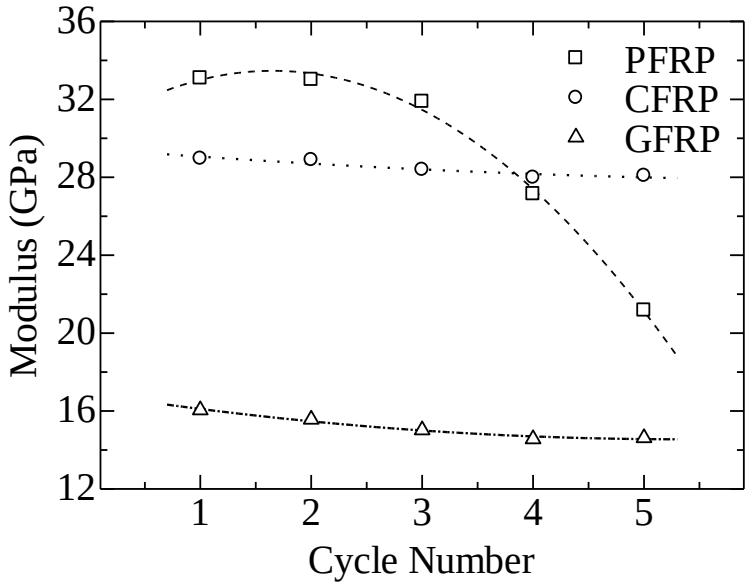


Fig. 3.6. Variation of modulus for the loading portions of each cycle.

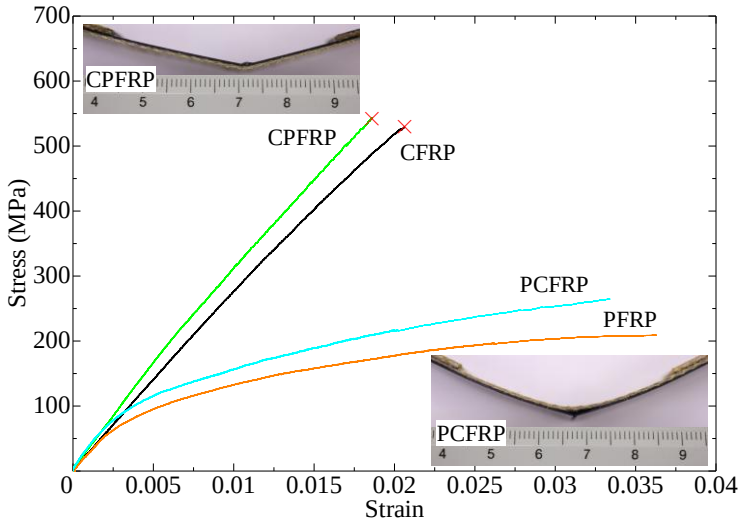


(a)

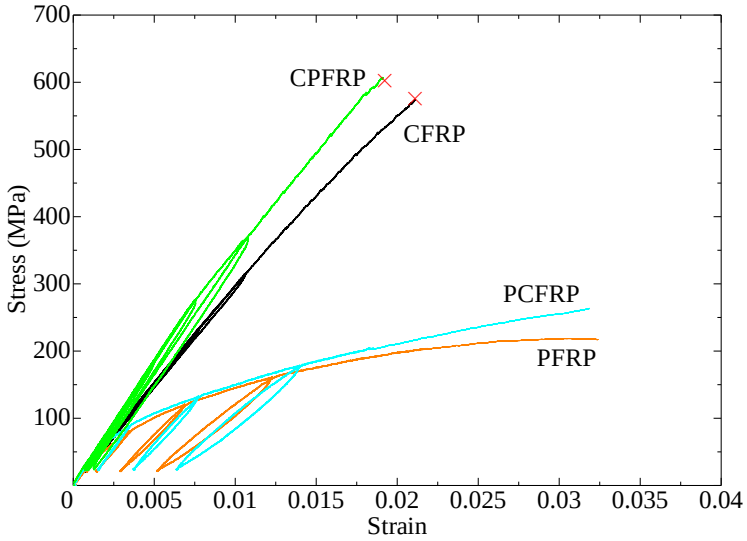


(b)

Fig. 3.7. Representative S-S curves of mono-fiber–reinforced and hybrid-FRP composites after a (a) bending test and a (b) load-unload cycled bending test.

To retain the advantages while minimizing the disadvantages of the composites, the hybridization of carbon and PBO fibers reinforced composite was manufactured [22]. Figure 3.7 shows representative S-S curves of CFRP, PFRP, and hybrid FRP after

bending tests and load-unload cycled bending tests. Two types of hybrid FRPs with different fibers on the compression side were manufactured. Based on the type of fiber placed on the compression side of this composite, one of two categories of S-S curves emerged: CFRP-like with higher strength and lower strain, or PFRP-like with lower stress but higher strain. Figure 3.7(a) shows a photo of CPFRP after a bending test; the specimen failed on the carbon-fiber side and formed an obtuse angle at the failure point. Figure 3.7(a) also shows a PCFRP specimen after a bending test; the specimen also failed on the carbon-fiber side, and delamination occurred between the carbon laminate and PBO laminate and holds a circularly deflected shape after the test, influenced by the presence of PBO fiber. Figure 3.7(b) shows that the areas between the loading and unloading portions for CPFRP are larger than those for CFRP, which can be attributed to the presence of PBO fibers. The curves of PCFRP and PFRP are much like each other; the residual irreversible plastic strain in PCFRP is as large as in PFRP. PBO fiber has a higher tensile strength than carbon fiber, but has a similar modulus and much lower strength in compression. Consequently, when the carbon laminate is on the compression side of the composite, CPFRP has higher strength than CFRP; when the PBO laminate is on the compression side, the composite performs like PFRP because of its lower compression strength. The carbon ultimately ruptures under tensile stress, leading to delamination.

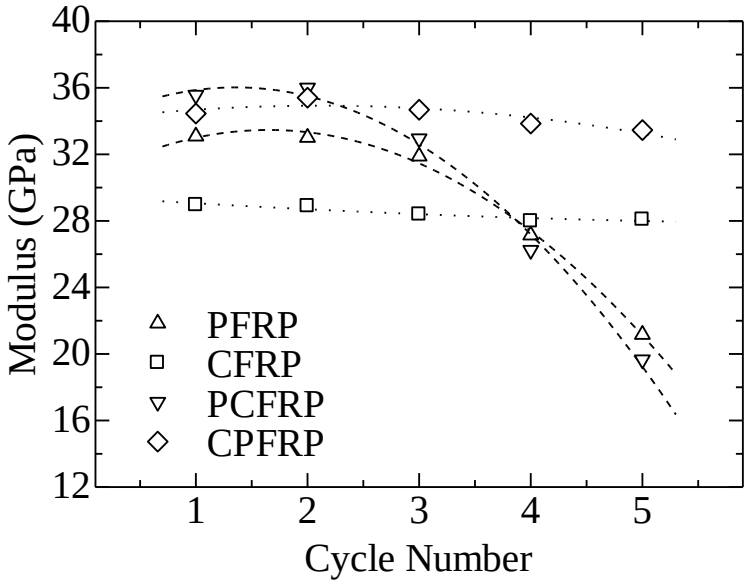


Fig. 3.8. Modulus variation between mono-fiber–reinforced and hybrid-FRP composites.

Figure 3.8 summarizes the slopes of the loading portions of hybrid-fiber– and mono-fiber–reinforced composite S-S curves, as introduced previously. The modulus of the hybrid CPFRP obviously improved, caused by the tensile modulus of the PBO fiber being higher than that of the carbon fiber. However, the modulus of PCFRP slightly improved. The variation of the modulus of CPFRP is like that of CFRP, showing a small linear change. The modulus of PCFRP has a similar trend to PFRP.

### 3.4 Summary

The properties of mono-fiber- and hybrid-fiber-reinforced plastic composites during pure bending moment and load-unload cycled bending tests were investigated. It is found that the failure mode of PFRP is different from those of CFRP and GFRP during pure bending. For hybrid-fiber-reinforced composites, the choice of fiber on the

compression side affects the failure mode of the composite. Load-unload cycled bending tests revealed that PFRP and PCFRP retained more irreversible plastic strain than CFRP, CPFRP, and GFRP did. Investigating the instantaneous modulus of each material revealed two disparate phenomena, one analogous to CFRP (little change) and the other to PFRP (significant decrease, but the residual modulus is still larger than that of GFRP). In further investigation the influence of other properties rather than the low compressive strength of PBO fiber, for example, the bonding behavior of between fiber and matrix, will be put into investigation to clarify the deformation behavior observed in this paper.

**References**

[1] C.W. Dolan and A. Nanni, Status of Fiber-Reinforced Plastic Reinforcement Development and Cement Based Research Needs, Advn Cem Bas Mat, 1 (1994) 185-191.

[2] J.L. Mena-Tun, A. Díaz-Díaz, P.I. Gonzalez-Chi, Non-linear characterization of PP twaron laminates based on a model of plasticity with damage, Composite structures, 93 (2011) 2808-2816.

[3] Z.M. Huang, A unified micromechanical model for the mechanical properties of two constituent composite materials. Part I: elastic behavior. J Thermoplast Compos, 13 (2000) 252-271.

[4] W.P. Lin, H.T. Hu, Parametric study on the failure of fiber reinforced composite laminates under biaxial tensile load. J Comp Mater, 36 (2002) 1481–1503.

[5] C.S. Lee, W. Hwang, H.C. Park, K.S. Han, Fatigue failure model for composite

laminates under multi-axial cyclic loading. Key Eng Mater, 183-187 (2000) 945-950.

[6] U.A. Khashaba, S.S. Behavior of unidirectional GFR/epoxy composites under tension-torsion biaxial loading. Proceedings of the seventh international conference on production engineering, design and control, vol. 3. Egypt: Alexandria University; (2001) 1977-1993.

[7] A.M. El-Assal, U.A. Khashaba, Combined torsional and bending fatigue of unidirectional GFRP composites. Proceedings of the second international conference on mechanical engineering. Adv.Tech for Indus Prod, vol. 1. Egypt: Assiut University; (1999) 206-216.

[8] A.C. Hansen, D.M. Blackketter, D.E. Walrath, An invariant-based flow rule for anisotropic plasticity applied to composite materials. Journal of Applied Mechanics, 58 (1991):881-888.

[9] W. Kim, C.T. Sun, Modeling Relaxation of a Polymeric Composite during Loading and Unloading, Journal of Composite Materials, 36 (2002) 745-755.

[10] C.T. Sun, J.L. Chen, A simple flow rule for characterizing nonlinear behavior of fiber composites. Journal of Composite Materials, 23 (1989) 1009-1020.

[11] T. Yokozeki, S. Ogihara, S. Yoshida, T. Ogasawara, Simple constitutive model for nonlinear response of fiber-reinforced composites with loading-directional dependence, Composites Science and Technology, 67 (2007) 111-118.

[12] J. Fritsch, S. Hiermaier, G. Strobl, Characterizing and modeling the non-linear viscoelastic tensile deformation of a glass fiber reinforced polypropylene, Composites Science and Technology, 69 (2009) 2460-2466.

[13] C.A. Weeks, C.T. Sun, Modeling nonlinear rate-dependent behavior in fiber-reinforced composites, Composites Science and Technology, 58 (1998) 603-611.

[14] P.T. Curtis, S.M. Bishop, An assessment of the potential of woven carbon fibre-reinforced plastics for high performance applications, Composites, 15 (1984) 259-265.

[15] S. Bourbigot, X. Flambard, B. Revel, Characterisation of poly(p-phenylenylenebenzobisox- azole) fibers by solid state NMR, European Polymer Journal, 38 (2002) 1645-1651.

[16] X.D. Hu, S.E. Jenkins, B.G. Min, M.B. Polk, S. Kumar, Rigid-rod polymers: synthesis, processing, simulation, structure, and properties, Macromolecular Material and Engineering, 288 (2003) 823-843.

[17] S.A. Fawaz, A.N. Palazotto, C.S. Wang, Axial tensile and compressive properties of high-performance polymeric fibers, Polymer, 33 (1992) 100-105.

[18] P.J. Walsh, X.B. Hu, P. Cunniff, A.J. Lesser, Environmental Effects on Poly-p-phenylenebenzobisoxazole Fibers. I. Mechanisms of Degradation, Journal of Applied Polymer Science, 102 (2006) 3517–3525.

[19] L. Yu, X. Cheng, Tensile property of surface-treated poly-p-phenylenebenzobisoxazole (PBO) fiber-reinforced thermoplastic polyimide composite, Journal of Thermoplastic Composite Materials, (2011) 1-15, doi:10.1177/089270571 1423290.

[20] Property of unidirectional PBO fiber reinforced composite, http://www.toyobo.co.jp/seihin/kc/pbo/ud.pdf. Accessed 26 May 2013

[21] C. G'sell, J.J. Jonas, Yield and transient effects during the plastic deformation of solid polymers, Journal of Materials Science, 16 (1981) 1956-1974.

[22] G. Kretsis, A review of the tensile, compressive, flexural and shear properties of hybrid fibre-reinforced plastics, Composites, 18 (1987) 13-23.

CHAPTER FOUR

# Influence of aramid spread tow fabric on the mechanical properties of fiber reinforced plastic composite

# Chapter 4: Influence of aramid spread tow fabric on the mechanical properties of fiber reinforced plastic composite

## 4.1 Introduction

The aramid fibers had the highest strength-to-weight ratio comparing to the other when it was firstly introduced to the world in 1970s. With the characteristics of light weight, high strength, and high toughness the aramid fibers have let to the development of applications in composites, ballistics, tires, ropes, cables, asbestosreplacement, and protective apparel. The chemical composition of aramid fiber is poly para-phenyleneterephthalamide also known as PPD-T. This fiber is made from the condensation reaction of paraphenylene diamine and terephthaloyl chloride. The aromatic ring structure contributes high thermal stability, while the para configuration leads to stiff, rigid molecules that contribute high strength and high modulus. The para-aramid fibers are considered to be belonging to a class of materials known as liquid crystalline polymers. Because these polymers are very rigid and rodlike, in solution they can aggregate to form ordered domains in parallel arrays [1]. During the fiber manufacture process, the PPD-T was firstly dissolved in the solvent (concentrated sulfuric acid), then the solution was extruded through a sprinneret and drawn through an air gap, the liquid crystalline domains can orient and align in the axis direction of the manufactured fiber [2-4]. For the long, straight polymer chains align parallel to the fiber axis, confirmed by many researchers [5, 6], made the fiber be anisotropic, which means the strength and modulus in the fiber longitudinal direction is much higher than in the

radial direction, the orientation of the crystalline structure can be further improved when a high-temperature processing under tension was performed on the fiber which result in higher fiber modulus [7].

Spread Tow Fabric (STF) is a type of lightweight fabric. Its production involves the steps of spreading a tow in thin and flat uni-directional tape (Spread Tow Tape, STT), and weaving the tapes to a woven Spread Tow Fabric.[8] This technique increases the mechanical properties of the material and is also used to reduce weight on composites. In the composite reinforced by carbon fiber spread fabrics, the transverse crack and delamination are effectively suppressed because of the reduced laminate thickness, and the CAI properties are improved [9, 10].

In this research with the purpose of manufacturing composites strong and light weight, an aramid spread tow fabric is used to manufacture composites. The bending properties of the mono-fiber composite and hybrid composite reinforced by aramid STF and carbon fabric were investigated as well as the compression and tension properties of composite reinforced by aramid STF. Then the influence of aramid STF on the impact resistance properties of carbon fabric reinforced composite was investigated by the compression after impact (CAI) test method.

## 4.2 Materials and Experiment details

### 4.2.1 Specimens

The reinforcement fibers used in this research including carbon fiber (Torayca® CO6343 woven fabrics) purchased from Toray Industries, Inc., and two kinds of para-aramid fabrics, one is the ordinary fabric made by technnora yarn (Technnora®

manufactured by Teijin), and the other fabric is made by the technnora spread tow with thickness of 0.08mm got from Suncorona Oda co.,ltd. In order to weave the spread tow fabric the tow used in the ordinary fabric was firstly spread into a thin and flat unidirectional tape, and then spread tow fabric can be manufactured on a tape weaving machine. The aramid spread tow fabric was shown in figure 4.1. Laminated fabrics were used to manufacture fiber reinforced plastic composite by vacuum-assisted resin transfer molding (VaRTM). The epoxy resin (epoxy resin DENATITE XNR 6815, hardener DENATITE XNH 6815, Nagase ChemteX Corporation ) is employed as the matrix.

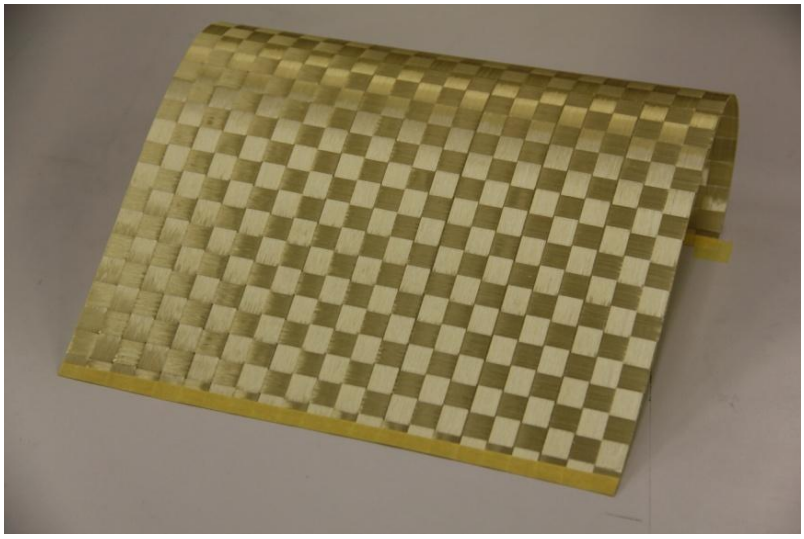

Fig. 4.1. Photo of aramid spread tow fabric.

4.2.2 Pure bending

In traditional bending test methods (like three-point bending and four-point bending) the test sample were with limitative thickness, for the purpose of using the thin aramid spread tow fabric as a reinforcement of composite to produce thin composite

with better mechanical properties, it is not necessary to laminate over 20layers thin fabrics to satisfy the experimental conditions. So the pure bending experiment is employed to test the bending properties of the thin spread tow fabric reinforced epoxy composite. The details of pure bending apparatus have been introduced in Chapter 3. For a comparison the three kinds of fabric reinforced epoxy was manufactured. One is the composite with 9layers aramid spread tow fabric, the second is with 3layers carbon fabric and the third is a hybrid composite with 1layer carbon fabric on compression side and 5layers of aramid spread tow fabric on tension side. The composites were cut into rectangular specimens with dimensions of 110×25×0.85mm. The diagram of the specimen is presented in figure 4.2.

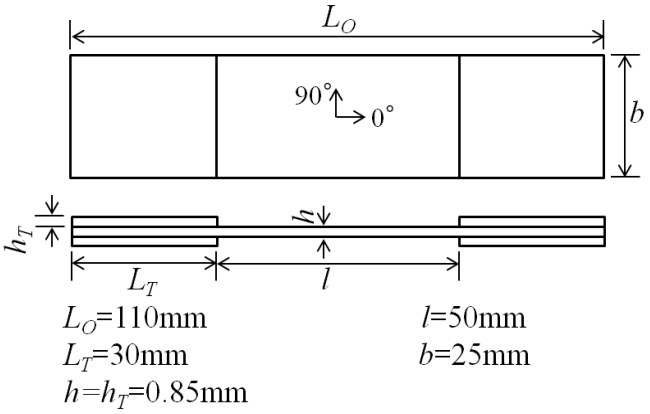


Fig. 4.2. Schematic showing the dimensions of the bending test specimens.

4.2.3 Tension

During the bending test, the specimen undergoes tension tress on one side and compression stress on the other, here the tension property of aramid spread tow fabric reinforced composite was studied. The laminations of the specimens were 6layers

ordinary aramid fabric; 9layers aramid spread tow fabric and 3layers of carbon fabric respectively. The composites were cut into rectangular specimens with dimensions of 2000×15×0.85mm (figure 4.3). Tabs were affixed at the ends of the specimens, avoiding damage from the clamps during tension test. The testing rate was 1mm/min. Also a triaxial strain (Kyowa Electronics, Inc.,) gage was glued in the center of the specimens.

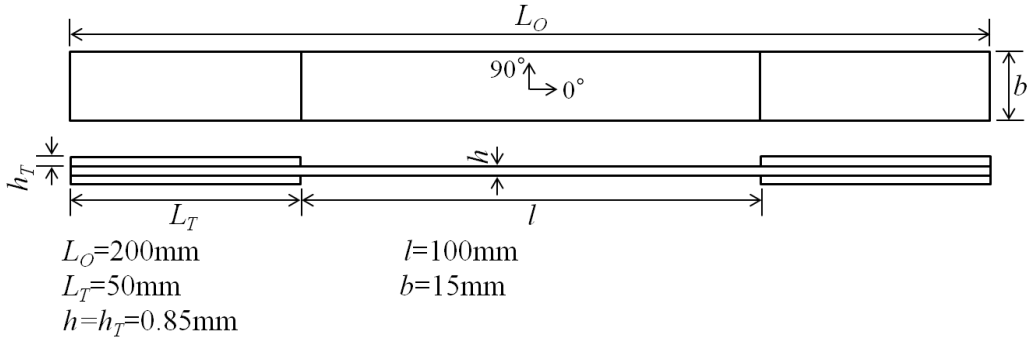


Fig. 4.3. Diagram of dimensions of tension test specimens.

4.2.4 Compression

During the compression test, the top and bottom edges of the specimens should be paralleled with each other and perpendicular to the loading axis as far as possible, because the compression results are very sensitive to the angle between the fiber orientation and loading direction. After being cut, the specimens were polished at the top and the bottom edges, and then the specimens were clamped in a specially made holding device, the compression test is performed on the autograph test machine, shown in figure 4.4. According to JIS K7161, two groups of specimens made of 8layers carbon fabric and 24layers aramid spread tow fabric respectively were compressed at a constant

displacement rate of 1mm/min. For a comparison, compression strength and modulus of the two kinds of composites were calculated using the equations (4.1) and (4.2):

$$\sigma = \frac{P_c}{A_m} \quad \text{Eq. (4.1)}$$

$$E_c = \frac{\Delta\sigma}{\Delta\varepsilon} \quad \text{Eq. (4.2)}$$

where $\sigma$ is compression strength (MPa); $P_c$ is compression loading (N); $A_m$ is the area in the cross section of the specimens ($mm^2$); $E_c$ is compression modulus (MPa); $\Delta\sigma$ is the increased compression strength when the compression strain increases $\Delta\varepsilon$.

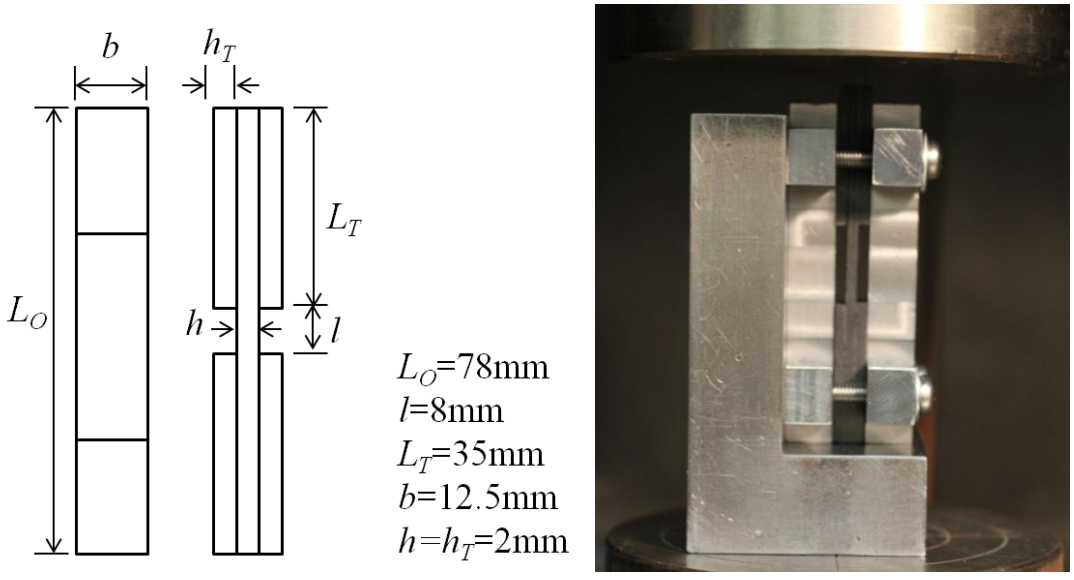


(a) (b)

Fig. 4.4. (a)Diagram of dimensions of tension test specimens and (b) Photograph of the settled test piece and the test device.

4.2.5 Impacting test and compression after impact

In order to find out the crashworthiness of the fiber reinforced epoxy composite, a Charpy impact tester (D-7900 type 510L 100/00, Zwick Gmbh & Co. KG) was used to add impact damage to the testing specimens. The Charpy impact tester is composed of a

machine body that provides both a stage for the test and an anvil supporting for the test specimen, and a pendulum striker, which is attached to a rotation axis supported by the machine body in the end of the pendulum arm; in the other end is a spherical impact head which is perpendicular to the pendulum arm with a 5mm radius of curvature. Also an acceleration transducer (Kyowa Electronics, Inc., AS-1000HA) is attached to the striker at the impact point in order to measure change of acceleration during impact test. The striker's center of mass is adjusted to the impact head, to insure of all the kinetic energy being applied on the specimens. The pendulum striker has a mass of 1149.4g, and a swing arm length also known as the length from rotation point to impact point is 390mm. A photograph of the charpy impact test machine is providing in figure 4.5 [11]. For a required kinetic energy or called impact energy, the pendulum will be raised to θ which is determined according to equation3:

$$E = WgR^2(1 - \cos\theta)/L \qquad \text{Eq. (4.3)}$$

where: W is the weight of the pendulum striker, g is G-forces, R is the length from rotation point to the striker's center of mass, L is the length from rotation point to impact point, and θ is the angle striker should be raised. There is no necessity to take the energy losses caused by bearing friction or air resistance into account, for their small influence on energy balance. In this paper two energy levels (1/1.5J/mm) for the impact test were decided, and five specimens were tested for each sample at each energy level.

The testing specimens' dimensions were 80×50×2.5, specified by the supplement in JIS K7089. After specimens being settled on the anvil support, the pendulum striker will be raised to θ, and then hit the center of the specimen. To avoid a secondary impact the pendulum striker should be held after the striker hitting the specimen and rebounding. During this impact processing the changing of acceleration was recorded by

the data collection unit via the bridge unit control software (Kyowa Electronics, Inc., DBU-120A).

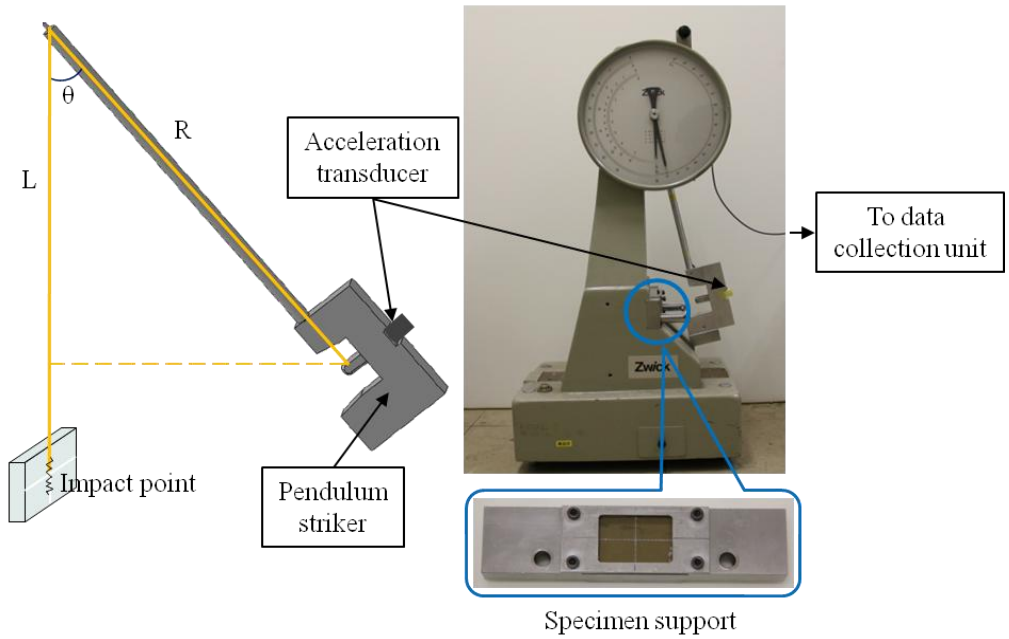


Fig. 4.5. Illustration of Sharpy impact machine.

After the impact test, the residual compression strength (RCS) was measured to evaluate the damage resistance of specimens, which is called compression after impact (the CAI test). RCS is sensitive to the damage caused by localized buckling of sublaminates created by delamination, leading to stress concentration around the region of reduced stiffness [12-15]. CAI test was performed using a mechanical property test machine (TMI UTM-10T; Toyo. Baldwin Co., Ltd.) with a loading cell of 100kN based on JIS K7089, and specimens are with the same dimensions used in impact test. The specimens were compressed at a constant displacement rate of 1mm/min. As mentioned in compression test, compression results were sensitive to fiber orientation relative to loading direction and the top and bottom edges are required to be parallel to each other

and perpendicular to the loading axis, consequently the same polish treatment of the samples were made during preparation. The geometry of the fixture for the CAI test is shown in figure 6. The maximum failure force of the specimen was obtained to evaluate CAI strength. The maximum compression strength or CAI strength is calculated by equation (4.4):

$$\sigma_{ULT} = \frac{P}{bt} \qquad \text{Eq. (4.4)}$$

where $\sigma_{ULT}$ is the ultimate compression strength, P is the ultimate compression loading, b is the specimen width, and t is the average thickness.

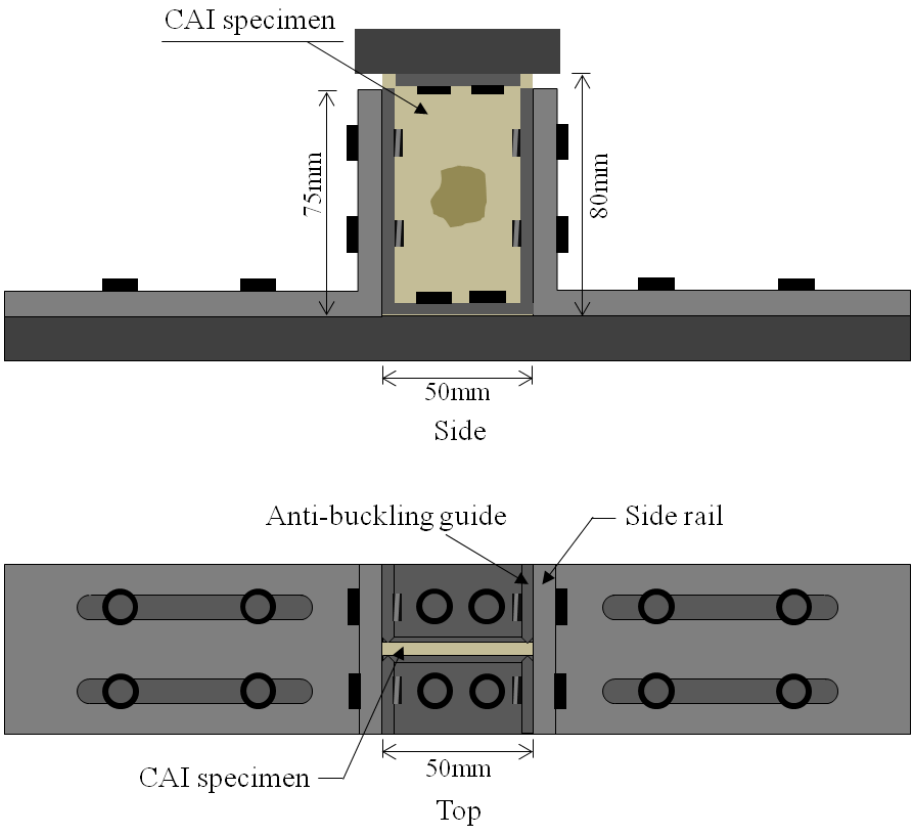


Fig. 4.6. Illustration of compression fixture.

## 4.3 Results and discussion

### 4.3.1 Pure bending

As shown in figure 4.7, the relationships between curvature and moment of aramid STF and carbon fabric reinforced composites are different from each other. The C-M curve of CFRP is linear, and when the curvature is about $35m^{-1}$ the CFRP was broken. On the other hand, the slopes of the C-M curves change at the inflexion point $20m^{-1}$, become gentle. Even bent to the terminal of the equipment, the AFRP had not been broken. The tensile properties and compressive properties of CFRP and AFRP are laid out in figure 4.8 and figure 4.9 respectively. In CFRP the gap between its tensile properties and compressive properties is not as big as in the AFRP. Bending property is a compressive property dominated character, the failure occurs on the compressive side in the forming of micro buckling and kinking [16]. During compression, buckling occurs at small loading in the AFRP, on the other hand, the CFRP was failure in fiber broken, shown in figure 4.10.

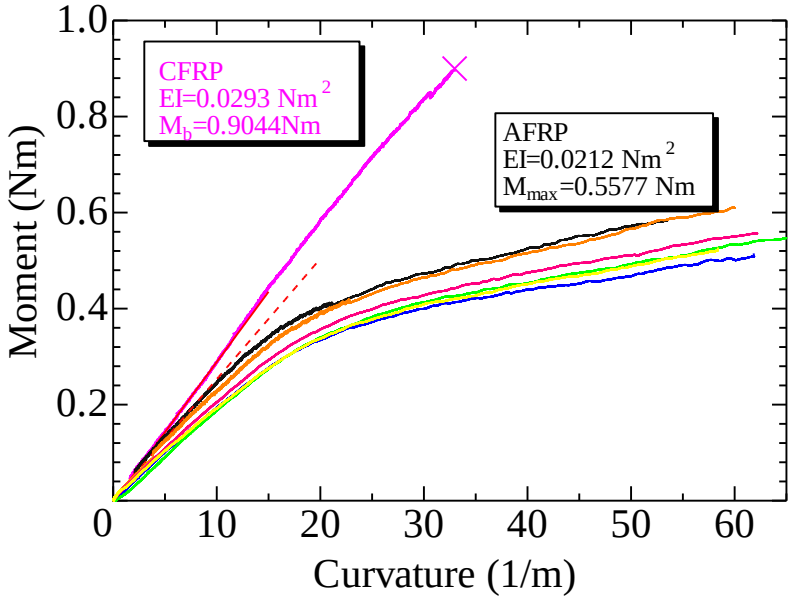

Fig. 4.7. Curvature-Moment curves of AFRP (9layers of aramid spread tow fabric) and CFRP (3layers of carbon fabric).

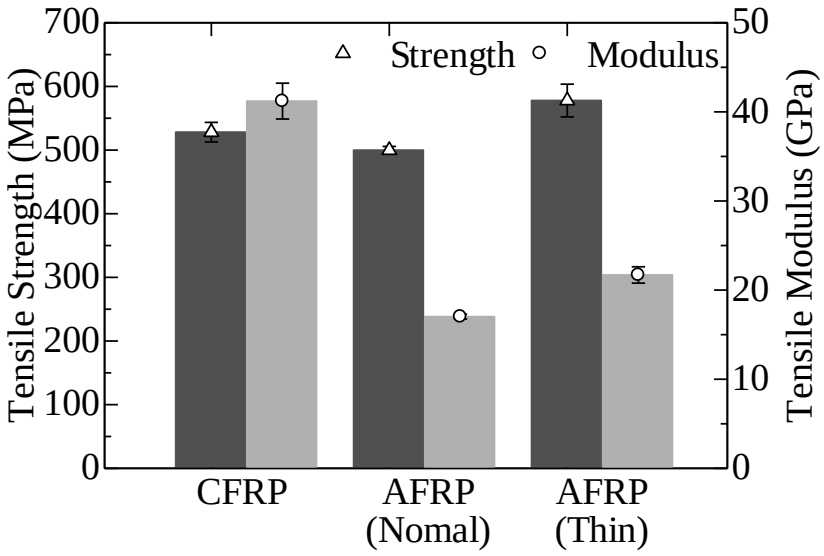


Fig. 4.8. Tensile strength and modulus of CFRP and AFRP.

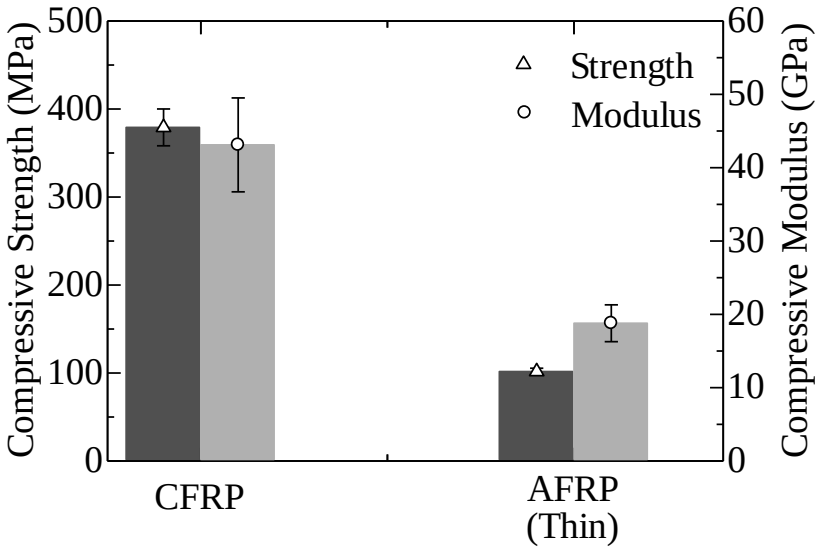


Fig. 4.9. Compressive strength and modulus of CFRP and AFRP.

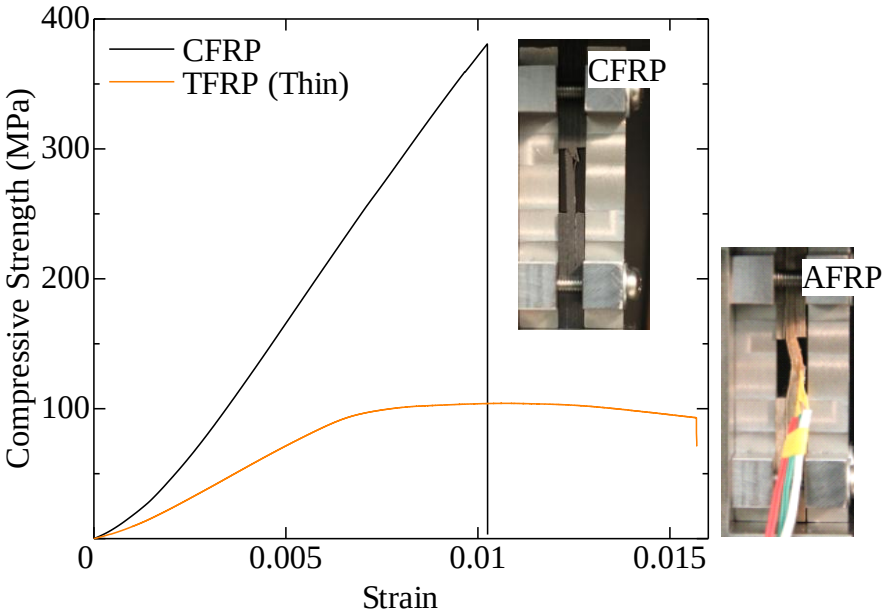


Fig. 4.10. Compressive Strain-Stress curves and failure mode of CFRP and AFRP.

A simple but effective way of manufacturing advanced FRP is the hybrid method [17, 18]. In the purpose of enhancing the bending properties of AFRP, the STF was hybrid with carbon fiber and glass fiber which are with better compression properties than aramid fiber. In figure 4.11 shows the Curvature-Moment curves of AFRP, CFRP and hybrid FRPs. With one layer of carbon fabric on the compressive side, significant enhancements both in failure moment and curvature were observed, that is to say the hybrid CAFRP can undergo large flexural load at large curvature. The glass fiber used in AGAFRP is in mat, and was laminated in the middle of the composite, so the enhancement is not as notable as the carbon fiber.

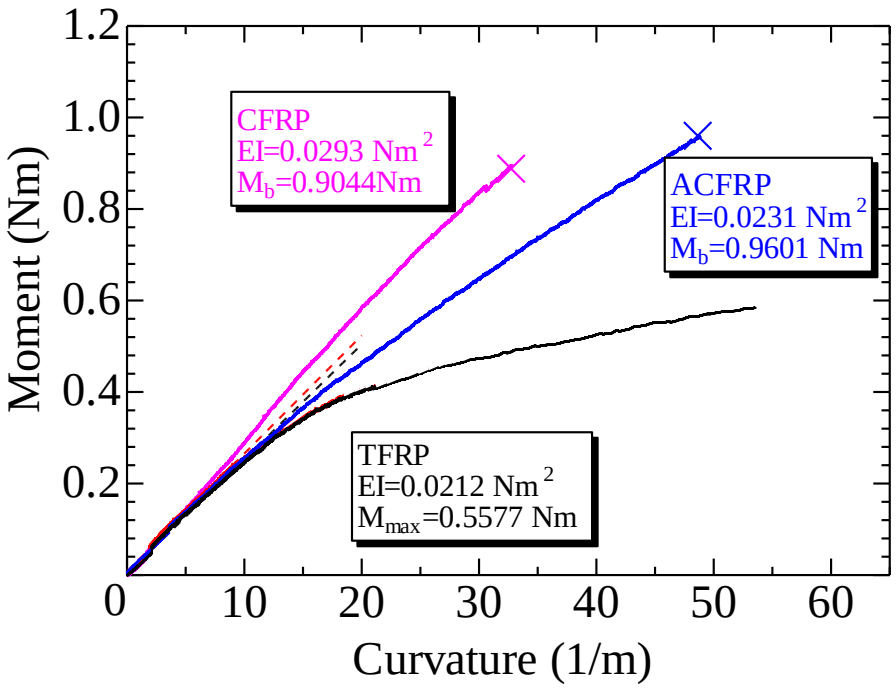


Fig. 4.11. Curvature-Moment curves of AFRP, CFRP and hybrid FRPs.

4.3.2 Impact properties

The materials generally absorb the impact energy by elastic deformation and plastic deformation, materials like rubber can tolerate large elastic deformation, that is to say most impact energy can be absorbed by elastic deformation without any failure. However, the ability of composites undergoing plastic deformation is extremely limited, the absorbed impact energies cause significant impact damage in the form of delamination, matrix cracking, or fiber breakage which is totally undetectable by visual inspection. The damage subsequently leads to reductions in both strength and stiffness [19, 20]. The impact load-time curves of CFRP, AFRP and their hybrid FRPs under different impact energies are shown in figure 4.12. The peak load in the curves is the composites can bear before major failure under certain impact energy [21]. In figure

4.12(a) there is one load peak in all the curves, which is related to initial failure like interface failure or generation of matrix cracking. Adding aramid STF reduces the value of the load peak when the aramid STF is less-than 6layers, the peak value increases with adding aramid STF sequentially. All the peaks concentrate in the former part of the impact action, except AFRP and its load peak value is as large as CFRP. There is no deformation or damage observed after impact, the main way for absorbing energy is elastic deformation. When the impact energy level is raised to 1.5J/mm, all impact load increase, and two load peaks can be observed in the samples with aramid STF less-than 18layers. The first one is initial failure, and the second one is the failure growth from the initial failure. The curve of the composite with 18layers aramid STF is still in the shape of plateau considered to be the merging of the initial failure and the following growth. The impact load increased significantly creating initial failure.

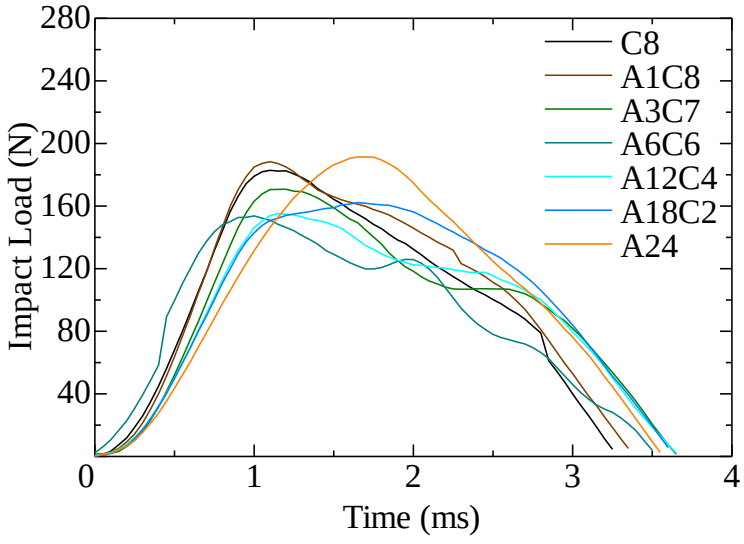


(a)

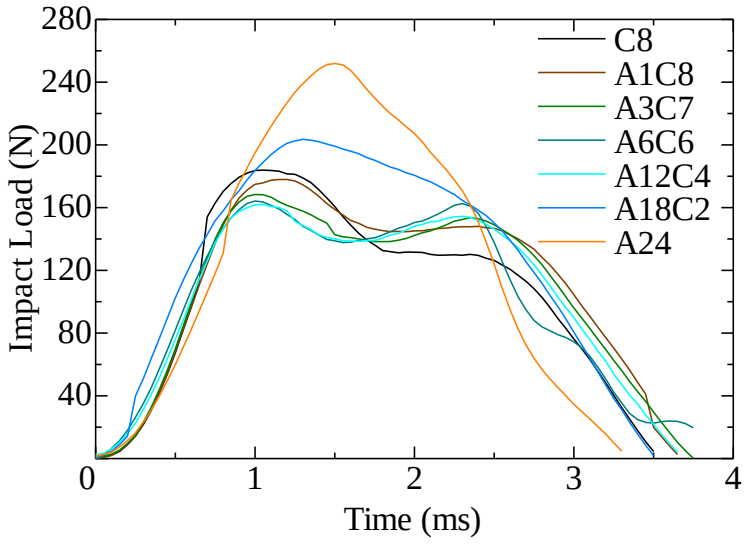


(b)

Fig. 4.12. Impact load-Time curves for (a) 1J/mm and (b) 1.5J/mm (C: carbon fabric, A: aramid STF).

### 4.3.3 Compression after impact

After impact test, compression test are performed to evaluate the impact damage on the samples. In figure 4.13, the residual strength after impact of CFRP and AFRP are presented. In all the two composites, the residual strength retention reduces with the increasing impact energy, because the large impact-induced damage leads to great weakness in composite structure [22]. But the strength retention in AFRP is higher than that in CFRP at the same impact energy level. It is considered that for low velocity impact loading, the ability of the fibers to store energy elastically appears to be the fundamental parameter in determining impact resistance. Aramid fibers, which have large areas under their stress/strain curves, offer excellent impact resistance [23]. Because of the excellent energy absorb ability in elastic deformation, the AFRP suffers

less failure such like interface separation or matrix cracking than CFRP dose, consequently, they have high retention.

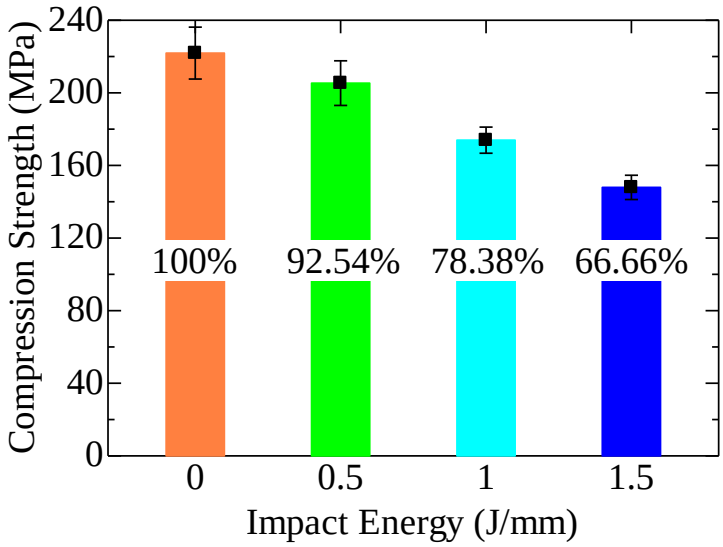


(a)

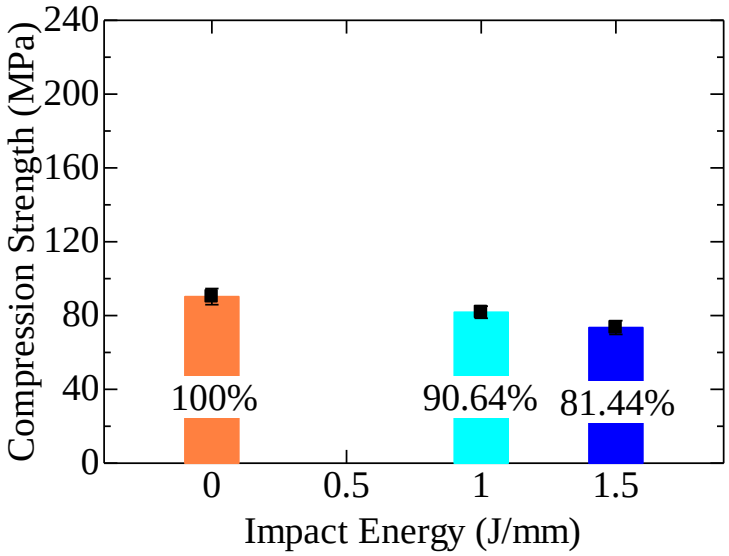


(b)

Fig. 4.13. CAI strength of (a) CFRP, (b) AFRP.

In designing materials, considering the practical application property, not only the

impact resistance but also the strength of the material should be considered synthetically. As shown in figure 4.14, the strength percentage is the ratio of composite comparing to CFRP after adding aramid STF, and strength retention is residual strength after impact comparing to strength without impact. Significant reduce in compression strength occurs when adding aramid STF; on the contrary, adding aramid STF doesn't bring persistent increasing in strength retention. For the balance of material strength and residual strength retention adding 3layers of aramid STF is promising in application. The strength retention after 1.5J/mm impact is with analogous change.

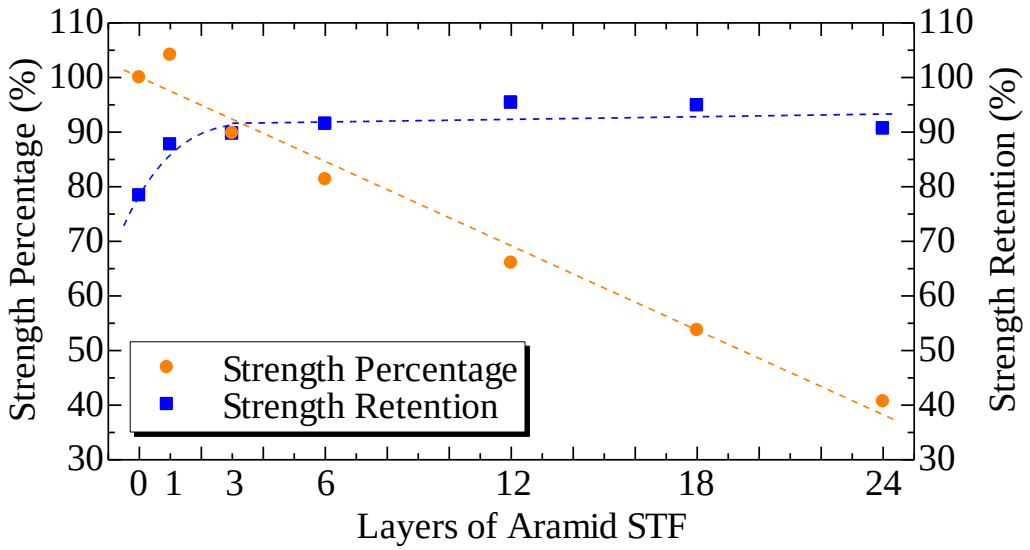


Fig. 4.14. Change of compression strength with and without impact.

The samples after CAI test are with different failure modes, as shown in figure 4.15, the left side is the front surface and the right side is back surface. With small amount of aramid STF, only shear failure can be observed, after that, the failure compose of shear failure in carbon side and buckling in aramid side, at last in AFRP only buckling is left, which are consistent with the compression result.

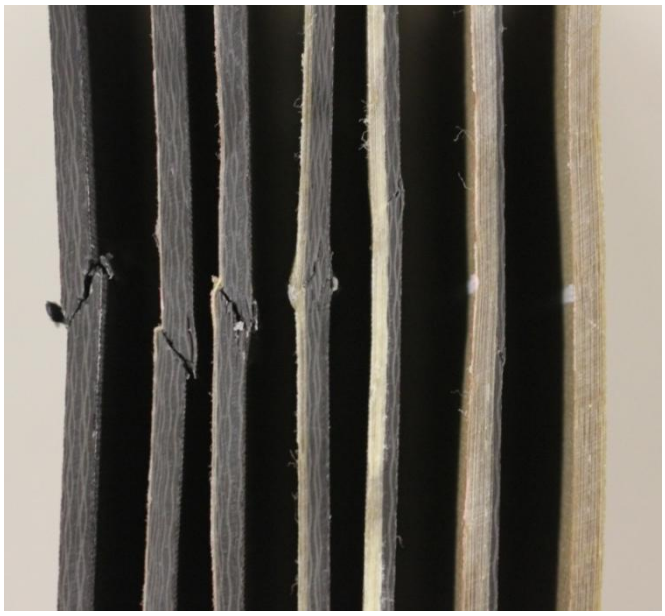

0 1 3 6 12 18 24

Fig. 4.15. Photograph in the profile of the samples after CAI test (Impact energy level 1J/mm).

## 4.4 Summary

In the purpose of producing advanced composite materials with small amount of raw materials the aramid STF were employed to manufacture hybrid composite with carbon fabric. Because of the hybrid effect, the hybrid ACFRP can undergo higher bending moment than AFRP and larger curvature than CFRP with only 1layer carbon fabric on the compressive side. By the hybrid method, the energy absorbing properties were changed, the impact-induced failure was controlled and it was promising to increase the residual strength retention from 80% up to over 90% even with aramid STF less-than 3layers. The possibility of producing advanced composite materials with small amount materials is supported by the results in this research.

**References**

[1] P.J. Flory, Molecular theory of liquid crystals, Advances in polymer science, 59 (1984) 1-36.

[2] P.W Morgan, Synthesis and Properties of Aromatic and Extended Chain Polyamides, Macromolecules, 10 (1977) 1381-1390.

[3] S.L. Kwolek, P.W. morgan、J.R.Schaefgen, and L.W.gulrich, Synthesis, Anisotropic Solutions, and Fibers of Poly(1,4-benzamide), Macromolecules, 10 (1977) 1390-1396.

[4] H.Blades, Dry jet wet spinning process, US 3767756 (1973)

[5] H.H yang, Kevlar aramid fiber, J. Chem. Educ., 71 (1994) A54.

[6] J W S Hearle, High-performance fibers, Woodhead Publishing Ltd.

[7] D. Tanner, A. K. Dhingra, J. J. Pigliacampi, Aramid fiber composites for general engineering, Journal of Materials, 38 (1986) 21-25

[8] N. Khokar, Method and apparatus for weaving tape-like warp and weft and material thereof, Canadian Patents CA 2594350.

[9] H. Takiuchi, H. Saito and I. Kimpara, Investigation of crack suppression mechanism of thin ply CFRP cross-ply laminate by cohesive element method, Journal of the Japan Society for Composite Materials, 38 (2012) 30-37.

[10] H. Saito, H. Takiuchi and I. Kimpara, Experimental evaluation of the damage growth restraining in 90° layer of thin-ply CFRP cross-ply laminates, Adcanced Composite Materials, 21 (2012) 57-66.

[11] W. Hufenbach, F. Marques Ibraim, A. Langkamp, R. Böhm, and A. Hornig, Charpy impact tests on composite structures-An experimental and numerical

investigation, Composite Science and Technology, 68 (2008) 2391-2400.

[12] A.J. Patel, N.R. Sottos, E.D. Wetzel, and S.R. White, Autonomic healing of low-velocity impact damage in fiber-reinforced composites, Composites Part A: Applied Science and Manufacturing, 41(2010) 360-368.

[13] Abrate S., Impact on laminated composite materials, Applied Mechanics Reviews, 44 (1991) 155-190.

[14] Abrate S. Impact on laminated composites: recent advances, Applied Mechanics Reviews, 47(1991) 517-544.

[15] Freitas MD, Reis L., Failure mechanisms on composite specimens subjected to compression after impact, Composite Structures, 42 (1998) 365–373.

[16] D.P.N. Vlasveld, W. Daud, H.E.N. Bersee, S.J. Picken, Continuous fibre composites with a nanocomposite matrix: Improvement of flexural and compressive strength at elevated temperatures, Composites Part A: Applied Science and Manufacturing, 38 (2007) 730–738.

[17] D. Short, J. Summerscales, Hybrids-a review: Part 1. Techniques, design and construction, Composites, 10 (1979) 215-222.

[18] D. Short, J. Summerscales, Hybrids-a review: Part 2. Physical properties, Composites, 11 (1980) 33-38.

[19] W.J. Cantwell and J. Morton, The impact resistance of composite materials - a review, Composites, 22(1991) 347-362.

[20] M.V. Hosur, M. Adbullah, S. Jeelani, Studies on the low-velocity impact response of woven hybrid composites, Composite Structures, 67 (2005) 253-262.

[21] Y. Hirai, H. Hamada, J. Kim, Impact response of woven glass-fabric composites I: Effect of fibre surface treatment, Composites Science and Technology, 58 (1998)

91-104.

[22] X. Zhang, G.A.O. Davies, D. Hitchings, Impact damage with compressive preload and post-impact compression of carbon composite plates, International Journal of Impact Engineering, 22 (1999) 485-509.

[23] D. F. Adams and A.K. Miller, An analysis of the impact behavior of hybrid composite materials, Materials Science and Engineering, 19(1975) 245-260.

CHAPTER FIVE

# Determination of Creep Life of Glass Fiber/Phenol Composite Filled with Carbon Nanotubes by Four-Point Flexural Creep Test

# Chapter5: Determination of Creep Life of Glass Fiber /Phenol Composite Filled with Carbon Nanotubes by Four-Point Flexural Creep Test

## 5.1 Introduction

Because of their high specific stiffness and strength, as well as their outstanding fatigue performance and high chemical resistance, fiber-reinforced plastic (FRP) composites are becoming one of the most important lightweight materials, particularly in aircraft, F-1 cars, and the wind-energy industry, and have become irreplaceable nowadays. Although the in-plane properties of laminated composites are fiber-dominated and appear to be strong for many structural applications, the Z-axis through-the-thickness properties of such composites, such as delamination resistance, are often not sufficient owing to the apparent low performance of the matrix-dominated interface. Therefore, a limited structural integrity and an application far below the full potential are observed. For their laminated structure, FRP materials are susceptible to the effect of the transverse load. The FRP materials are inhomogeneous and anisotropic making their damage behavior complex and entirely different from that of a metal. In laminated FRP components, the damage mode usually consists of local permanent deformations, fiber breakage, delamination, and matrix cracking [1]. Studies of carbon fiber reinforced plastic (CFRP) have indicated that failure under static or dynamic loads is known to involve microscopic damage, such as matrix cracks and delamination [2, 3]. Such damages may not be visible for they are always on a subsurface, but their presence

can result in considerable reductions in composite strength and stiffness, and then in the catastrophic failure of the materials. One of the potential ways for overcoming this defect is to add fillers to the resin. If the fillers can disperse between the fiber fabric layers in the thickness direction of the composites, the fillers that are preferentially oriented between the fiber layers in the thickness direction can lead to the interpenetration of the fillers and the fiber fabric, thus forming a new interface between the resin and the fiber fabric, to transfer the load from the matrix to the fiber reinforcement layer, more effectively [4].

Carbon nanotubes (CNTs), first discovered by Iijima in 1991 [5], not only have the mutual properties of nanofillers, such as nanometric size, which leads to large specific surface areas exceeding 1000 $m^2/g$ [6], but also have excellent mechanical properties [7-10] and electrical and thermal conductivities [11, 12]. CNTs are considered to be high-potential nanoparticles for improving mechanical and physical polymer properties. For example, adding only 1 wt% CNTs to thermoplastic poly(vinyl alcohol) improves its tensile modulus by 80% [13]. Previous works have demonstrated that the key factor to achieving superior mechanical properties is the dispersion of nanofillers, and the higher performance of CNT-polymer composites strongly depends on the extent of load transfer from the matrix to the fillers [14, 15]. A perfect dispersion not only makes more filler surface area available but also prevents the aggregation of the fillers. The aggregated fillers act as stress concentrators in the composites and also cause nanotube slippage during composite loading, all of which greatly decrease the performance of FRP composites.

There are many research papers on FRP composites reinforced by CNTs; most of them focus on improving the mechanical properties of the composites [16-18]. In this

work, the influences of the amount of nanotubes on flexural and interlaminar shear properties were confirmed. To find a simple and convenient way for evaluating the durability under static loads of FRP composites modified by CNTs, the four-point flexural creep test was performed.

## 5.2 Experimental Procedure

### 5.2.1 Materials

Phenol resin has a three-dimensional network structure when polymerized, and it has some advantageous features, such as its electrical characteristics and mechanical properties, particularly its flame retardancy and thermotolerance. Therefore, phenol resin was used as the matrix in this study. The phenol matrix used consists of Shonol BRL-240 (phenol resin) and a curing agent (FRH-30A), both supplied by Showa Highpolymer. Considering the performance-to-cost ratio, glass fiber cloth (glass cloth WF230 100BX, supplied by Nitto Boseki) was used for reinforcement. The phenol resin was first modified by CNTs (CT-12k) at different mass fractions by Hodogaya Chemical.

### 5.2.2 Manufacture of samples and test method

Taking into account that during the resin transfer molding (RTM) process, the reinforcement fiber may block the transfer of CNTs, making the distribution of the CNTs uneven, hand lay-up molding was employed in this case. Nine plies of glass cloth were stacked to achieve a thickness of 2mm. After being saturated by the phenol resin

modified by CNTs, FRP samples were cured at 60 ℃ for 2h with a hot press machine and after-cured at 100 ℃ for another 4h in a heating oven. The color of the FRP subsequently changed from white to russet, indicating that the resin was fully cured, as seen in Figure 5.1.

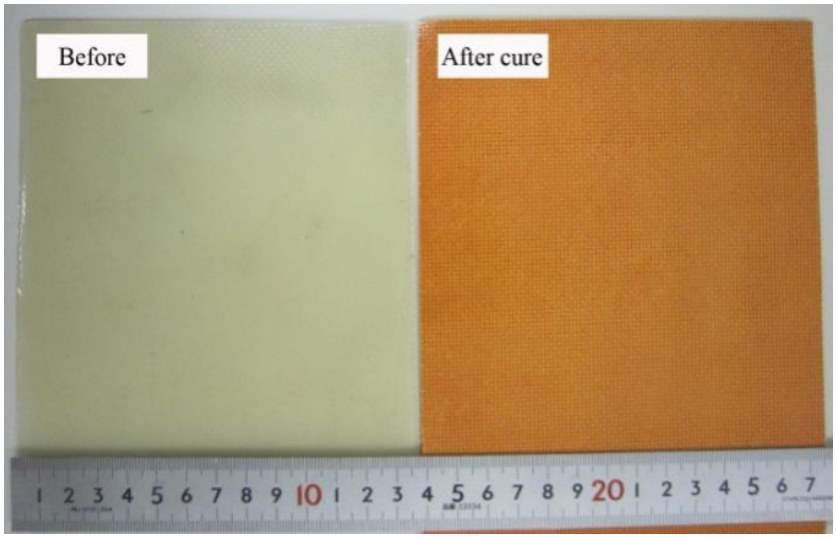


Fig. 5.1. Samples before and after after-cure.

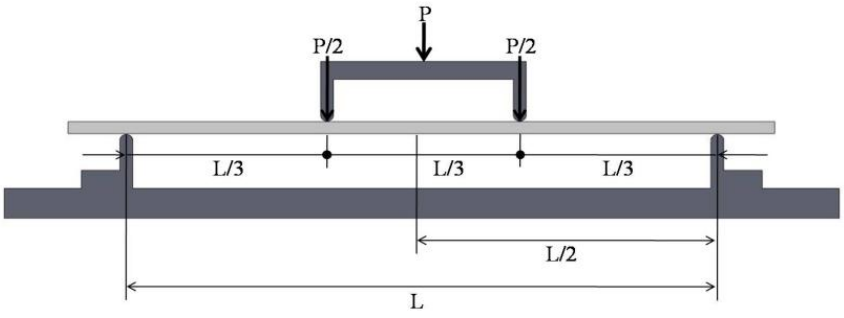


Fig. 5.2. Diagram of four-point bending test.

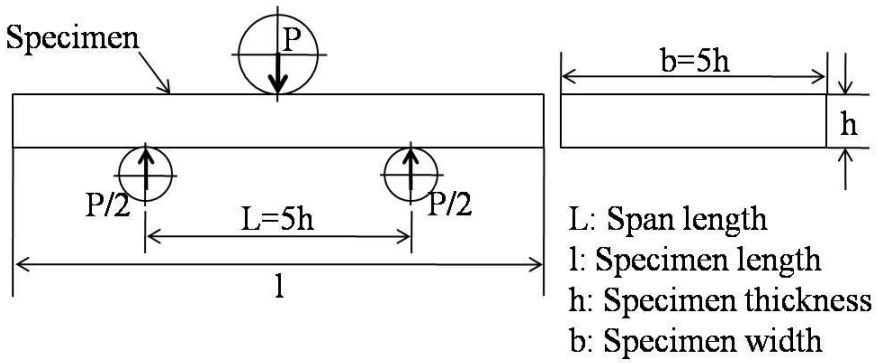


Fig. 5.3. Diagram of short beam test.

Using JIS K7017 (fiber-reinforced plastic composite for the determination of flexural properties), a four-point bending test (Figure 5.2) was performed on Shimadzu Autograph. A short-beam method based on JIS K7057 (fiber-reinforced plastic composites for the determination of apparent interlaminar shear strength by short-beam method) was used to measure the interlaminar shear strength of the FRP samples. Figure 5.3 presents the schematic graph.

In this work, a four-point flexural creep test was performed to confirm the static durability of GFRP materials with CNTs. In practice, it may be a long time before materials reach the end of their lifetime; however, under the testing conditions, the time should be reduced. Therefore, an acceleration test (see JIS Z8115, glossary of terms used in reliability) has been conducted.

As is well known, relaxation and creep occur owing to molecular motion, andthey become more rapid as the temperature increases. Temperature is a measure of molecular motion. The time-temperature superposition principle indicates that with viscoelastic materials, time and temperature are equivalent to the extent that data at one temperature can be superimposed upon data at another temperature by shifting the curves along a logarithmic time axis. The time-temperature superposition principle allows an

estimation of the relaxation modulus and other properties over many decades of time [19]. In this study, on the basis of the results of a four-point bending test, the creep test was performed by imposing 40 and 60% flexural fracture loads on the sample using JIS K7088 (test methods for flexural creep of carbon fiber reinforced plastics) at different temperatures, with an Intesco creep test instrument. After a one-hundred-hour test, we obtained curves for the deflection against time. Curves occurring under different temperatures but with the same load were obtained to form a master life curve according to the time-temperature reciprocation law.

## 5.3 Results and Discussion

### 5.3.1 Mechanical properties

Figure 5.4 illustrates the four-point bending test results for the GFRP filled with CNTs. The flexural modulus increased slightly after adding CNTs to the phenol matrix, indicating that GFRP composite properties are fiber-dominated. The bending strength increased slightly with CNTs below 2 wt%, while at 2 wt%, it markedly increased, indicating that 2 wt% is a suitable mass fraction for enhancing this GFRP composite within the test range. Finally, the flexural modulus and bending strength improved, probably because after adding CNTs, the interlaminar strength and rigidity of the GFRP increased.

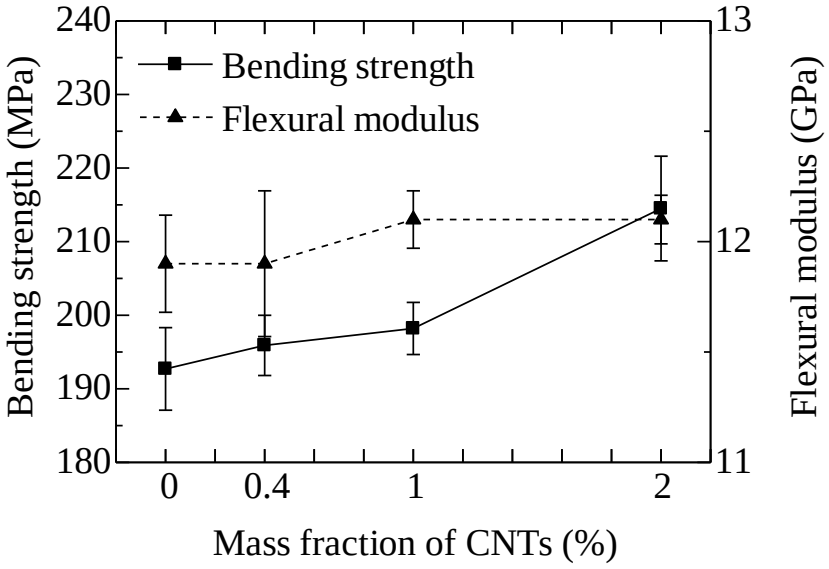


Fig. 5.4. Bending strength and flexural modulus of FRP filled with CNTs.

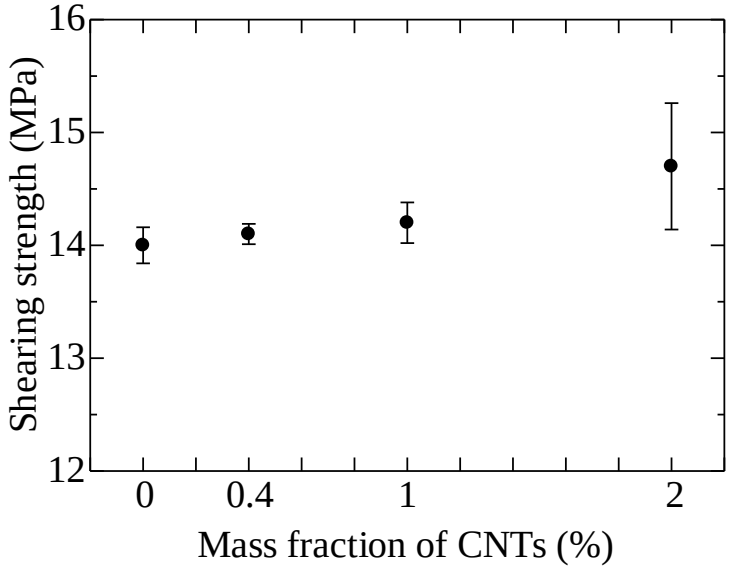


Fig. 5.5. Shear strength of GFRP.

Delamination along ply interfaces due to fiber/matrix debonding is one of the major failure modes in laminated FRP composite structures, subject to transverse and compression loading. Major factors that determine such Z-axis properties include the

fracture toughness of resin and the interfacial properties between fibers and the matrix. One of the major methods for promoting the fiber-matrix adhesion and improving the interfacial shear strength is modifying the interface using nanofillers. The interlaminar shear strength (ILSS) of the GFRP is illustrated in Figure 5.5. The ILSS was improved by adding CNTs owing to the stitching effect of CNTs between the fiber and the matrix. The ILSS with different mass fractions of CNTs tends to vary similarly to the bending strength, indicating that the improvement in bending strength is directly related to the ILSS. With an enhanced ILSS, FRP materials can effectively transfer load from one lamina to another, which can be considered as the most important factor for improving mechanical properties.

### 5.3.2 Creep life test

Every single creep test takes a long time; thus, to save time, samples with 0, 1, and 2 wt% CNTs, which exhibited an obvious enhancement in the bending test, were chosen for the flexural creep test. Some of the test results are presented in Figure 5.6. The deflection increased with increasing temperature, and the sample was broken with a 60% load imposed on it when the temperature was 60 ℃. The results indicate that the GFRP has time-dependent properties.

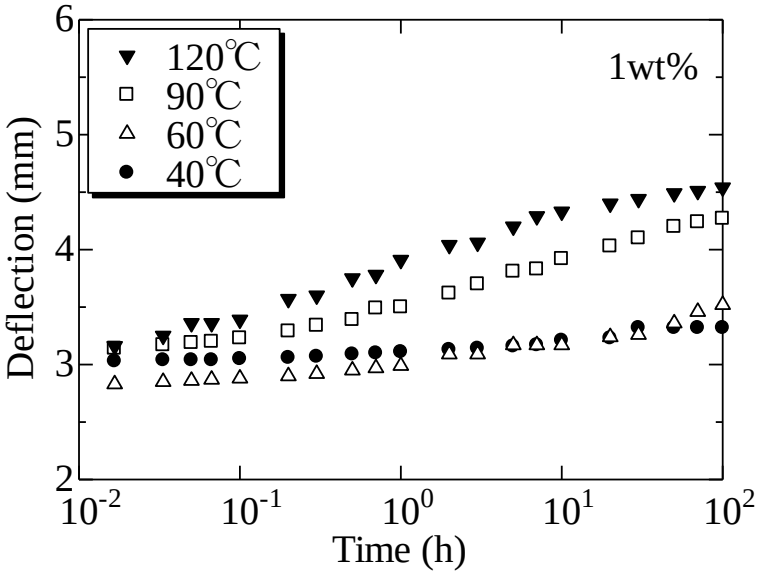


(a)

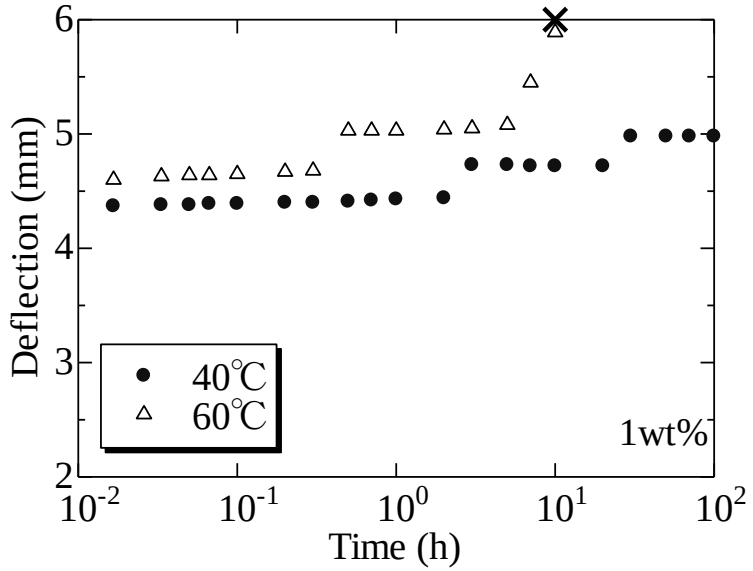


(b)

Fig. 5.6. Creep curves of GFRP with 1wt% CNTs under loads of (a) 40 and (b) 60% (×: broken down).

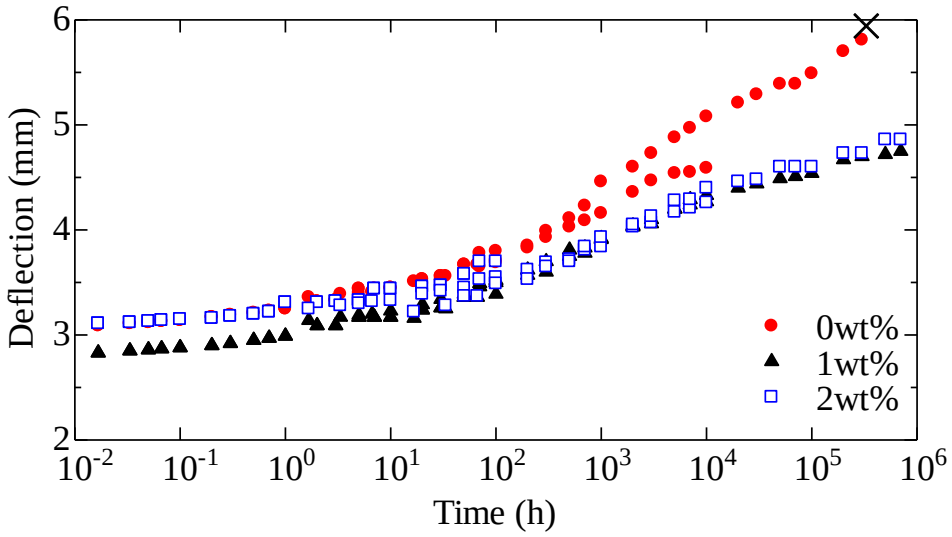


(a)

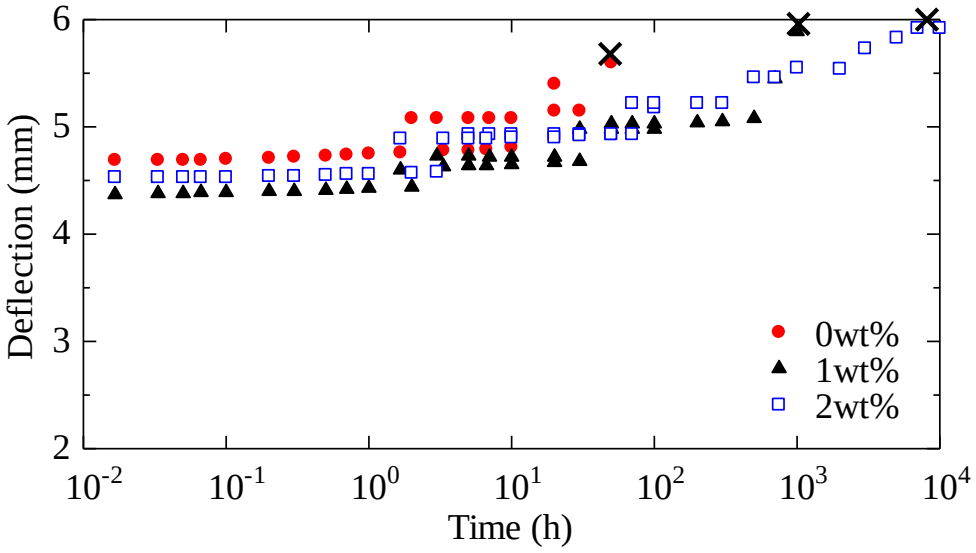


(b)

Fig. 5.7. Master curves under (a) 40 and (b) 60% loads (×: broken down).

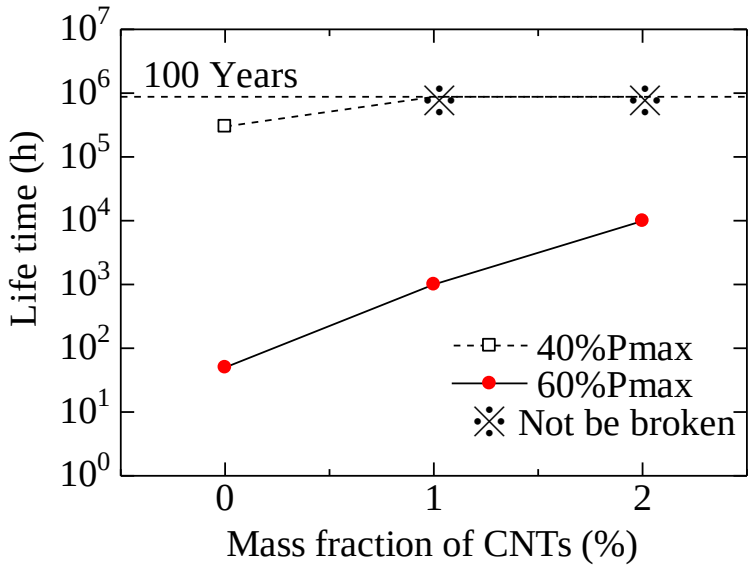


Fig. 5.8. Longevities of GFRP under 40 and 60% loads

The master life curves (Figure 5.7) were determined by the method of drawing master curves from short-term creep data based on the time-temperature reciprocation law [19]. A longevity comparison of FRPs with and without CNTs is given in Figure 5.8. Considering the master curves with a 40% load, samples with CNTs did not break even after $10^6$h, which is more than 100 years; it is evident that samples with CNTs formed a new balance on the molecular level that cannot be overcome at a 40% load. Further work should be carried out to determine the type of the new balance. The master curves of samples with a 60% load indicate an obvious enhancement of the lifetime of GFRP materials by adding CNTs. The almost straight climb in longevity indicates that CNTs effectively improved the lifetime of GFRP materials. However, the enhancing mechanism of CNTs has not been found. Here, we can only make a hypothesis that the enhancement of CNTs at the interface of two fiber laminae makes it possible for the fiber to reinforce the matrix effectively.

### 5.3.3 Prediction of longevity of GFRP materials with CNTs

The creep flexural rigidity (EIc) and static four-point bending rigidity (EI*) were calculated by the creep and bending tests, respectively, and the curve of the proportion of creep flexural rigidity to that of the bending test was determined [Figure 9(a)]. Linear fitting can be carried out by using the least-squares method and the results are shown in Figure 9(b). The gradients of the fitting straight lines and the correlation coefficients to original curves are presented in Table 5.1. The closer the correlation coefficient is to 1, the more reliable the fitting result is. The comparison of the absolute values of these gradients shows that the sample without CNTs has a greater gradient than those filled with CNTs under both 40 and 60% loads, which indicates that the decrease rate of the original sample is higher than those of the samples filled with CNTs and the failure of original sample is much more rapid. Since shearing test results have demonstrated that the ILSS is enhanced by CNTs, and the bending property is also enhanced, the lifetime of the GFRP is improved. In addition, the CNTs also improve the thermal properties [20] of the GFRP, resulting in a better performance even at higher temperatures. These findings suggest that samples filled with CNTs maintain a higher retention ratio of flexural rigidity than those without CNTs, indicating that the gradients of the EIc/EI* curves can be used for the longevity prediction of FRP materials with CNTs.

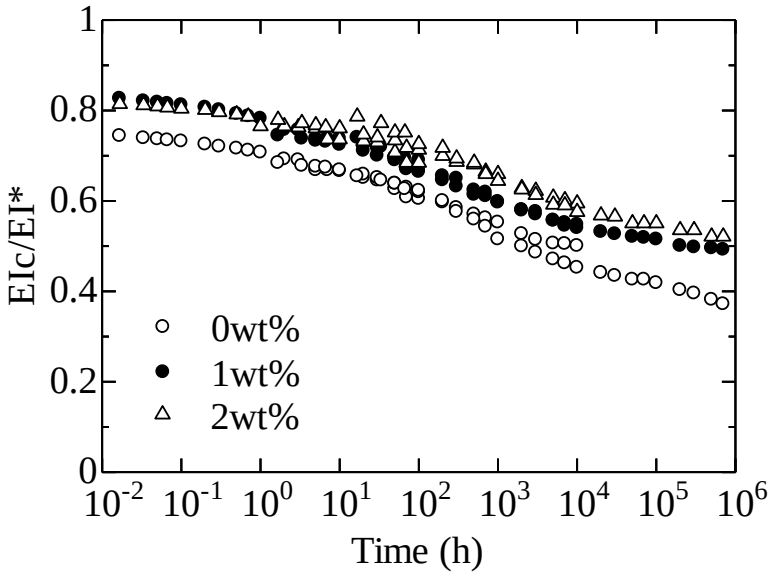


(a) Proportion of creep flexural rigidity (EIc) to static four-point flexural rigidity (EI*).

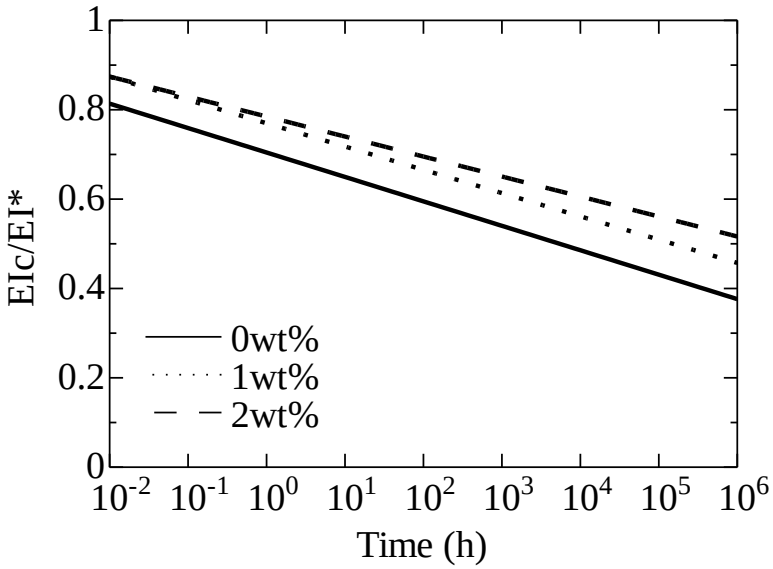


(b) Fitting a straight line of rigidity ratio curves.

Fig. 5.9. Comparison of rigidity ratio curves (under 40% load).

Table 5.1. Comparison of gradients of the rigidity ratio curves.

| | Sample (wt%) | Gradient | Correlation coefficient |
|---|---|---|---|
| 40% | 0 | -2.38 | 0.980 |
| | 1 | -2.26 | 0.988 |
| | 2 | -1.94 | 0.967 |
| 60% | 0 | -2.36 | 0.923 |
| | 1 | -1.80 | 0.919 |
| | 2 | -1.64 | 0.955 |

## 5.4 Summary

In this study, phenol resin, glass cloth, and CNTs were used to manufacture GFRP test samples and the bending and shearing properties and the creep lifetime of the samples were investigated. The conclusions obtained are summarized as follows.

Adding CNTs improved the bending strength flexural modulus and ILSS. Within the test range, the sample with 2 wt% CNTs exhibited the highest degree of strengthening, owing to the stitching effect of CNTs between the laminae. In samples with CNTs exceeding 2 wt%, the CNTs bunched together, reducing the degree of enhancement. New dispersion methods that can fill more CNTs into a matrix are essential for the further improvement of the materials.

In the creep test with an imposed 40% load, only the sample without CNTs broke; samples with 1 and 2 wt% CNTs did not break, even after a long time. With an imposed 60% load, the samples failed in the order of 0, 1, and 2 wt%. These findings were due to the stitching effect and improved thermal properties of CNTs. The longevity of the FRP can be predicted by comparing the flexural rigidities of samples with and without CNTs.

**References**

[1] D. Chakraborty, Delamination of laminated fiber reinforced plastic composites under multiple cylindrical impact, Materials and Design. 28 (2007) 1142-1153.

[2] N. Takeda and S. Ogihara, In situ observation and probabilistic prediction of microscopic failure processes in CFRP cross-ply laminates. Composites Science and Technology, 52 (1994) 183-195.

[3] N. Takeda and S. Ogihara, Initiation and growth of delamination from the tips of transverse cracks in CFRP cross-ply laminates, Composites Science and Technology, 52 (1994) 309-318.

[4] L. Sun, Y. Zhao, Y. Duan, and Z. Zhang, Interlaminar Shear Property of Modified Glass Fiber reinforced Polymer with Different MWCNTs, Chinese Journal of Aeronautics 21(2008) 361-369.

[5] S. Iijima, Helical microtubules of graphitic carbon, Nature 354 (1991) 56-58.

[6] A. Peigney, Ch. Laurent, E. Flahaut, R. R. Bacsa, and A. Rousset, Specific surface area of carbon nanotubes and bundles of carbon nanotubes, Carbon 39 (2001) 507-514.

[7] E. T. Thostenson and T. W. Chou, On the elastic properties of carbon nanotube-based composites: modelling and characterization, Joural of Physics D: Applied Physics 36 (2003) 573.

[8] M. F. Yu, O. Lourie, M. J. Dyer, K. Moloni, T. F. Kelly, and R. S. Ruoff, Strength and Breaking Mechanism of Multiwalled Carbon Nanotubes Under Tensile Load**,** Science 287 (2000) 637-640.

[9] M. F. Yu, B. S. Files, S. Arepalli, and R. S. Ruoff, Tensile Loading of Ropes of Single Wall Carbon Nanotubes and their Mechanical Properties, Physical review letters 84 (2000) 5552-5555.

[10] C. Li and T. W. Chou, Elastic moduli of multi-walled carbon nanotubes and the effect of van der Waals forces, Composites Science and Technology, 63 (2003) 1517-1524.

[11] D. J. Yang, S. G. Wang, Q. Zhang, P. J. Sellin, and G. Chen, Thermal and electrical transport in multi-walled carbon nanotubes, Physics Letters A 329 (2004) 207-213.

[12] S. Berber, Y. K. Kwon, and D. Tománek, Unusually High Thermal Conductivity of Carbon Nanotubes, Physical review letters, 84 (2000) 4613-4616

[13] M. Cadek, J. N. Coleman, V. Barron, K. Hedicke, and W. J. Blau, Morphological and mechanical properties of carbon-nanotube-reinforced semicrystalline and amorphous polymer composites, Applied Physics Letters, 81 (2002) 5123-5125.

[14] P. M. Ajayan, L. S. Schadler, C. Giannaris, and A. Rubio, Single-Walled Carbon Nanotube±Polymer Composites: Strength and Weakness, Advanced Materials, 12 (2000) 750-753.

[15] R. Andrews, D. Jacques, D. Qian, and T. Rantell:, Multiwall Carbon Nanotubes: Synthesis and Application, Accounts of Chemical Research, 35 (2002) 1008-1017.

[16] D. C. Davis, J. W. Wilkerson, J. Zhu, and V. G. Hadjiev, A strategy for improving mechanical properties of a fiber reinforced epoxy composite using functionalized carbon nanotubes, Composites Science and Technology 71 (2011) 1089-1097.

[17] V. Kostopoulos, A. Baltopoulos, P. Karapappas, A. Vavouliotis, and A. Paipetis, Impact and after-impact properties of carbon fibre reinforced composites enhanced with multi-wall carbon nanotubes, Composites Science and Technology, 70 (2010) 553-563.

[18] J. Zhu, A. Imam, R. Crane, K. Lozano, V. N. Khabashesku, and E. V. Barrera, Processing a glass fiber reinforced vinyl ester composite with nanotube enhancement of interlaminar shear strength, Composites Science and Technology, 67 (2007) 1509-1517.

[19] K. K. Biswas and S. Somiya, Study of the Effect of Aging Progression on Creep Behavior of PPE Composites, Mechanics of Time-Dependent Materials, 3 (1999) 335-350.

[20] S. Wang and J. Qiu, Enhancing thermal conductivity of glass fiber/polymer composites through carbon nanotubes incorporation, Composites: B, 41 (2010) 533-536.

CHAPTER SIX

# Conclusions

# Chapter 6: Conclusions

There are still some imperfections of the fiber reinforced polymer matrix composite materials, in this thesis focused on the molding method of manufacturing continuous fiber reinforced thermoplastic composite materials with high fiber volume fraction and mechanical properties; by introducing organic fibers into CFRP, the reshaping and reprocessing possibility of FRP materials was investigated; the fiber with good energy absorbing property was used to improve the impact resistance, and the stacked sequence was also put into investigation; at last the CNTs was employed to improving the interlaminar shear strength and the creep life time properties. The conclusions are collected in this chapter.

In chapter one, an introduction on the manufacture method and the mechanical properties of advanced fiber reinforced polymer matrix composite materials was made.

In chapter two, Vacuum-assisted solution impregnation prepreg thermoplastic composite molding method for improving the fiber volume fractions of continuous fiber reinforced thermoplastic composite materials was proposed and investigated. After pre-impregnation of the reinforcing fibers with thermoplastic resin solution, a vacuum was employed for further impregnation and solvent volatilization in the prepreg manufacturing process. The treatment time for the fabric and the solution conditions were determined (10 s/20 cm and 25 wt%, respectively) based on bonding tests. Under the determined manufacturing conditions, the fiber volume fraction in the thermoplastic composite material reached 60%, which is similar to those of laboratory-produced fiber-reinforced thermosetting composites. The tensile strength and tensile modulus were improved to levels similar to those of PFRP after the fiber volume fraction of

PFRTP was improved. Tensile tests and comparisons confirmed the effectiveness of vacuum-assisted solution impregnation. The feasibility of the proposed method was confirmed.

Application of the method in manufacturing continuous carbon fiber reinforced thermoplastic indicated that it is promising in the manufacture of other continuous fiber reinforced thermoplastic composites with high fiber volume fraction when the reinforcing materials are in the form of fabric.

In chapter three, the properties of mono-fiber- and hybrid-fiber-reinforced plastic composites during pure bending moment and load-unload cycled bending tests were investigated. It is found that the failure mode of PFRP is different from those of CFRP and GFRP during pure bending. For hybrid-fiber–reinforced composites, the choice of fiber on the compression side affects the failure mode of the composite. Load-unload cycled bending tests revealed that PFRP and PCFRP retained more irreversible plastic strain than CFRP, CPFRP, and GFRP did. Investigating the instantaneous modulus of each material revealed two disparate phenomena, one analogous to CFRP (little change) and the other to PFRP (significant decrease, but the residual modulus is still larger than that of GFRP). In further investigation the influence of other properties rather than the low compressive strength of PBO fiber, for example, the bonding behavior of between fiber and matrix, will be put into investigation to clarify the deformation behavior observed in this paper.

In chapter four, in the purpose of producing advanced composite materials with small amount of raw materials the aramid STF were employed to manufacture hybrid composite with carbon fabric. Because of the hybrid effect, the hybrid ACFRP can undergo higher bending moment than AFRP and larger curvature than CFRP with only

1layer carbon fabric on the compressive side. By the hybrid method, the energy absorbing properties were changed, the impact-induced failure was controlled and it was promising to increase the residual strength retention from 80% up to over 90% even with aramid STF less-than 3layers. The possibility of producing advanced composite materials with small amount materials is supported by the results in this research.

In chapter five, phenol resin, glass cloth, and CNTs were used to manufacture GFRP test samples and the bending and shearing properties and the creep lifetime of the samples were investigated. The conclusions obtained are summarized as follows.

Adding CNTs improved the bending strength flexural modulus and ILSS. Within the test range, the sample with 2 wt% CNTs exhibited the highest degree of strengthening, owing to the stitching effect of CNTs between the laminae. In samples with CNTs exceeding 2 wt%, the CNTs bunched together, reducing the degree of enhancement. New dispersion methods that can fill more CNTs into a matrix are essential for the further improvement of the materials.

In the creep test with an imposed 40% load, only the sample without CNTs broke; samples with 1 and 2 wt% CNTs did not break, even after a long time. With an imposed 60% load, the samples failed in the order of 0, 1, and 2 wt%. These findings were due to the stitching effect and improved thermal properties of CNTs. The longevity of the FRP can be predicted by comparing the flexural rigidities of samples with and without CNTs.

# List of publications

1. Anchang Xu, Hiroshi Nozaki, Limin Bao, Kiyoshi Kemmochi. Determination of Creep Life of Glass Fiber/Phenol Composite Filled with Carbon Nanotubes by Four-Point Flexural Creep Test. Japanese Journal of Applied Physics, 51(1), 01AK03-1-5 (2012)
2. 鮑　力民，黒田　勇貴，徐　安長，剣持　潔, FRP 層間破壊靭性に充てん中空フィラーが及ぼす影響, 日本複合材料学会誌, 38(3), 101-106(2012)
3. Anchang Xu, Limin Bao, Mitsuo Nishida, Atsuhiko Yamanaka. Molding of PBO Fabric Reinforced Thermoplastic Composite to Achieve High Fiber Volume Fraction. Polymer Composites, 34, 953–958 (2013)
4. Anchang Xu, Limin Bao. Manufacture of Fabric Reinforced Thermoplastic Composites with High Fiber Volume Fraction. Advanced Materials Research, 796, 301-305(2013)
5. Limin Bao, Anchang Xu, Takuro Fujii, Kiyoshi Kemmochi, Mitsuo Nishida. Development of the Molding Methods of FRTP to Achieve a High Fiber Volume Fraction. Reinforced Plastics, 59, 6-9(2013)

# Scientific presentation

**International conference**

1. Limin Bao, Anchang Xu and Yuji Umena. Friction Decrease of Airbags with Air. 7th China International Silk Conference, September 10-12, 2010, Suzhou, China.
2. M.Musadiq, L.Bao, T. Kishima, S. Uyama and A. Xu. Study on Influence of Dust

Dislodgement Efficiency of Bag Filter's Structure. 7th China International Silk Conference, September 10-12, 2010, Suzhou, China.

3. Danna Qian, Anchang Xu, Limin Bao and Masayuki Takatera. Improvement of Erosion Behavior and Mechanical Strength of UP Resin Composites Filled with VGCF. The 6th China-Japan International Conference on Mechatronics 2010, September 10-12, 2010, Zhenjiang, China.
4. Anchang Xu, Hiroshi Nozaki and Limin Bao. Creep Life of GFRP Composite Filled with CNTs. 3rd International Symposium on Advanced Plasma Science and its Applications for Nitrides and Nanomaterials (ISPlasma 2011), March 6-9 2011, Nagoya, Japan.
5. Xu Anchang, Bao Limin, Inayoshi Shinki. Molding Technique and Mechanical Evaluation of PBO Continuous Fiber Reinforced Thermoplastic Composite. 6th International Conference on Advanced Fiber/Textile Materials, December 7-9, 2011, Ueda, Japan.
6. Anchang Xu and Limin Bao. Creep Life Time of Glass Fiber / Phenol Composite Filled with Carbon Nanotubes. POLYCHAR 21 World Forum on Advanced Materials, March 11-15, 2013, Gwangju, Republic of Korea.
7. A. Xu, L. Bao. PBO Fabric Reinforced Thermoplastic Composite Manufactured by Solution Impregnation Method. 19th International Conference on Composite Materials, July 28-Auguest 2, 2013, Montreal, Canada.
8. Anchang Xu, Jian Shi, Limin Bao. Study on the Plasticity of Fiber Reinforced Plastic Under Bending Moment. The 42nd Textile Research Symposium, August 28-30, 2013, MT. FUJI, Japan.

# Acknowledgments

It is my pleasure to write this message and express my gratitude to all those who have directly or indirectly contributed to the creation of this thesis.

First of all, I would like to express my deepest gratitude to ***Prof. Limin Bao***, my supervisor, for his continuous instruction with important suggestion, precious advice as well as his enduring patience, fruitful encouragement and large support thorough my doctoral course in Shinshu University.

I would like to express my gratitude to the reviewers, Prof. Isao Kinbara, Hideaki Morikawa, Qingqing Ni, and Shunmei Natsuki, for their kind supports and their invaluable comments and insights. Their advice, insightful comments and suggestions provided significant support on this work.

Naturally, these studies have joint efforts with many other researchers. Thanks also would be given to my group-mates, senior members and juniors (*Ms. Danna Qian, Mr. Jian Shi, Mr. Fangtao Ruan, Mr. Liang Xu, Mr. Daichi Sugiyama, Mr. Shinya Soma, Mr. Ryoji Muramatu, Mr. Takuro Fujii, Mr. Kameel, Mr. Yuki Miura, Mr. Yuji Nanki, Mr. Shunsuke Sato, Mr. Takuya Okazawa, Mr. Bing Liu,*) for their joining part of experiment work, as well for pleasant and enjoyable work environment that they made.

I am sincerely appreciative of Global COE of Shinshu University and for research funding from April 2011 to March 2012, and Grant-in-Aid for the Grants for Excellent Graduate Schools by MEXT, Japan from December 2012 to March 2014.

I also acknowledge with pleasure to ***Prof. Zhijuan Pan***, who encouraged me to further my studies in Japan, ***and Prof. Lun Bai,*** College of textile and clothing engineering of Soochow University (China), for their kind guidance and constant

encouragements.

I would like to say that I am very lucky to meet lots of kind friends during learning career in Ueda. They are always there, to laugh with me in the happy times and to lend a helping hand, when I meet difficulties. We share many experiences and help each other. I am heartily grateful to all my friends at Shinshu University for playing along with me and making the wonderful clips and precious memories of my twenties lives.

I dedicate my greatest thanks to my beloved family. Words fail to express my deep gratitude to my parents for their patience, understanding, love, meticulous care and unlimited support over the years.